University of Szeged

Faculty of Pharmacy

Institute of Pharmaceutical Technology and Regulatory Affairs
Head: Dr. habil. Ildikó Csóka *Ph.D.*

Crystal habit optimization by means of impinging jet crystallization method

Ph.D. Thesis

By

Tímea Tari *Pharm.D.*
Pharmacist

Supervisor:

Dr. habil. Zoltán Aigner *Ph.D.*

Szeged
2019

LIST OF ORIGINAL PUBLICATIONS

I. **Tímea Tari**, Zoltán Fekete, Piroska Szabó-Révész, Zoltán Aigner: Reduction of glycine particle size by impinging jet crystallization. *International Journal of Pharmaceutics,* 478 (1) (2015) 96-102.
DOI: 10.1016/j.ijpharm.2014.11.021

IF (2015): 3.994
Citation: 3

II. **Tímea Tari**, Rita Ambrus, Gerda Szakonyi, Dániel Madarász, Patrick Frohberg, Ildikó Csóka, Piroska Szabó-Révész, Joachim Ulrich, Zoltán Aigner: Optimizing the crystal habit of glycine by using additive for impinging jet crystallization. *Chemical Engineering and Technology,* 40 (2017) 1323-1331.
DOI: 10.1002/ceat.201600634

IF (2017): 1.588
Citation: 3

III. **Tímea Tari**, Piroska Szabó-Révész, Zoltán Aigner: Effect of additive on glycine crystal habit by impinging jet crystallization. *BIWIC 2016* - 23rd International Workshop on Industrial Crystallization, Conference Proceedings, pp. 40-45, Magdeburg, Germany, 06-08. 09. 2016
ISBN: 978-3-7369-9322-8

IV. **Tímea Tari**, Zoltán Aigner: Folyamatos kristályosítási eljárás fejlesztése impinging jet módszerrel. *Acta Pharmaceutica Hungarica,* 87 (043) (2017) 69-75.
ISSN: 001-6659

V. **Tímea Tari**, Piroska Szabó-Révész, Zoltán Aigner: Comparative study of different crystallization methods in the case of cilostazol crystal habit optimization. *Crystals – Special issue: Antisolvent crystallization* – under review

(IF (2017): 2.144)

PRESENTATIONS RELATED TO THE THESIS

1. **Tímea Tari**, Zoltán Aigner: Impinging jet kristályosítási eljárás alkalmazása glicin szemcseméret-csökkentésében.
   Local Scientific Student's Association, Szeged, Hungary, p. 180, 14. 02. 2013

2. **Tímea Tari**, Zoltán Aigner: Impinging jet kristályosítási eljárás alkalmazása glicin szemcseméret-csökkentésében.
   National Conference of Scientific Student's Association, Szeged, Hungary, p. 374, 02 - 05. 04. 2013

3. **Tímea Tari**, Zoltán Aigner: Impinging jet kristályosítási eljárás alkalmazása glicin szemcseméret-csökkentésében.
   Hungarian Chemical Society - Crystallization and Drug Formulation Department 6th Conference, Balatonszemes, Hungary, p. 27, 06 - 07. 09. 2013

4. Zoltán Aigner, **Tímea Tari**, Zoltán Fekete, Piroska Szabó-Révész: Particle size reduction by impinging jet crystallization.
   9th World Meeting on Pharmaceutics, Biopharmaceutics and Pharmaceutical Technology, Lisboa, Portugal, p. 73, 31. 03 - 04. 03. 2014

5. **Tímea Tari**, Zoltán Fekete, Piroska Szabó-Révész, Zoltán Aigner: Szemcseméret csökkentése impinging jet kristályosítással.
   Congressus Pharmaceuticus Hungaricus XV., Budapest, Hungary, p. 49, 10 - 12. 04. 2014

6. **Tímea Tari**, Zoltán Aigner: Additívek alkalmazása impinging jet kristályosítási eljárás során.
   Hungarian Chemical Society - Crystallization and Drug Formulation Department 8th Conference, Balatonszemes, Hungary, p. 11, 15 - 16. 05. 2015

7. **Tímea Tari**, Zoltán Aigner: Kálium-klorid hatása glicin szemcsék habitusára impinging jet kristályosítás során.
   Hungarian Chemical Society - Crystallization and Drug Formulation Department 9th Conference, Balatonszemes, Hungary, p. 11, 06 - 07. 05. 2016

8. **Tímea Tari**, Piroska Szabó-Révész, Zoltán Aigner: Effect of KCl additive on glycine crystal habit by impinging jet crystallization.
   5th International School of Crystallization, Granada, Spain, p. 116, 03 - 05. 06. 2016

9. **Tímea Tari**: Glicin kristályok habitusának optimalizálása impinging jet kristályosítással. *XII. Ottó Clauder Memorial Competition*, Budapest, Hungary, p. 34, 20 - 21. 10. 2016

10. **Tímea Tari**, Zoltán Aigner: Development of continuous antisolvent crystallization process of glycine using impinging jet method.
6th FIP Pharmaceutical World Congress, Stockholm, Sweden, p. 1, 21 - 24. 05. 2017

11. **Tímea Tari**, Zoltán Aigner: Optimization of cilostazol crystal habit by impinging jet crystallization.
4th European Crystallography School, Warsaw, Poland, pp. 102–103, 02 - 07. 07. 2017

12. **Tímea Tari**, Zoltán Aigner: Folyamatos kristályosítási eljárás fejlesztése impinging jet módszerrel.
Hungarian Chemical Society - Crystallization and Drug Formulation Department 11th Conference, Balatonszemes, Hungary, p. 18, 04 - 05. 05. 2018

OTHER PRESENTATION

1. **Tímea Tari**: Bioszimiláris gyógyszerkészítmények liofilizálási ciklusának fejlesztése.
XIII. Ottó Clauder Memorial Competition, Budapest, Hungary, p. 48, 22 - 23. 11. 2018

TABLE OF CONTENTS

ABBREVIATIONS

API	Active pharmaceutical ingredient
AS	Antisolvent crystallization method
BCS	Biopharmaceutics Classification System
CSD	Cambridge Structural Database
CIL	Cilostazol
CV	Coefficient of variation
D [4,3]	the mean diameter over volume, the DeBroukere mean
d (0.5)	the diameter where half of the population lies below this value
DMF	N,N-dimethylformamide
DMSO	Dimethyl sulfoxide
DSC	Differential scanning calorimetry
EDS	Energy dispersive X-ray spectroscopy
EtOH	Ethanol
FAAS	Flame atomic absorption spectrometry
ff	Flow function
GI	Gastrointestinal
Gly	Glycine
hGC	Headspace gas chromatography
ICH	International Conference on Harmonization
IJ	Impinging jet
MeOH	Methanol
PFT	Powder flow tester
PSD	Particle size distribution
R^2	Root mean square error
REV	Reverse antisolvent crystallization method
SD	Standard deviation
SEM	Scanning electron microscopy
SGF	Simulated gastric fluid
s.gr.	Space group
US	Ultrasound
XRPD	X-ray powder diffractometry

1. INTRODUCTION

During the past decades the number of poorly water-soluble drug candidates has increased extraordinarily in pharmaceutical research and development. According to recent evaluations, approximately 75 % of the new candidates belong to BCS Class II (low solubility-high permeability) and Class IV (low solubility-low permeability) categories [1]. In order to overcome the major obstacles that these drug substances possess, such as poor solubility, low dissolution and oral bioavailability, new approaches and possibilities should be taken into consideration. Many of these technologies have already been examined and aimed to be used in pharmaceutical industry, for example particle size reduction, micronization, cyclodextrin complexation, co-crystallization, solid dispersion preparation, solid lipid nanoparticles, polymeric micelles, freeze-dried liposomes, the use of different salt forms, additives, co-solvents, or solubilizing agents, just to name a few [2–7].

As the majority of APIs and excipients can be produced by crystallization, significant progress is also essential in the control of crystallization processes to refine attributes of the crystalline product [8; 9]. Namely, different crystallization techniques could result in agglomerated particles, unstable polymorphic forms, poor flow, needle like crystals, or the product could contain impurities which can decrease stability and efficacy. Therefore, already in the early phase of development, the choice of the most appropriate crystallization method and the optimization of crystallization parameters are crucial to achieve a high quality product [10; 11].

Crystallization methods that are commonly used in the pharmaceutical industry include cooling, antisolvent and precipitation processes. However, with these techniques the particle size can be reduced only within certain limits [12; 13]. New methods are therefore sought to decrease the particle size of APIs with high percentage yield and good reproducibility, such as the use of impinging jet crystallization and the application of multiple inlet vortex mixers [14; 15]. Most of these crystallization processes are performed in batches, but because of the productivity and batch-to-batch variability problems, continuous technologies gain increasing attention. However, not every batch process has been suitable for continuous crystallization thus far, but only a continuous mode would offer potential economic advantages as well as high product efficiency [16; 17].

2. AIMS

In pharmaceutical technology great efforts have been made to develop cost-effective, time-saving particle size reduction techniques which are suitable for the production of uniform crystalline products and can be built into the process of the manufacturing of pharmaceutical formulations.

The main focus of this thesis is on the development of a robust and fast crystallization technique which can result in high quality crystalline product with proper physico-chemical properties besides high productivity and stability. Process intensification and optimization of operating conditions using batch technology have been accomplished, as well as the conversion of the parameters to continuous mode. The goal is to achieve significant particle size reduction, narrow particle size distribution, optimal crystal shape and stable polymorphic form in the case of a model material and a poorly water-soluble drug. Furthermore, the crystal habit modification effect of different crystallization methods is investigated and compared with each other.

The main steps in the experiments were as follows:

A Investigation of particle size reduction efficacy by impinging jet antisolvent crystallization method with self-developed impinging jet device and comparison of the effect on crystal habit with conventional crystallization methods in the case of a model material, glycine.

B Optimization of crystal habit by adjusting operating conditions with innovative solutions based on factorial design during impinging jet crystallization.

C Determination of particle size reduction effect of impinging jet method in the case of poorly water-soluble drug, cilostazol with the use of a full factorial design.

D Development of continuous crystallization method using the self-equipped impinging jet unit with both a model material and a poorly water-soluble drug.

3. LITERATURE SURVEY

3.1. Crystallization

Each crystallization process involves two subsequent steps: nucleation and crystal growth. During crystallization a certain level of supersaturation is needed for nucleation, where a non-equilibrium system occurs and the solution tends to crystallize. Locally, the concentration in the solution is impermanent, and molecules can form aggregates as well as small clusters. In case the formation of stable nuclei overcomes the associated energy barrier, the nuclei can grow, otherwise it dissolves again [18].

Crystallization is an important pharmaceutical industrial process, not only in the field of pharmaceutical, but also food and cosmetic industries. The majority of APIs and excipients can be produced by crystallization and one of the main purposes of this step is to generate an appropriate form of the compound in terms of manufacturability. The APIs of commercial products have to be produced usually in large scale, and the well-chosen crystallization method with high efficacy and productivity can significantly decrease cost and time of production and provide an energy-efficient manufacturing step. The crystallization process determines the chemical purity and physical properties of the product, including particle size, PSD, morphology, polymorphic form, purity, tap density, flowability, compactibility, hygroscopicity and dissolution rate. These quality attributes influence the further processability of drug substances [19–21]. Those crystallization methods are preferable which can produce reproducible products in the simplest possible way, and the material can be directly applied in the formulation of pharmaceutical dosage forms [22–24].

3.1.1. Crystal habit

The crystal habit, such as particle size, shape and surface, plays a decisive role in pharmaceutical formulation. These parameters have a crucial impact on bioavailability, influence the dissolution rate, and determine the tabletability of the drug substances. Direct tablet compression requires sufficiently large and isodimensional particles. In contrast, a small average particle size with a narrow particle size distribution is preferred and frequent requirement for poorly water-soluble APIs. In the case of these drugs, which belong to BCS Classes II or IV, the crystal habit is particularly important, as they have limited aqueous solubility, slow dissolution in the GI tract, in addition the low systemic absorption and erratic oral bioavailability lead to sub-

optimal efficacy in patients [25–27]. Crystal engineering, which can attain small particle size of the final crystallized product, can increase dissolution rate, solubility and releasing quantity from dosage forms; improve the bioavailability of the drug products; as well as enhance the stability and the uniformity of the API incorporated in tablets [28]. A spherical crystal shape favours flowability and fluency during the tableting processes. The smooth surface decreases the agglomeration propensity of the particles, assures the presence of individual particles, therefore fast filtration is facilitated [29]. Overall, these properties appreciably influence the manufacturability and the processability of the given active agent [30; 31].

3.1.2. Effect of additives

Additives selectively inhibit or enhance the growth of crystal faces via several mechanisms and effectively change the crystal morphology. The control of morphology is affected by particular functional groups which can promote crystal growth or conversely inhibit it via two main mechanisms depending on the additives' aggregation state. On the one hand, the aggregated additives can provide a planar surface and the crystallizing material can adsorb onto that surface, and this way the nucleation is promoted. On the other hand, the molecularly dispersed additive can adsorb onto the growing crystallizing material or incorporate into the crystal lattice, and therefore inhibits the attachment of additional crystalline material and further crystal growth is inhibited [32–34]. Parameters such as the concentration and type of the additives can influence the occurrence of the different polymorphs [35–37]. The additives used for the crystallization process can improve the dissolution rate, the hardness, and therefore even the efficiency of the tablets [38–41].

Kaialy et al. successfully engineered xylitol crystals by conventional antisolvent crystallization technique in the presence of various hydrophilic additives. Xylitol crystallized with polyvinylpyrrolidone or polyvinyl alcohol demonstrated improvement in the hardness of directly compressed tablets which contained a poorly water-soluble model material, indomethacin [42]. *Lyn et al.* applied a solvent evaporation and a slow crystallization method with the use of different solvent mixtures and polymers as additives in the case of piroxicam. Incorporation of a polymer resulted in the formation of different crystal forms, the additive formed a hydrophilic film on the surface of drug crystals and had improved dissolution but not solubility [27]. *Yang et al.* investigated the effects of sodium chloride on the nucleation and transformation of two polymorphs of glycine. They found that the aqueous solution of NaCl

favoured the formation of the γ-form, and the final crystals were larger than the initial crystal size [43]. *Sekar and Parimaladevi* applied a slow evaporation method for glycine crystallization using a high concentration of potassium chloride (4-18 %, i.e., 4000-18000 ppm) as additive. They observed that the additive preferentially adsorbed on the (011) crystal face of α-glycine and inhibited its growth along the c-axis, while enhancing the growth along the a-axis [44]. *Han et al.* examined the effects of malonic and DL-aspartic acids as additives on the growth of γ-glycine and DL-alanine side faces. These amino acids usually grow with a needle-like morphology from their aqueous solutions and are elongated along the polar c-axis. It was found that both of the additives inhibited the side growth along the c-axis [45].

In summary, the additives are clearly shown to affect the crystal morphology in the case of long-lasting crystallization methods, but for fast crystallization methods like impinging jet crystallization, the effects of additives on morphology control have not yet been investigated [25].

3.1.3. Conventional crystallization methods

Conventional crystallization methods, i.e. antisolvent, reverse antisolvent and cooling crystallization techniques are frequently used in the pharmaceutical industry. The crystallization conditions, such as temperature, cooling rate, solvent-antisolvent ratio and quality, material concentration, mixing factors, etc. can influence the physicochemical properties of the product [46–48]. However, the conventional route can influence the particle size only within certain limits. Therefore, several alternative processes have been developed for the control and modification of the solid state properties of APIs. Based on the literature, ultrasound application in crystallization is suitable for modifying the quality of the crystals. It can reduce the metastable zone width, and generate rapid, uniform mixing, which reduces the agglomeration of particles [49]. Higher sonication intensity and longer sonication time favour the formation of smaller crystals with narrow size distribution [50–52]. Combining cooling and antisolvent crystallization is also advantageous regarding the greater control of the process. With the application of different cooling and feeding policies not only the yield but PSD can be improved as well [53].

3.1.4. Impinging jet crystallization method

Midler et al. introduced and adapted the impinging jet technique in crystallization [54]. The general use of this technique is a relatively new field for the researchers in the pharmaceutical

manufacturing and industrial crystallization [55; 56]. However, it is proved that this method effectively reduces particle size, as well as having the potential advantage to produce reproducible products with small average particle size and narrow PSD [57]. In the course of IJ crystallization, the rich solution of the API and the antisolvent flow through two jet nozzles arranged diametrically opposite each other, and it generates high-intensity micromixing of fluids to achieve high supersaturation before the onset of nucleation at the impinging point [58]. This process potentially results in rapid crystallization in the absence of concentration gradients and produces a monodisperse population of small crystals with a high surface area. The impinging jet element can be used in a crystallization reactor or operated in non-submerged mode. It is often used in combination with ultrasound to achieve a further reduction in particle size. The direct production of small uniform crystals with high surface area that meet the bioavailability and dissolution requirements can eliminate the need for milling, which can give rise to dust issues, yield losses, long production times, polymorphic transformation or amorphization [46; 59–64]. The currently applied unit, which was used during our experiments, was a self-developed and designed device.

3.1.5. Continuous crystallization

Due to a high demand to accelerate time-to-market developments for new therapies and critical medicines, a keen interest in robust and cost efficient continuous technology has leapt into the limelight. Regulators also encourage manufacturers for the development of continuous processes, since it gives the opportunity to gain more information on process parameters and collect more data to demonstrate that the procedure is consistent within the acceptable operating ranges [65; 66]. However, nowadays, it is still a great challenge to convert technologies from batch to continuous mode in the pharmaceutical industry. The application of scalable and flexible continuous processes is clearly becoming more and more widespread, since continuous manufacturing has a lot of advantages, such as faster process, better percentage yield, uniform product, thus the variations between batches can be avoided, and precision control and monitoring of critical quality attributes can also be achieved more easily. The main advantages of these techniques are that they have the merits of flexible change in production quantities and ease of scale-up, which are important in commercial manufacturing, however certain processes require parameter adjustment for prolonged operation [67].

The development of conventional batch crystallization begins with lab-scale in small-volume reactors and during scale-up the parameters often need to be widely adjusted to achieve the same quality of the product. High-volume reactors and expensive equipment are needed in industrial scale, which require a lot of space to arrange them and have huge time-consuming purification steps. During continuous mode a small-size reactor is sufficient even in industrial-scale due to an ongoing removal of the product [68–72]. The development of a continuous system that is capable of filtering, washing, and drying the crystallized APIs is also advantageous. The system should be tested for success criteria of achieving comparable cake purity and consistent PSD compared with the crystallized material [73].

3.2. Polymorphism

Polymorphism in the solid state occurs when the same molecule exists as multiple crystalline phases in the crystal lattice [74]. The most common technological factors which can induce polymorphism are i.a. scale-up, optimization of crystallization, change of solvent, drying, compression, and grinding/milling [75]. For the pharmaceutical industry, the main concern is the effect of the appearance of unwanted polymorphs during the production, because certain forms have different physico-chemical properties, such as stability, solubility or even toxicity. Therefore, this phenomenon must be very well monitored throughout the whole production chain, and the different forms have to be identified and fully characterized [76; 77].

3.3. Drug substances

3.3.1. Glycine

Glycine is a widely used material for crystallization experiments [78–80]. Gly crystals grow rapidly and the crystal size is typically quite large, therefore it is an ideal model material for particle size reduction studies and for the demonstration of the efficacy of crystallization methods [81; 82]. Figure 1 shows its chemical formula.

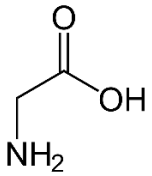

Figure 1 *Chemical formula of glycine.*

Gly exists in three polymorphic forms under ambient conditions and under high pressure, δ- and ζ-polymorphs have also been observed [83]. α-glycine is metastable under ambient conditions and in aqueous solutions, it develops by spontaneous nucleation as the main polymorph. Its crystal structure is monoclinic (s.gr. $P2_1/n$) [79; 84]. β-glycine is the least stable form at all temperatures, and its formation is driven by the addition of methanol or ethanol to the aqueous solutions. It is also characterized by a monoclinic crystal structure (s.gr. $P2_1$). Thermodynamically, γ-glycine is the most stable form under ambient conditions, although most commonly the α-form crystallizes in aqueous solutions and it does not usually transform into the γ-form under these conditions. The γ-form is known to develop in acidic and basic water solutions containing additives like acetic acid, ammonia, or inorganic salts. Its crystal structure is trigonal (s.gr. $P3_1$). The addition of ethanol to an aqueous Gly solution induces precipitation of the β-form [57; 85; 86]. The crystallization methods and conditions, the pH of the solution, and the presence of additives also influence the crystal morphology and the polymorphism [28]. These three polymorphs exist in the zwitter-ionic form within the crystals, and they differ in terms of how the $^{+}NH3–CH2–COO^{-}$ groups are linked by the hydrogen bonds [25; 87; 88].

Aigner et al. examined the effects of several crystallization methods and their parameters (cooling, reverse antisolvent and antisolvent crystallization with ultrasound) on the average particle size, PSD and roundness of glycine, and found that these methods are capable of reducing the average particle size only within a certain range. The particle size varied in a relatively wide range: in cooling crystallization 268-680 μm; in reverse antisolvent crystallization 160-466 μm; and in antisolvent crystallization with the use of ultrasound 82-232 μm were the range of the produced crystals particle size [47]. In order to reduce the glycine particle size, *Louhi-Kultanen et al. (2006)* studied the effects of ultrasound during cooling crystallization on the polymorphism, crystal size distribution and heat transfer in batch cooling crystallization. Sonocrystallization proved to be a good tool for optimizing and controlling the nucleation and crystallization of glycine, and can be used as a size reduction method to produce a final product with uniform crystal morphology. The smallest average particle size achieved was about 100 μm [89].

3.3.2. Cilostazol

Cilostazol, 6-[4-(1-cyclohexyl-1H-tetrazol-5-yl)butoxy]-3,4-dihydro-2(1H)-quinolinone is a phosphodiesterase III inhibitor, which supresses platelet aggregation and has a direct arterial vasodilator effect [90–92]. It exists in three polymorphic forms in a monotropic system. Form A

is thermodynamically the most stable, orthorhombic polymorph, Forms B and C are metastable, and Form C has a monoclinic crystal structure [93]. Cilostazol belongs to the BCS Class II group, and accordingly, it is poorly soluble in water and highly permeable. Due to its poor aqueous solubility and low oral bioavailability, the therapeutic usage of cilostazol is limited. Therefore, several researchers have attempted to increase the solubility and oral bioavailability of cilostazol by using various procedures [94–96]. *Gouthami et al.* established that different solvent-antisolvent compositions influence the crystal habit, methanol-hexane and ethanol-hexane resulted in hexagonal and rod shaped habits. The raw material cilostazol has needle-shaped crystals in general, and currently in commerce its average particle size is between 10-15 μm [97]. *Kim et al.* used supercritical antisolvent (SAS) process to reduce the particle size of cilostazol. Remarkable dissolution rate enhancement was observed due to the increased specific surface area [98]. *Jinno et al.* applied, among others, different mechanical milling processes, such as hammer-mill and jet-mill technologies. These methods resulted in particles with mean diameters of 13 μm and 2.4 μm, respectively [99]. Figure 2 shows its chemical formula.

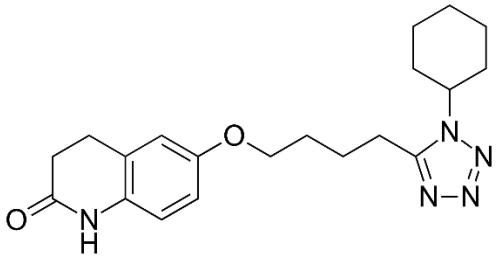

Figure 2 *Chemical formula of cilostazol.*

4. MATERIALS AND METHODS

4.1. Materials

Glycine was purchased from VWR International Ltd., Debrecen, Hungary. Cilostazol was generously provided by Egis Pharmaceuticals Plc., Budapest, Hungary.

All the applied solvents were of analytical grade. Ethanol 96%, methanol and acetone were supplied by VWR International Ltd., Debrecen, Hungary; neutral oil (Miglyol 812) was purchased from Sasol Germany GmbH, Hamburg, Germany; N,N-dimethylformamide and dimethyl sulfoxide were supplied by Scharlau, Barcelona, Spain; and purified water of Ph. Eur. quality was used for the experiments. Polysorbate 80 (VWR International Ltd., Debrecen, Hungary) was applied for sample preparation during particle size distribution analysis. Simulated gastric fluid without enzymes (10.0 g NaCl, ~59.4 g 37% HCl ad 5000 ml purified water, pH = 1.2 ± 0.1), and phosphate buffer (385 ml 0.2 M NaOH, 34.0 g KH_2PO_4 ad 5000 ml purified water, pH = 6.8 ± 0.1) were used during dissolution investigations.

4.2. Methods

4.2.1. Crystallization methods

4.2.1.1. Conventional crystallization methods

Conventional crystallization methods were implemented in a 250-mL flat-bottomed, double-walled crystallization reactor with constant room temperature provided by the Julabo F32 (Julabo GmbH, Seelbach, Germany) cryothermostat controlled by the Julabo EasyTemp 2.3e software. Ongoing mixing was carried out with a magnetic stirrer by using an egg-shaped magnetic stir bar. In the case of the antisolvent system, supersaturation was achieved by exposing the saturated API solution to the antisolvent at room temperature with fast addition (24 mL min^{-1}) by means of a peristaltic pump. Reverse addition of the solutions was applied in the case of reverse antisolvent crystallization, thus the saturated product solution was added to the antisolvent with the same constant velocity at 25 °C. In both cases the experiments were accomplished with and without the use of high power ultrasound device (Hielscher UP 200S Ultrasonic Processor, Germany).

4.2.1.2. Impinging jet crystallization

The impinging jet unit was a self-developed device which included 0.6-mm-diameter nozzles and was arranged in a non-submerged mode. Two calibrated peristaltic pumps (Rollpump Type

5198, MTA Kutesz, Budapest, Hungary) fed the near-saturated solution of APIs and the antisolvents to the IJ unit at defined temperatures. Crystallization experiments were carried out in a 250-mL round-bottomed, double-walled Schmizo crystallization reactor (Schmizo AG, Oftringen, Switzerland) equipped with an IKA Eurostar digital overhead stirrer (IKA-Werke GmbH & Co., Staufen, Germany) and an Anker-type mixer with constant stirring speed. Temperatures were adjusted with a Thermo Haake P5/C10 (Thermo Haake, Karlsruhe, Germany) thermostat and a Julabo F32 (Julabo GmbH, Seelbach, Germany) cryothermostat controlled by the Julabo EasyTemp 2.3e software. After the preparation of saturated API solution, further solvent (2 ml) was added consequently to avoid crystallization in the nozzles. The feeding was accomplished with certain linear velocity and with different solvent–antisolvent ratio, with various temperature differences between the solutions. The crystallized products were filtered in a porcelain filter and were washed with antisolvent, to minimize the quantity of residual solvent. After 24 hours of vacuum drying at 40 °C, the products were stored in closed containers under normal conditions. The schematic drawing of the experimental apparatus is outlined in Figure 3.

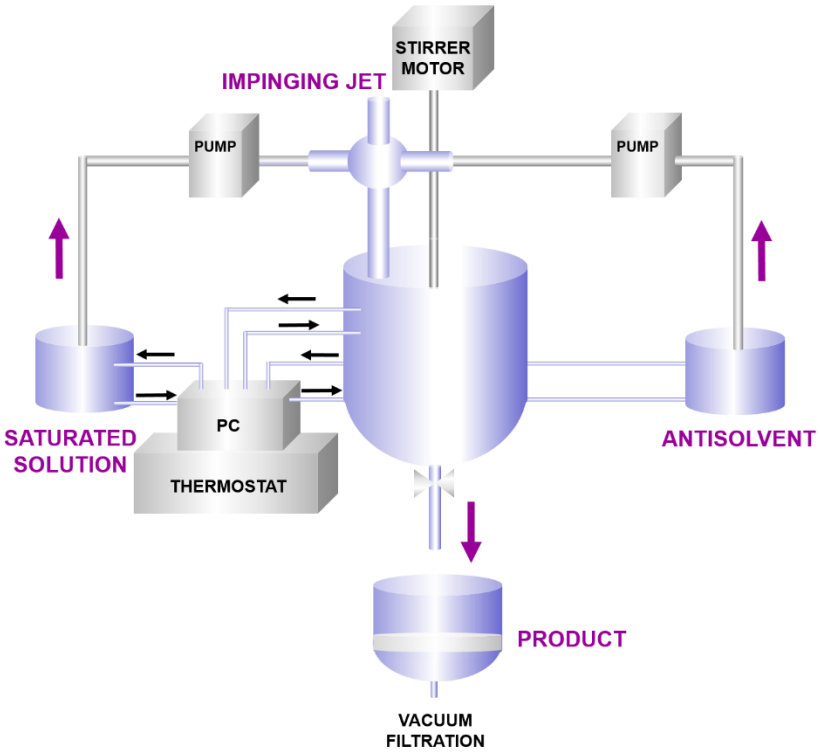

Figure 3 *Self-developed experimental apparatus of impinging jet crystallization.*

4.2.1.3. Continuous crystallization

During the continuous experiments the self-equipped impinging jet mixer was applied in non-submerged mode in a double-walled crystallization reactor (Schmizo AG, Oftringen, Switzerland), and the continuous mixing was achieved by an IKA Eurostar digital overhead stirrer (IKA-Werke GmbH & Co., Staufen, Germany) equipped with an Anker-type mixer with constant stirring speed. Constant temperatures of both of the API solution and the antisolvent were set by Thermo Haake P5/C10 (Thermo Haake, Karlsruhe, Germany) thermostat and Julabo F32 (Julabo GmbH, Seelbach, Germany) cryothermostat controlled by Julabo EasyTemp 2.3e software. The solutions were dosed in high volume by two calibrated peristaltic pumps (Rollpump Type 5198, MTA Kutesz, Budapest, Hungary). In the case of the glycine experiments the nearly saturated API solution, which contained 200 ppm KCl, and the antisolvent, 96% ethanol flowed through the nozzles with constant velocity (4.06 m s^{-1}) in the ratio of 1:1 to the impinging point. During cilostazol experiments those parameters were set as well, which resulted the most appropriate product in the case of batch process. The nearly saturated API solution and the antisolvent, purified water were dozen to the impinging unit with constant 4.06 m s^{-1} velocity in the ratio of 1:1.

Ongoing filtration was implemented of the crystallized product with porcelain filters without post-mixing. Fractions were separated from the crystallized product at given intervals in order to investigate the physico-chemical properties of the crystals in the pipeline. After 24 hours of vacuum drying at 40 °C, the products were stored in closed containers under ambient conditions.

4.2.2. Determination of solubility

The solubility of glycine and cilostazol was determined by using gravimetric method in pure water, EtOH, MeOH, DMSO, DMF, acetone and in mixtures of different volume ratios of solvents at ambient temperature. The effect of different concentrations of additives (NaCl and KCl) to solubility was also evaluated. Three parallel measurements were carried out and for each it took 24 hours to reach the equilibrium. After the sedimentation of the suspended particles, the clear solution was sampled into a vessel with a known mass.

4.2.3. Product characterization

4.2.3.1. Determination of crystal morphology

Light microscopy

The crystal shape of the crystallized products was analysed using the Leica Image Processing and Analysis System (Leica Q500MC; Leica Cambridge Ltd., Cambridge, UK). It can provide detailed information about the morphology of single particles in terms of crystal length, breadth, surface area, perimeter and roundness. The products were suspended in Miglyol 812 with ultrasound for 2 minutes in order to ensure the presence of individual particles. Approximately 1000 particles per sample were measured and the roundness value was evaluated of high priority.

Roundness is a shape factor giving a minimum value of unity for the circle shape. The roundness value for the perfect sphere shape equals 1.00. Roundness is calculated as the ratio of the perimeter squared and the surface area. The adjustment factor of 1.064 corrects the perimeter for the effect of the corners produced by the digitization of the image. The following equation was applied:

$$Roundness = \frac{Perimeter^2}{4 \cdot \pi \cdot Area \cdot 1.064}$$

Scanning electron microscopy

The morphology of the crystallized products was investigated by SEM (Hitachi S-4700, Hitachi Scientific Ltd., Tokyo, Japan). The working distance was 15 mm with an accelerating voltage of 10 kV and an emission current of 10 mA. A sputter coating apparatus (Bio-Rad SC 502, VG Microtech, Uckfield, UK) was applied to induce electric conductivity on the surface of the samples applying a gold-palladium coating. The argon gas pressure was 1.3–13.0 mPa and the time was 90 sec.

Particle size distribution analysis

PSD was determined by a Malvern Mastersizer 2000 laser diffraction analyser (Malvern Instruments Ltd., Malvern, UK) in dry method with a Scirocco dry powder feeder, using air as the dispersion agent in the case of Gly samples. CIL was investigated with wet analysis using the Hydro S dispersion unit (capacity 100–150 mL), and the samples were dispersed in purified water which was saturated with CIL with a brief period (3 min) of sonication, and 0.02 mL Polysorbate 80 was added to the solution in order to avoid the reagglomeration of the particles. In both cases measuring range of 0.02–2000 μm was defined. Two repeated measurements were performed on each sample and the mean value was calculated. The tables with the results contain d (0.5), the diameter where half of the population lies below; and D [4,3], the mean diameter over the volume.

4.2.3.2. Identification of polymorphism

X-ray powder diffractometry

Crystal structures were identified by XRPD, the experiments were performed with a Bruker D8 Advance diffractometer (Bruker AXS GmbH, Karlsruhe, Germany). Scattered intensities were measured with a Våntec-1 line detector, symmetrical reflection mode with Cu Kα radiation (λ = 1.5406 Å), and Göbel Mirror bent gradient multilayer optics were used. Relevant measurement conditions were as follows: angular range, from 3° to 40° in steps of 0.01°; target, Cu; filter, Ni; voltage, 40 kV; current, 40 mA; measuring time, 0.1 s/steps. The diffraction patterns of the crystallized samples were compared with those of the structures available in the Cambridge Structural Database (Cambridge Crystallographic Data Centre, Cambridge, UK).

Differential scanning calorimetry

A Mettler Toledo DSC 821^e thermal analysis system, equipped with the STAR^e software version 9.30 (Mettler-Toledo AG, Greifensee, Switzerland) was applied for the determination of melting points of the samples. The measuring parameters were as follows: 10 °C min^{-1} linear heating rate, argon as carrier gas (100 mL min^{-1}), 2–5 mg sample weight, and 25–300 °C temperature interval. A sealed 40-µL aluminium crucible with three leaks in the lid was used for the measurements.

4.2.3.3. Flowability properties

The device was generously provided by Gedeon Richter Plc., Budapest, Hungary for our research work. A Brookfield Powder Flow Tester (PFT230, Brookfield Engineering Labs, Inc., Middleboro, USA) equipped with Powder Flow Pro software (Powder Flow Pro V1.3 Build 23, Brookfield Engineering Labs, Inc., Middleboro, USA) for automated instrument control and data acquisition, was used to measure the Gly samples with the running of standard Flow Function Test. The products were scooped into the trough (230 cc, 6-inch diameter) and the scraping tool was used to evenly distribute the powder and form the sample. Lid Type: Vane Lid, 304 s/s, 33 cc, and 6-inch diameter.

4.2.3.4. Determination of wettability by contact angle measurement

Contact angle measurements were conducted under ambient conditions with a DataPhysics Contact Angle System OCA 20 (DataPhysics Instruments, Filderstadt, Germany). CIL compacted pastilles were produced with a manual hydraulic press (Specac Ltd., Orpington, UK). 150 mg CIL powder was filled into the 13-mm die and compressed to tablets at a compression

force of 0.5 ton with a dwell time of 30 s. The sessile drop method was used to determine the contact angle: 5.2 µl of purified water was placed on a compact. The contact angle was measured immediately after the drop reached a quasiequilibrium shape. Triplicate determinations were carried out for each compact.

4.2.3.5. Residual solvent quantity

Glycine samples

The residual solvent content was analysed by a headspace gas chromatographic method using a Varian CP-3800 gas chromatograph (Varian, Walnut Creek, CA, USA) with a DB-624 capillary column (60 m · 0.25 mm · 1.4 mm, nominal) equipped with a Tekmar Dohrmann 7000 headspace autosampler and a flame ionization detector. The conditions for the GC analysis were optimized for quantitative determination of ethanol.

Cilostazol samples

Residual solvent content was measured by a hGC method using a Perkin Elmer Clarus Gas Chromatograph with a DB-624 capillary column (30 m · 0.32 mm · 1.8 µm, nominal) equipped with a Turbomatrix 110 headspace autosampler and a flame ionization detector. The conditions were optimized for DMF concentration determination.

4.2.3.6. Analysis of residual additive content

Qualitative determination of the additive content

SEM (Hitachi S-4700 cold field emission microscope type II) with EDS (Röntec XFlash energy dispersive X-ray spectrometer, Berlin, Germany) was used to examine the topology, the composition, and the elemental map of the samples. The resolution limit of this unit was 1.5 nm; the rate of magnification was 2500 x. The samples were made conductive by sputter-coating, producing an approximately 3-nm gold-palladium surface layer to avoid charging effects (Bio-Rad SC 502, VG Microtech, Uckfield, UK).

Quantitative determination of the additive content

Determination of the KCl concentration of the samples was performed by FAAS. A Perkin Elmer 4100 ZL (Überlingen, Germany) flame atomic absorption spectrometer equipped with a deuterium background correction system and an air-acetylene burner was used for the determination of the potassium content. The conventional working parameters for the instrument were as follows: a wavelength of 766.5 nm, a spectral bandwidth of 0.7 nm, an acetylene flow rate of 2.5 L min^{-1}, and a nebulizer flow rate of 8.0 mL min^{-1}. The concentration of the standard

potassium stock solution was 1000 ppm (Acidum-2 Ltd., Debrecen, Hungary); the calibration series were made using a 0.2 M HNO_3 solution and the stock solution in various quantities. The sample solutions were also prepared using the 0.2 M HNO_3 solution.

4.2.3.7. Investigation of dissolution rate

The dissolution rate of the CIL samples was examined by a Ph. Eur. dissolution apparatus with a modified paddle method (Type PTW II, PharmaTest Apparatebau AG, Hainburg, Germany), using 11.11 mg of pure CIL powder, which corresponds to the dose of the product on the market, in 100 mL of SGF at a pH value of 1.2 ± 0.1. The suspension was agitated at 100 rpm and sampling was performed up to 120 min (sample volume 5.0 mL). Aliquots were withdrawn at 5, 10, 15, 30, 60, 90, 120 min, and immediately filtered through 0.2-μm cellulose filters (Phenomenex Syringe filters). At each sampling time, an equal volume of fresh medium was added, and the correction for the cumulative dilution was calculated. Each experiment was run in triplicate. After filtration and dilution, the API contents of the samples were determined UV-spectrophotometrically (λ_{SGF} = 260 nm).

4.2.4. Factorial design and statistical analysis

The IJ experiments were implemented by a 3^2 full factorial design to identify the relevant factors which affect the solid state properties of the crystallized product. Different crystallization parameters were investigated, i.a. linear velocity, post-mixing time, temperature difference on independent variables, i.e. on roundness, d (0.5), D [4,3], percentage yield or dissolution rate. The experiments were performed in a randomized sequence. The following equation describing the interactions of the factors was used to determine the response surface and the relative effects of each factor investigated (b):

$$y = b_0 + b_1x_1 + b_2x_2 + b_3x_1^2 + b_4x_2^2 + b_5x_1x_2$$

Statistica for Windows 12 AGA software (StatSoft Inc., Tulsa, USA) was used for these calculations. The confidence interval was chosen to be 95%, i.e. the differences were regarded as significant at $p < 0.05$.

Significant differences between the conventional and the IJ methods were also discovered in terms of the mean particle size (d (0.5)) and roundness. GraphPad Prism 5 Portable statistical software (GraphPad Software Inc., La Jolla, CA, USA) was applied for the statistical analysis by means of an unpaired t-test.

4. RESULTS AND DISCUSSION

4.1. Glycine particle size reduction

4.1.1. Solubility of glycine

The solubility of Gly was measured in water-ethanol mixtures, so was in the pure solvents at ambient conditions in order to identify the saturated concentration in water and determine the optimal solvent-antisolvent ratio which occurs in the crystallization reactor after feeding of the solutions. The low solubility of Gly in that mixture prevents the dissolution of small crystals and improve the yield. Figure 4 shows that in the case of 1:2 ratio of water:ethanol the solubility is decreased appreciably and further increasing of ethanol quantity is not reasonable. It is worth to take into consideration the ratio of 1:1, because solubility of Gly is even low, and the lower ethanol concentration favors the presence of the more stable α polymorphic form. Therefore, 1:2 or 1:1 ratio can be chosen for the experiments to ensure high productivity and percentage yield during crystallization.

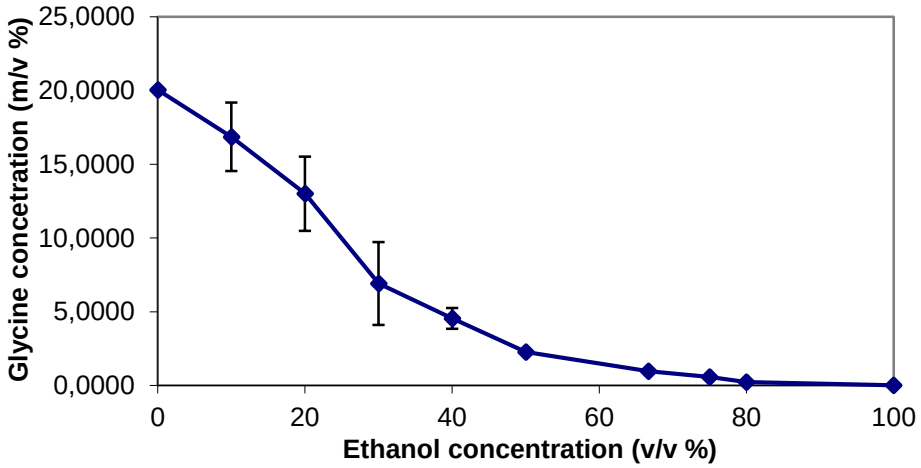

Figure 4 *Glycine solubility in water-ethanol mixture.*

4.1.2. Factorial design

The IJ experiments were accomplished in two series and laid out by a 3^2 full factorial design. In the case of series A the influence of the linear velocity (1.41; 2.77; 4.06 m s^{-1}) and the post-mixing time (0; 5; 10 min) in three different levels, and in series B the influence of the temperature difference (0; 12.5; 25 °C) and the post-mixing time (0; 5; 10 min) were investigated on three operational parameters: roundness, d (0.5) and D [4,3].

4.1.3. Crystal habit of the crystallized products

In series A, 1:1 water:ethanol solvent ratio was applied and remarkable particle size reduction was experienced compared to the initial material. One of the investigated dependent variables had inverse effect: increase of the post-mixing time improved the roundness, but increased the particle size of the product, which was in contrast with the announced goal. The average particle size increased to a greater extent particularly at a post-mixing time of 10 min. As the crystallization parameters had opposite effects on the particle size and roundness, it was favourable to apply a post-mixing time reduction. In series B, the solvent ratio was modified to 1:2 water:ethanol ratio. However, neither the temperature difference nor the post-mixing time influenced the particle size or roundness of the crystallized products significantly, but each individual parameter setting resulted in significantly smaller particles as compared with series A. The percentage yield in series B was higher due to the lower solubility of glycine in the 1:2 solvent–antisolvent mixture. The filterability of all the crystallized products was satisfactory.

Figure 5 *SEM images of the initial glycine (A); product of series A (B); product of series B (C).*

In Figure 5 the differences in crystal size and morphological parameters are demonstrated. The original glycine contained large isodimensional crystals with a smooth surface. By contrast, the products with the smallest average particles in the two crystallization series consisted of small, irregular-shaped, needle-form crystals with a smooth surface and poorer roundness. The crystallized products exhibited a slight tendency to aggregate due to the small particle size, but this did not cause any problem for the laser diffraction particle size analysis measurements and allowed the application of the dry method.

The results of particle size and shape for the two series are presented in Table 1 and Table 2. Each assay was repeated three times; the Tables show the average results of roundness, d (0.5), D [4,3] and percentage yield.

Table 1 *IJ crystallization results for series A [57].*

Sample	Linear velocity ($m\ s^{-1}$)	Post-mixing time (min)	Roundness	d (0.5)	D [4,3]
A1	1.41	0	2.977	15.792	21.497
A2	1.41	5	2.292	15.808	20.295
A3	1.41	10	2.089	31.222	37.498
A4	2.77	0	2.715	16.770	22.530
A5	2.77	5	2.251	26.057	31.610
A6	2.77	10	2.033	34.285	40.650
A7	4.06	0	2.116	14.029	17.175
A8	4.06	5	2.363	13.778	17.784
A9	4.06	10	1.961	31.948	38.076

Table 2 *IJ crystallization results for series B [57].*

Sample	Temperature difference (°C)	Post-mixing time (min)	Roundness	d (0.5)	D [4,3]
B1	0	0	1.825	10.142	13.329
B2	0	5	2.429	9.249	11.241
B3	0	10	2.935	9.368	11.563
B4	12.5	0	2.851	8.335	10.889
B5	12.5	5	2.186	8.524	10.803
B6	12.5	10	2.292	9.664	12.662
B7	25	0	2.071	8.575	11.599
B8	25	5	2.166	10.204	13.849
B9	25	10	2.513	8.835	11.636

4.1.4. Polymorphism of the crystallized products

4.1.4.1. XRPD analysis of the crystallized products

The polymorphism of the initial material and the products was examined with XRPD and compared with the structures in the CSD (Figure 6). It was found that both the initial material and the series A products consisted of the pure stable α-polymorph. In contrast, the series B products contained mostly the less stable β-polymorph, and a small amount of the α-polymorph. According to the literature data [85; 86], the appearance of the β-polymorph is caused by the higher concentration of ethanol in the crystallization process. While the 1:1 solvent–antisolvent ratio favoured the formation of the stable α-form, the 1:2 ratio resulted in the appearance of the less stable β-polymorph.

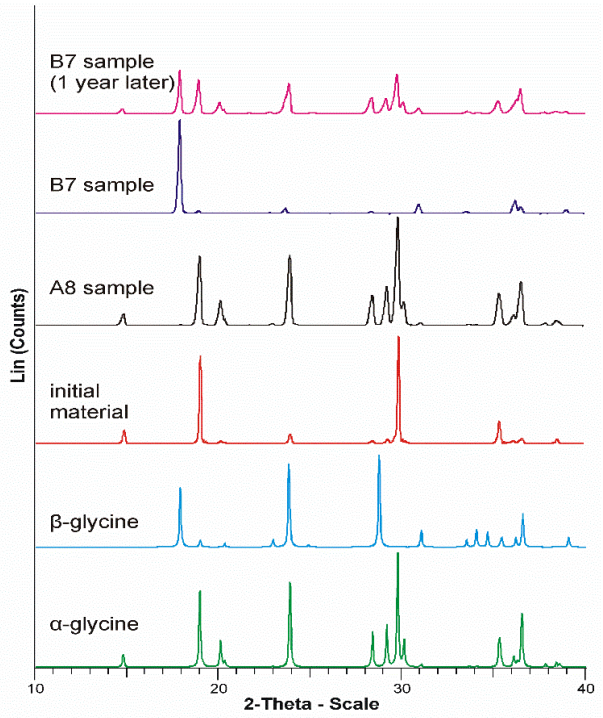

Figure 6 *XRPD diffractograms of the α- and β-glycine, and IJ crystallized products with the most appropriate morphology in series A and B after preparation and after one year of storage.*

4.1.4.2. Determination of the transformation of the polymorphic forms

Transformation of the β-form into the α-polymorph began during storage. The exact characterization of polymorphic alteration and the ability to monitor the effect of process parameters are crucial, therefore a novel XRPD calibration approach was developed for the monitoring of this phenomenon in the case of glycine.

The procedure of the pure β-form production based on the literature data [87] and was optimized for higher productivity in our laboratory. Powder mixtures of various compositions (0 + 100, 10 + 90, 20 + 80 Form α + Form β, and so on) were prepared from the two polymorphs and the calibration curve was recorded. The calibration curve based on the characteristic peak area of the α-form (peaks at 29.225, 29.827 and 30.172 2θ) was as follows:

$$y\ (\alpha\text{-form}\ \%) = -1.7465 \times (\text{net area}) + 158.25\ (R^2 = 0.991).$$

It was specified that the initial β-form content of the series B samples was between 72 and 96%. After 1 year of storage under normal conditions, the β-form content had decreased to 13–17%. The series A products did not change during this storage period. It was found that the 1:1 solvent ratio used in the crystallization processes was critical for the formation of the stable polymorphic form.

4.1.4.3. DSC results of the crystallized products

DSC studies confirmed the results of the powder X-ray analysis. The thermograms of the initial material and the series A products contained one endothermic peak at about 257 °C, which corresponds to the melting point of the α-form. In contrast, the thermograms of the series B samples displayed two endothermic peaks. The lower-temperature peak corresponded to the melting point of the β-form, while the second peak was caused by the melting of the α-form. It was not possible to specify the proportion of the polymorphs because the two endothermic peaks overlapped. After storage for one year, the thermograms of the series B samples were similar to the previously recorded ones. It has been reported that the phase transition of the γ-form to the α-polymorph causes a small endothermic peak at about 179 °C [35]. Our results indicated that our samples did not contain any γ-form (see Figure 7).

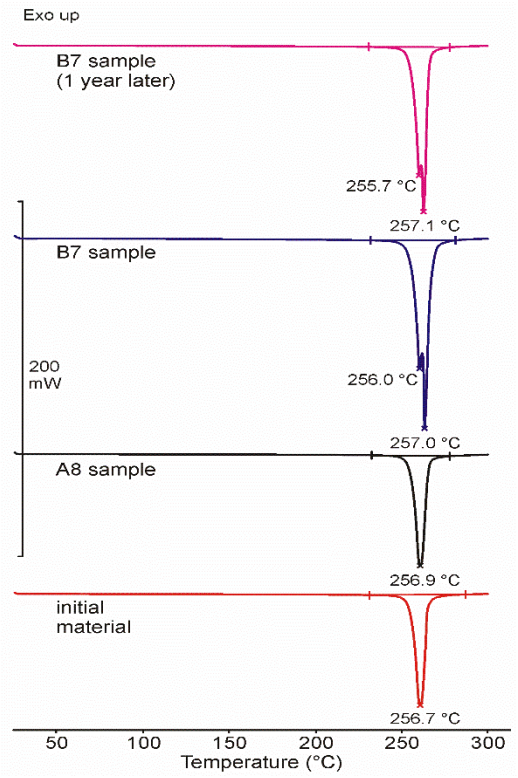

Figure 7 *DSC thermograms of the initial material and the IJ crystallized products in series A and B.*

4.1.5. Residual solvent quantity

The growth of the crystals during IJ crystallization is fast, due to the homogeneous and high degree of supersaturation. Therefore, there is a high risk for the occurrence of solvent (antisolvent) inclusions in the crystals that is associated with such an extremely rapid

crystallization technique. Ethanol (used as antisolvent) belongs in the ICH Q3C(R7) Guideline Class 3 group, where the residual solvent concentration is at most 5000 ppm, and it was therefore necessary to determine its concentration in the crystallized products [100]. The residual solvent contents of the crystallized samples were determined by hGC. Our results indicated that the ethanol content of the initial sample was less than the limit of quantification, and it was therefore assumed that ethanol was not used in the preparation of this material. The maximum residual solvent content of the series A samples was 9 ppm, while the samples in series B contained a maximum 145 ppm of ethanol. The measured residual solvent content of the samples was low relative to the maximum values prescribed in the ICH requirements, which demonstrated the applicability of the IJ method in the antisolvent crystallization of glycine despite the extremely rapid nucleation.

4.1.6. Effects of dependent variables

Statistical analysis of the results relating to the effects of the crystallization parameters on the roundness and particle size are presented in Table 3, where the statistically significant factors are underlined. In the case of series A, only the post-mixing time exhibited a significant linear relationship with the changes in roundness, d (0.5) and D [4,3] results (the response surface R^2 results were 0.858, 0.937 and 0.943, respectively). Neither the linear nor the quadratic relationship of the linear velocity and the interaction effect of the two independent variables displayed a significant effect on the change in these dependent variables. An increase of the post-mixing time increased the average particle size, but reduced the roundness, and the post-mixing time therefore had to be reduced to achieve the desired small particles. We assume that an increase of the linear velocity would cause a further particle size reduction, but the pump capacity was limited, so that the velocity could not be increased as compared with the original parameters described in the crystallization studies. Surface plot diagrams were also taken for demonstration the significant parameters (see Figure 8). The investigated parameters did not cause significant changes in the particle size and roundness in series B.

Table 3 *Factorial design results (series A) [57].*

Dependent variable	Polynomial function	R^2
roundness	$y = 2.32 - 0.31x_1 - \underline{0.58x_2} + 0.04x_1^2 - 0.01x_2^2 + 0.37x_1x_2$	0.858
d (0.5)	$y = 22.19 - 1.02x_1 + \underline{16.94x_2} + 5.29x_1^2 - 5.46x_2^2 + 1.25x_1x_2$	0.937
D [4,3]	$y = 27.47 - 2.09x_1 + \underline{18.32x_2} + 6.24x_1^2 - 6.34x_2^2 + 2.45x_1x_2$	0.943

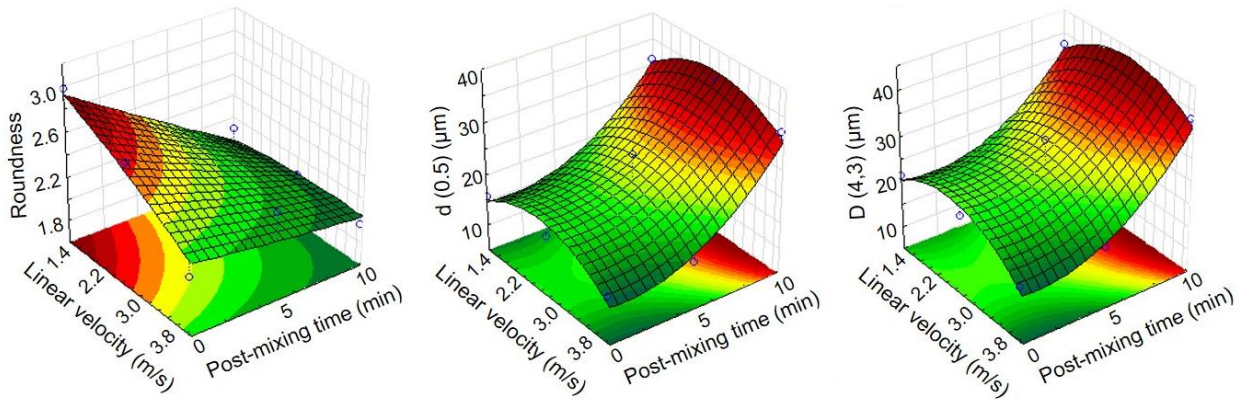

Figure 8 *Surface plot diagrams of the series A products, investigating the effect of mixing time and liner velocity on average size (d (0.5) and D [4,3]), and roundness.*

4.1.7. Comparison with conventional crystallization methods

The application of the IJ crystallization technique resulted in significantly smaller particle size as compared with the previously investigated conventional crystallization methods. The parallel crystallization processes with the same parameters produced the same particle size distribution, which confirmed the reproducibility of the methods.

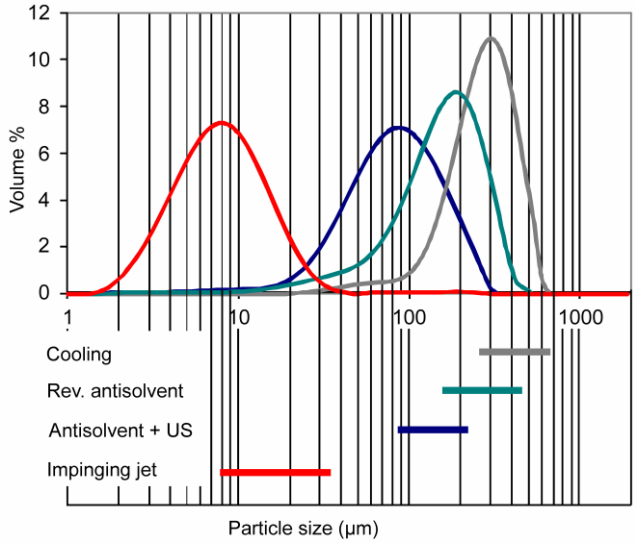

Figure 9 *Particle size distribution and average particle size range produced by different crystallization methods (top: particle size distribution of the product with the smallest average particle size achieved with the given method; bottom: average particle size ranges (d (0.5)) attained with the given method).*

Figure 9 illustrates the particle size distributions of the products with the smallest particles and the average particle size ranges produced by IJ crystallization and the previously investigated crystallization methods [47]. The largest particles were achieved by conventional cooling

crystallization. The reverse antisolvent and antisolvent methods with the application of ultrasound were also able to achieve slight reductions in the average particle size of glycine. The IJ technology resulted in a further one order of magnitude reduction in particle size [57].

4.1.8. Conclusion

Application of the self-developed IJ method in antisolvent crystallization led to a reproducible decrease in the average particle size of glycine with suitable low residual solvent quantity. The average particle size was an order of magnitude smaller (d (0.5) = 8–35 μm) as compared with the results of several other crystallization methods (cooling, reverse antisolvent and antisolvent crystallization with the application of ultrasound, where d (0.5) was between 82 and 680 μm. Production of the stable polymorphic form required the application of a 1:1 water–ethanol ratio. The IJ crystallization method has proved to be a good tool for optimizing and controlling the nucleation and crystallization of organic materials such as glycine.

However, the IJ method resulted in needle-shaped crystals which is considered as an unfavourable shape, therefore improvement of the roundness is necessary with further optimization of process parameters [57].

4.2. Optimization of glycine crystal habit with the use of additive

Based on thorough literature search it was found that inorganic salts are capable to modify glycine crystal habit in the case of long-lasting crystallization methods, like slow evaporation or cooling crystallization [43–45]. In the course of these methods high concentration of additives was applied to reach the desired effect on crystal habit. Their efficacy concerning either fast crystallization methods or low concentration levels (below 1000 ppm) has not been detected so far.

4.2.1. Selection of additives

First of all, the impact of inorganic salts on glycine solubility was determined, in order to keep later on the proper saturated level during the feeding of the API solution. Solubility of glycine varied due to the usage of different concentrations and types of additives. The presence of an additive increased the solubility of glycine from 0.20 g ml^{-1} to 0.24 g ml^{-1}, but the higher concentration of both NaCl and KCl increased the solubility with just a small amount compared with the lower concentrations. Furthermore, solubility of KCl and NaCl was measured in the

mixtures of different ratio of water:ethanol, to determine their optimal concentration for IJ experiments. For the first time, those maximum additive concentrations were selected, which can ensure that the additive still remains in solution in the ratio of 1:1 of water:ethanol, thus the quantity of the crystallized additive is minimized in the bulk solution.

NaCl was applied in 5000-15000 ppm concentration as additive in the case of glycine IJ crystallization and it resulted in mainly needle and irregular shaped crystals, in addition the high additive content caused the appearance of other polymorphic form as well. Based on these, NaCl was not included in our further investigations with the IJ device (see Figure 10).

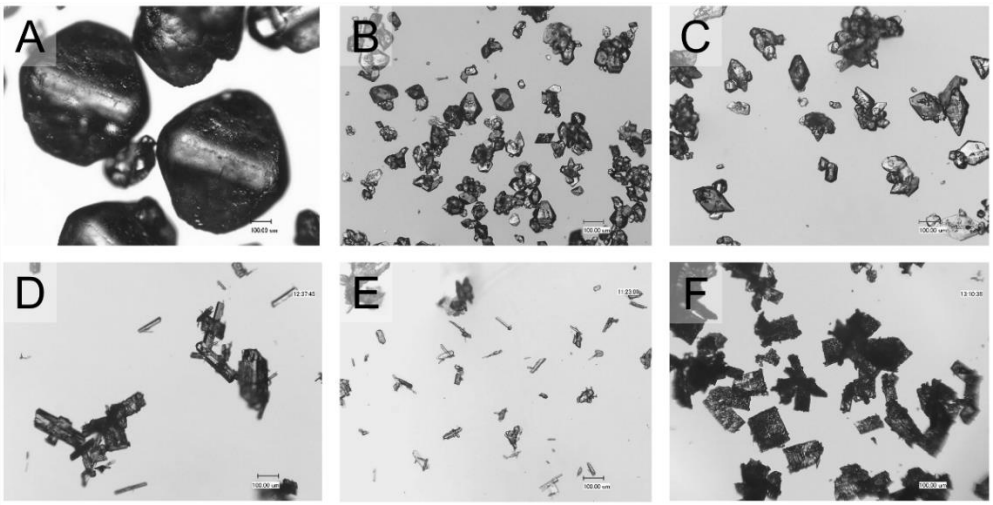

Figure 10 *Light microscopy images of IJ crystallized products with high concentration of additives: A: Initial Gly; B: IJ Gly with 5000 ppm KCl; C: IJ Gly with 8000 ppm KCl; D: IJ Gly with 5000 ppm NaCl; E: IJ Gly with 10000 ppm NaCl; F: IJ Gly with 15000 ppm NaCl*

In our initial pilot research, a high concentration (5000-8000 ppm) of KCl resulted in more appropriate morphology in the case of the IJ method. The lower concentration, 2000 ppm approached our final goal mostly. Thus, in series I, the concentration of additive was decreased, and the concentration range of 1000-2000 ppm of KCl was found to produce the desired effect. In series II, the additive concentration was decreased further with one order of magnitude (100-200 ppm) to find the lowest effective concentration of the additive and to reduce the residual KCl quantity in the products.

4.2.2. *Crystal morphology of IJ products with the use of various concentrations of KCl additive*

The crystallization results for the two series of experiments are presented in Table 4 and Table 5, showing the percentage yield, the average values of roundness, the particle size (d (0.5) and D [4,3]), and the residual potassium content of the products. In series I the applied concentration of KCl improved the crystal roundness, besides particle size reduction was experienced. An increasing post-mixing time was found to adversely affect these properties. The additive concentration of 1000 ppm KCl and 0 min of post-mixing time were demonstrated to yield crystals with the most favourable properties, indicating that a lower concentration of additive contributes to the optimal glycine particle shape and to a lower level of residual impurity in the case of IJ crystallization.

Table 4 *IJ crystallization results in series I [25].*

KCl concentration (ppm)	**Post-mixing time** (min)	**Percentage yield** (m%)	**Roundness** Mean	SD	**Particle size** d (0.5) (μm)	D [4,3] (μm)	**Residual potassium** (ppm)
0	0	52.27	2.36	1.05	37.728	44.959	1
0	5	56.53	2.62	1.36	39.662	46.803	1
0	10	56.81	2.34	0.95	39.082	44.206	1
1000	**0**	**54.55**	**1.86**	**0.63**	**31.929**	**41.233**	**123**
1000	5	60.97	2.03	0.84	34.162	38.606	167
1000	10	61.62	2.25	0.84	36.125	40.441	182
2000	0	51.56	2.16	0.93	36.682	42.789	184
2000	5	61.90	2.09	0.82	37.031	48.429	233
2000	10	61.81	2.20	0.90	40.854	46.361	364

In series II, the additive concentration was decreased sharply. The morphology of the glycine crystals was also found to be modified, even by a small amount of KCl added, in comparison to the samples without additive. This series of experiments clearly demonstrated that using low concentrations of KCl resulted in even better properties of the crystal habit compared to using higher concentrations of the additive. Even 100 ppm of additive appreciably improved the roundness of the crystals. A KCl concentration of 200 ppm and 0 min of post-mixing time were found to yield the smallest particle size and the most favourable roundness.

Table 5 *IJ crystallization results in series II [25].*

KCl concentration (ppm)	**Post-mixing time** (min)	**Percentage yield** (m%)	**Roundness** Mean	SD	**Particle size** d (0.5) (µm)	D [4,3] (µm)	**Residual KCl** (ppm)
0	0	52.27	2.36	1.05	37.728	44.959	1
0	5	56.53	2.62	1.36	39.662	46.803	1
0	10	56.81	2.34	0.95	39.082	44.206	1
100	0	58.48	1.68	0.42	37.814	44.684	33
100	5	58.78	1.65	0.39	33.970	40.311	30
100	10	60.88	1.67	0.48	38.446	43.444	31
200	**0**	**59.58**	**1.63**	**0.41**	**30.877**	**38.443**	**35**
200	5	56.29	1.65	0.36	33.562	39.237	22
200	10	60.78	1.62	0.38	36.083	41.909	48

The laser diffraction analysis of all samples demonstrated a monodisperse PSD. In Figure 11, the PSD diagrams of the most favourable samples of series I and II, and of the sample without additive, are illustrated and compared to each other. Differences in particle size between the samples produced by the different parameters can be recognized.

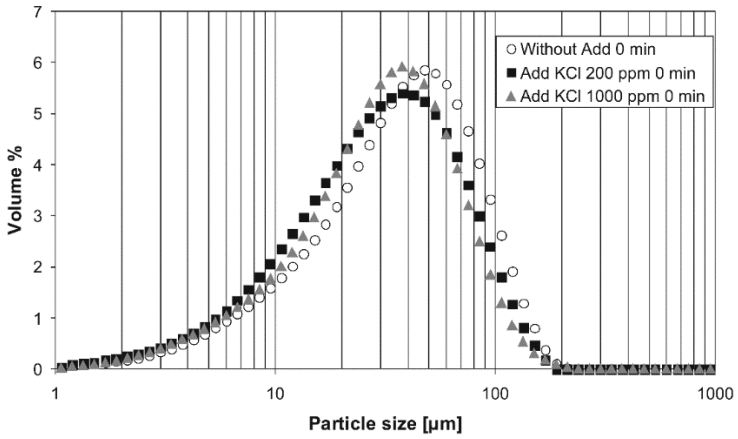

Figure 11 *Particle size distribution of the IJ crystallized products without the use of additive and with the use of additive in series I and II [25].*

The SEM images show the differences in crystal size and morphological parameters of the experimental products. Those crystals with the smallest average particle size and the most favourable roundness are presented in Figure 12. The original glycine contained large isodimensional crystals with a smooth surface. The products yielded by the IJ crystallization process were shown to have a significantly smaller average particle size. The sample without additive consisted of irregularly shaped, needle-like crystals with a smooth surface and poor

roundness, and also exhibited a slight tendency to aggregate. On the other hand, the products crystallized with the KCl additive contained bipyramidal-shaped, small-size, individual crystals with a smooth surface. The crystals produced by using 200 ppm of the additive show the most favourable morphology, as confirmed by the analytical data.

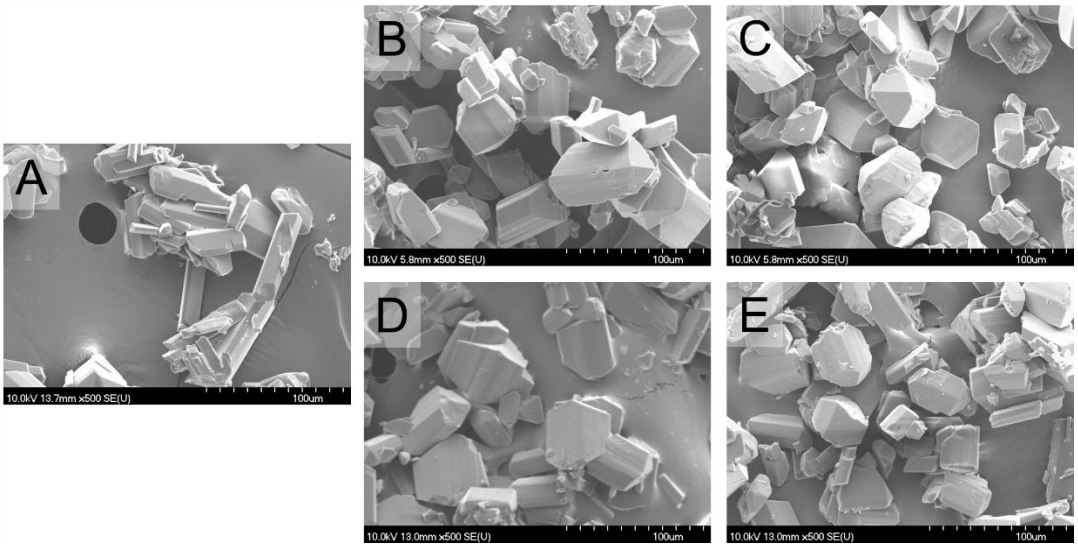

Figure 12 *SEM images of glycine crystals. A: without additive; B: with KCl 1000 ppm; C: with KCl 2000 ppm; D: with KCl 100 ppm; E: with KCl 200 ppm.*

The percentage yield in the two series ranged between 52 and 62 %. An increasing effect of the KCl addition was noticeable for this parameter. The presence of KCl increased the solubility of glycine; therefore, the increased saturation concentration of glycine resulted in a higher supersaturation value in the same water-ethanol mixture. Hence, if a bigger amount of glycine was dissolved, higher supersaturation occurred. This condition is preferred over the higher percentage yield. The supersaturation also influenced the crystal habit; it increased the nucleation rate and was favourable for the smaller particle size, and it also improved the crystal roundness. The optimal supersaturation and KCl concentration were achieved in series II. Besides, the percentage yield also depended on the post-mixing time: with increasing post-mixing time, the yield was also increased. During post-mixing, crystal growth could be considered to increase the percentage yield. Without post-mixing time, the nuclei had no time to grow further, since they were filtered off immediately. The filterability of all the crystallized products was satisfactory in our small-volume system, since the obtained filter cake did not inhibit the removal of the solution and did not decrease the flow rate of the dispersion medium.

4.2.3. Polymorphism

The polymorphism of the initial material and the products was examined immediately after vacuum drying, by both XRPD and DSC, in parallel. The XRPD diffractograms were compared with the structures available in the CSD (Figure 13). Based on the XRPD analysis, both the initial material and all the products were found to contain only the stable α-polymorph.

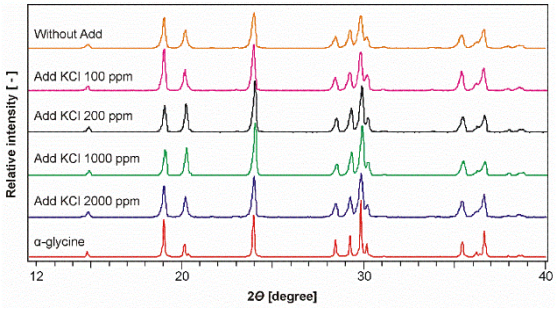

Figure 13 *XRPD diffractograms of the α-glycine and IJ products of series I and II.*

The DSC measurements, however, revealed two polymorphs, as this analytical method is more sensitive to the presence of β-glycine (Figure 14). The thermograms of the original glycine and of the products also contained two endothermic peaks at about 251 and 254 °C. The first peak corresponds to a small amount of the less stable β-form. The second one is the melting point of the α-form. It was not possible to specify the proportion of the polymorphs because the two endothermic peaks overlapped. Based on the literature, a higher additive concentration favours the formation of γ-glycine. The phase transition of the γ-form to the α-polymorph causes a small endothermic peak at about 179 °C. Our results indicate that our samples did not contain any amount of the γ-form, supporting the notion that the low concentrations of KCl applied did not change the crystal structure and the initial α-form was preserved in all the crystallized products.

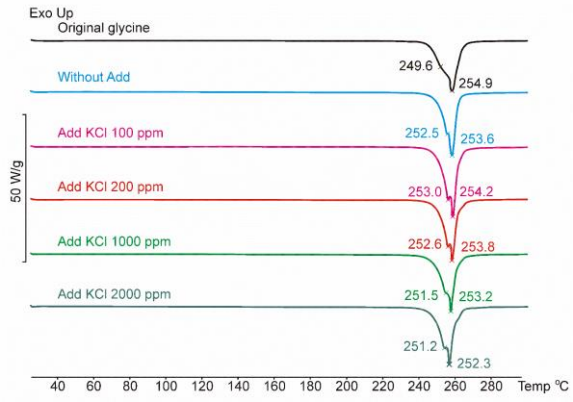

Figure 14 *DSC thermograms of the initial Gly and the IJ crystallized samples in series I and II.*

4.2.4. Residual solvent content

The residual ethanol content of the samples was analysed by hGC. As mentioned above, ethanol belongs to the ICH Q3C(R7) Guideline Class 3, with an upper limit of residual concentration of 5000 ppm [100]. The ethanol contents of the products of series I and II were between 38 and 80 ppm, which is minimal compared to the maximum value defined in the ICH requirements.

4.2.5. Residual potassium content

4.2.5.1. Qualitative analysis of potassium chloride

The arrangement of the residual KCl content within the samples was examined by SEM-EDS. Within the products containing high concentrations (5000 ppm) of the additive, the KCl crystals were found to be arranged separately and individually, as seen in Figure 15 visualizing K and Cl as red and green spots, respectively. In the case of low additive concentrations (100-200 ppm) well-defined separate KCl crystals were not recognized in the SEM-EDS elemental maps; KCl was only found to be adsorbed widespread on the crystal faces all over the sample surfaces. In the case of higher concentrations, those K and Cl ions not able to adsorb to the faces because of their high quantity arranged themselves separately and individually next to the glycine crystals. Based on the literature, KCl prefers to adsorb to the (011) crystal face of glycine and inhibits further incorporation of glycine molecules into the crystal lattice along the “c” direction [44]. Thus, the adsorption of KCl inhibits the lengthwise growth of the crystals: in the case of this rapid crystallization method, the enhancing effect of KCl in the “a” direction is smaller than the inhibiting effect displayed in the c direction, while crystal growth in direction “b” is not affected by KCl. This way, it is possible that the additive also has a decreasing effect on the particle size. During the post-mixing period, the growth in directions “a” and “b” becomes prominent, as the faces have more time to grow without limit. Presumably, the lack of the post-mixing period causes the more favourable roundness [25].

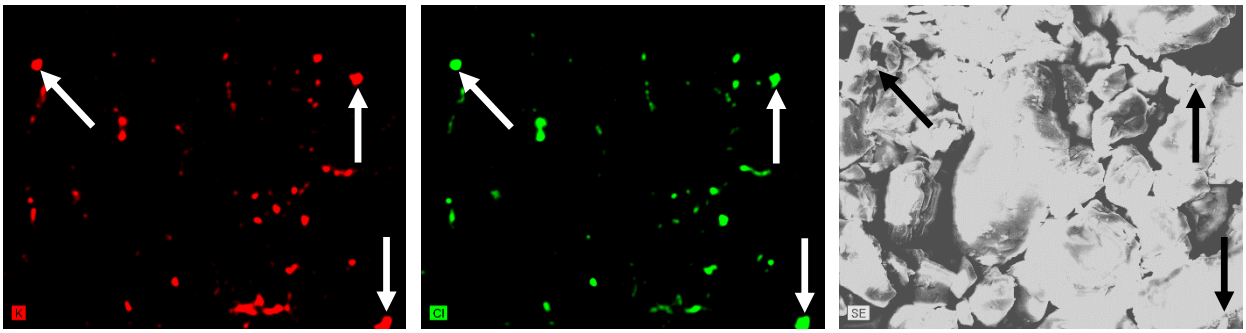

Figure 15 *SEM image and EDS elemental maps of potassium (red spots) and chlorine (green spots) for the arrangement of KCl crystals within the IJ Gly products containing 5000 ppm of additive.*

4.2.5.2. Analysis of residual potassium quantity

The quantitative measurement of the residual potassium content of the products was carried out by FAAS, as this is the most frequently used detector technique for the quantitative determination of this element. It was pointed that the residual KCl quantity in the samples strongly depended on the washing procedure during filtration. Therefore, several compositions of washing solutions and the washing procedures were investigated previously. The optimal circumstances were as follows, the final composition was 1:1 ratio of water:ethanol mixture (20 ml) and after vacuum filtration the washing solution was remained on the filter for 30 sec, and it was repeated twice. That way the residual additive concentration was reduced to the tenth in the samples. The other relevant parameter regarding the residual quantity was the additive concentration in the API solution.

The crystal samples produced by using a higher concentration (1000-2000 ppm) of KCl as additive were found to have a residual potassium content of 123-364 ppm. These values were found to be proportional to the length of the post-mixing time. A longer post-mixing time increased the residual potassium content because a higher amount of KCl was allowed to get adsorbed on the surface of the glycine crystals. The products generated in series II contained by one order of magnitude less potassium (22-48 ppm) compared to those produced in series I [25].

4.2.6. Statistical analysis

The statistical analysis aimed to explore the effects of the crystallization parameters on the roundness and particle size of the crystals, and the results can be seen in Table 6.

Table 6 *Factorial design results (x_1: KCl concentration; x_2: post-mixing time) [25].*

Dependent variable	Polynomial function	r^2
I. Roundness	$y = 2.21 - 0.29\ x_1 + 0.14\ x_2 - 0.25\ x_1^2 + 0.05\ x_2^2 + 0.03\ x_1x_2$	0.74
I. d (0.5)	$y = 37.03 - 0.64\ x_1 \mathbf{+ 3.24\ x_2 - 4.43\ x_1^2} - 0.12\ x_2^2 + 1.41\ x_1x_2$	0.99
I. D [4,3]	$y = 43.76 + 0.54\ x_1 + 0.68\ x_2 \mathbf{- 5.50\ x_1^2} + 1.28\ x_2^2 + 2.16\ x_1x_2$	0.77
II. Roundness	$y = 1.92 \mathbf{- 0.79\ x_1} - 0.03\ x_2 \mathbf{- 0.38\ x_1^2} + 0.08\ x_2^2 - 0.03\ x_1x_2$	0.97
II. d (0.5)	$y = 36.36 \mathbf{- 5.32\ x_1} + 2.40\ x_2 + 0.58\ x_1^2 - 0.94\ x_2^2 + 1.93\ x_1x_2$	0.76
II. D [4,3]	$y = 42.67 \mathbf{- 5.46\ x_1} + 0.49\ x_2 + 0.22\ x_1^2 - 0.82\ x_2^2 + 2.11\ x_1x_2$	0.71

In series I, the KCl concentration was revealed to exhibit a significant quadratic effect on the particle size, while it had no significant effect on the roundness because of outlier data. However, in series II, a tendency between the obtained data and an effect of the x_1 factor was noticeable. The KCl concentration was found to have a significant linear relationship with the changes in roundness, as well as with the d (0.5) and D [4,3] values. Thus, increasing the concentration of the additive within a certain range (0-200 ppm) was shown to improve the roundness and to reduce the average particle size. For all significant effects, $p < 0.036$. In Figure 16, a surface plot diagram demonstrates the significant effects of the investigated parameters.

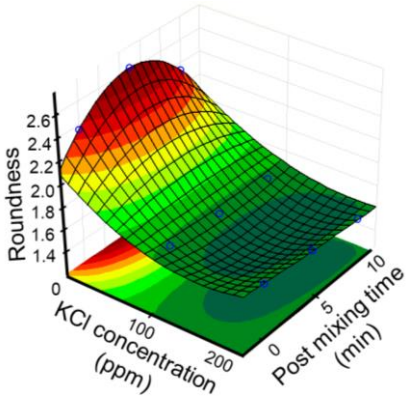

Figure 16 *Surface plot diagram of the series I products, investigating the effect of KCl concentration and mixing time on roundness.*

4.2.7. Conclusion

To our knowledge, the current research is the first example of combining the IJ crystallization method with the application of different concentrations of potassium chloride as an additive to modify the crystal habit of glycine particles. Further aims were to adjust the optimal concentration of the additive and to optimize the crystallization and washing parameters.

Even low concentrations of the additive proved sufficient for an appropriate effect: as little as 100 and 200 ppm of KCl could significantly improve the roundness and reduce the particle size of the glycine crystal products. Based on the 3^2 full factorial design applied to identify the relevant factors affecting the impinging jet-crystallized product, the post-mixing time was demonstrated to be another important process parameter. A KCl concentration of 200 ppm and 0 min of post-mixing time were found to yield the smallest particle size and the most favourable roundness. Residual KCl crystals were found to be arranged separately and individually within the products containing high concentrations of the additive, while those containing low concentrations of the additive were found to have residual KCl adsorbed on the crystal faces all over the sample surfaces. The crystallized product was characterized by low residual solvent and potassium contents. The newly applied jet crystallization method yielded a stable polymorph. Therefore, this study supports the notion that combining IJ crystallization with the application of an additive produces microparticles with the desired crystal morphology when the parameters of crystallization are chosen correctly [25; 41].

4.3. Poorly water-soluble drug, cilostazol particle size reduction

Many researchers have made a great effort to improve the oral bioavailability and systemic absorption of cilostazol with the use of various particle size reduction methods as it was mentioned above [97–99]. However, this is the first study on the application and optimization of the IJ crystallization method in the case of this molecule. In our previous experiments the most influencing crystallization factors were discovered and the process parameters were optimized for our model material, glycine, and these observations were converted to the current experiments and were further devised specifically for the BCS II material, cilostazol.

4.3.1. Solubility of cilostazol

Based on our measurements the solubility of CIL increases in the following order according to the type of solvent: water < ethanol 96 % < methanol < DMSO < acetone < DMF. DMSO resulted in an opalescent solution, and the majority of the solvents dissolved CIL only in a very small amount. At ambient conditions DMF resulted in a clear API solution, the saturated solution concentration was 0.0947 g ml^{-1}, therefore it was chosen as a solvent for CIL crystallization experiments. Furthermore, it was observed that the solubility of CIL depends on temperature, the

lower temperature of the antisolvent resulted in even lower solubility and higher supersaturation value in the same water-DMF mixture.

4.3.2. Crystal morphology

A 3^2 full factorial design series was accomplished in the case of IJ crystallization method. The dependent parameters were selected according to our preliminary results with Gly. The post-mixing time and the temperature difference between antisolvent and solvent influenced mostly the crystal morphology, therefore cooling crystallization was combined with the antisolvent IJ method. The average particle size ((d (0.5)) of CIL was between 3.6-4.8 μm. The increase in post-mixing time made the particle size systematically larger, as well as improving percentage yield, but not affecting roundness appreciably. The higher temperature differences between the saturated API solution and the antisolvent decreased the particle size due to the higher supersaturation which occurred in the water-DMF bulk solution after feeding. The roundness of the particles was between the values of 1.53-1.71, which means a remarkable improvement compared to the original material. IJ CIL-1; 4 and 7 samples revealed the most appropriate crystal habit and it was found that if the temperature difference is 20 °C between the API solution and the antisolvent, and the experiments are carried out without post-mixing, this results the most proper quality.

In order to determine the effectiveness of the developed IJ method in the case of CIL, it was compared with the conventionally and generally applied crystallization methods in the pharmaceutical industry, which are also aimed at particle size reduction. AS and REV methods were implemented with and without the application of US. The parameters of crystallization were similar to the IJ process where relevant (solvents, concentration, temperature, feeding velocity, stirring speed, filtration, washing procedure, etc.). Conventional AS resulted in approximately thrice bigger crystals compared to the impinging results, and roundness deteriorated spectacularly. REV resulted in smaller particles and more favourable roundness compared to AS. With the application of US particle size reduction was attained with both methods. The US parameters were optimized in our previous experiments with the contribution of an outstanding expert of crystallization, *Béla Farkas*, and the most effective cycle time and amplitude were implemented. Among the conventional processes, REV equipped with US resulted in the most appropriate crystal habit. In Table 7 the investigated parameters and the results of the IJ series and conventional methods are summarized.

Table 7 *Operating parameters and the results of the original, the IJ, and the conventionally crystallized CIL products.*

Sample code	Temp. difference (°C)	Post mixing time (min)	US amplitude (ppm)	US cycle time (min)	Percentage yield (m%)	Round-ness Mean	Particle size d (0,5) (µm)	Particle size D [4,3] (µm)
IJ CIL-1	0	0	-	-	79.62	1.56	3.887	5.281
IJ CIL-2	0	5	-	-	81.94	1.57	4.259	5.653
IJ CIL-3	0	10	-	-	87.01	1.58	4.801	6.027
IJ CIL-4	10	0	-	-	79.41	1.63	3.810	5.171
IJ CIL-5	10	5	-	-	85.53	1.67	4.134	5.423
IJ CIL-6	10	10	-	-	86.80	1.71	4.557	6.578
IJ CIL-7	**20**	**0**	**-**	**-**	**75.40**	**1.53**	**3.626**	**5.158**
IJ CIL-8	20	5	-	-	84.05	1.66	3.714	5.200
IJ CIL-9	20	10	-	-	83.63	1.63	3.759	4.824
AS	0	0	0	0	88.70	4.39	14.411	19.218
AS + UH	0	0	70	0.30	90.39	2.95	11.246	15.738
REV	0	0	0	0	55.97	2.36	9.906	12.802
REV + UH	0	0	70	0.30	92.93	2.27	8.028	12.006
Original CIL	0	0	-	-	-	2.08	23.563	60.639

The laser diffraction analysis of all IJ samples revealed monodisperse particle size distribution. The original material and the product of REV combined with US showed polydisperse distribution as can be seen in Figure 17. Overall, based on the results it can be stated that IJ resulted in remarkably smaller average particle size and improved the roundness compared to the initial material and conventional methods, not even with the application of US.

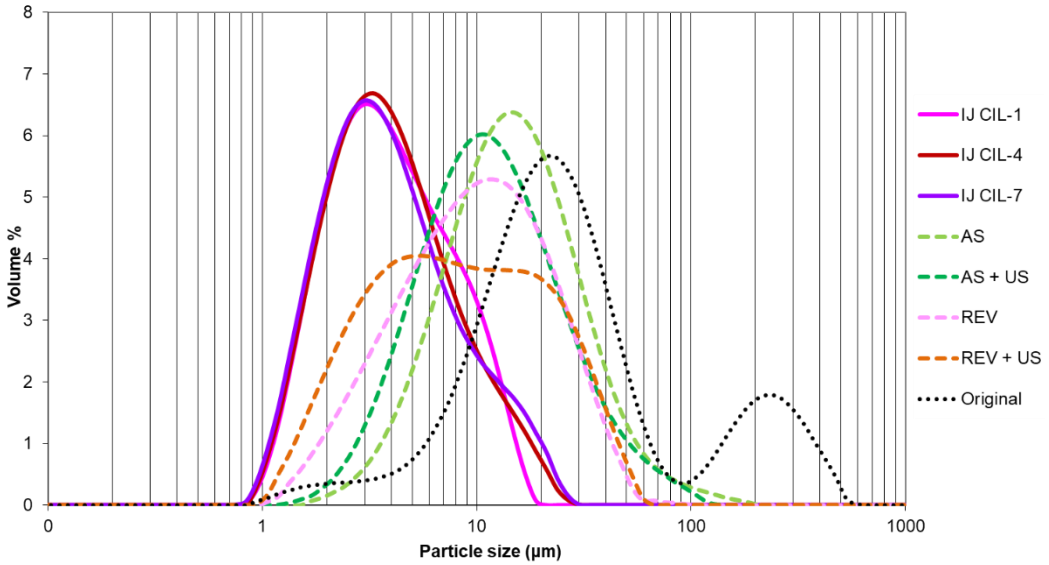

Figure 17 *Comparison of particle size distributions of samples made with different crystallization methods.*

Figure 18 demonstrates the disparities in the appearance and morphology of the obtained crystals produced by different crystallization methods. The original CIL contained large, fragmented crystals with an irregular shape, and small pieces of crystal debris can be observed, which suggests that the material was ground in advance. The conventional crystallization products consisted of bigger-sized, needle-like crystals, and exhibited a slight tendency to aggregate. The effect of US is obviously noticeable, in both cases, AS and REV, the application of US reduced the particle size appreciably, but with a wide PSD. In contrast, the IJ product with the most favourable crystal habit shows significantly smaller average particle size, smooth surface, rounded crystal shape and uniform, individual crystals.

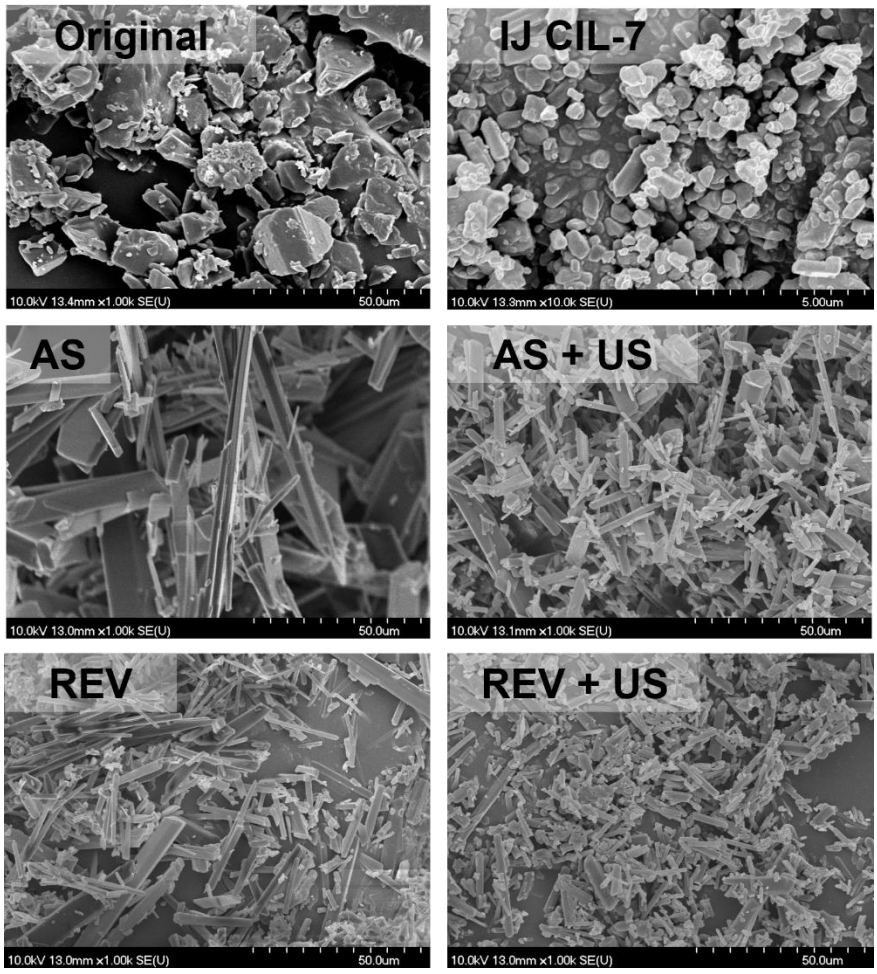

Figure 18 *SEM images of the ground initial CIL crystals (Original), IJ sample with the most appropriate morphology properties (IJ CIL-7) and the products of the different conventional crystallization methods (AS; AS + US; REV; REV+ US).*

4.3.3. Polymorphism

According to the XRPD analysis the initial material contains the orthorhombic A polymorph, which is the most stable form at ambient conditions. The diffractograms of each product were compared with CSD structures. It was found that all kinds of the crystallization methods resulted in the most stable orthorhombic A form, and any other polymorphic forms were not detected (see Figure 19).

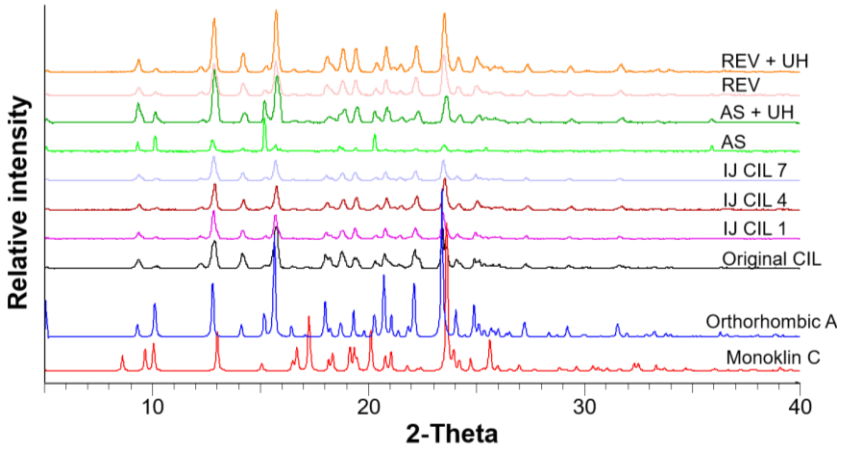

Figure 19 *XRPD diffractograms of the crystallized products with different types of methods.*

In Figure 20 the results by DSC measurements can be seen, which confirm the XRPD results. The thermograms of both the initial CIL and the products contained one endothermic peak at about 160 ºC. Based on the literature, this peak corresponds to the melting point of Form A. Our results indicate that our samples did not contain any of the B- or C-forms, supporting that the crystallization methods applied did not change the crystal structure, and the initial orthorhombic form was preserved in all the crystallized products.

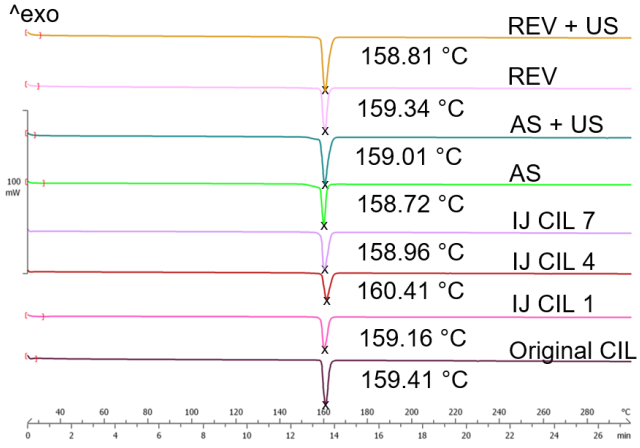

Figure 20 *DSC thermograms of the crystallized products.*

4.3.4. Wettability

Wetting is the first step for a solid oral system to dissolve, in addition, it can influence the disintegration time in the medium. Wettability describes the spreading of a liquid on a surface, which is usually indicated by contact angle. The limits of contact angle are 0° for complete wetting and 180° for no wetting [101; 102]. Table 8 shows our results. IJ products' contact angle was lower compared to the products made with conventional methods, which could be correlated to higher solubility values. The smaller particle size resulted in lower contact angle values in every case at 5 second. Presumably, in the case of the more uniform and individual crystals, the higher porosity of the surface also favoured the infiltration of the water droplet into the deeper layers. Therefore, the pharmaceutical formulation which contains one of the IJ products could reach faster disintegration time and higher dissolution rate.

Table 8 *Contact angle of the crystallized products.*

Time (sec)	Original	AS	AS + US	REV	REV + US	IJ CIL 1	IJ CIL 4	IJ CIL 7
0	72.7	65.0	66.0	64.7	61.8	58.0	61.0	55.7
1	67.8	64.0	64.5	61.8	60.1	56.9	58.6	50.6
2	65.8	63.1	62.3	60.7	58.4	55.4	57.2	49.4
3	64.3	62.5	61.2	59.8	57.0	54.2	55.9	48.4
4	63.0	62.0	60.6	59.1	55.8	53.1	54.4	47.6
5	62.4	61.7	59.9	58.5	54.6	52.1	53.3	46.9
6	61.9	61.3	59.5	57.9	53.4	51.1	52.3	46.2
7	61.6	61.0	59.2	57.2	52.2	50.0	51.1	45.5
8	61.6	60.7	59.0	56.7	51.1	49.3	50.2	44.9
9	60.7	60.4	58.3	56.1	50.0	48.5	49.2	44.3
10	59.7	60.1	57.7	55.6	48.9	47.6	48.3	43.7
11	58.8	59.8	57.1	55.1	47.8	46.8	47.3	43.1
12	57.6	59.5	56.6	54.6	46.8	46.0	46.4	42.6
13	56.6	59.3	56.1	54.1	45.7	45.2	45.5	42.1
14	56.5	59.0	55.6	53.7	44.7	44.4	44.5	41.5
15	56.4	58.7	55.1	53.2	43.7	43.9	43.8	40.9
16	56.1	58.5	54.6	52.6	42.6	43.1	42.8	40.4
17	55.4	58.2	54.2	51.2	41.6	42.4	42.0	39.8
18	54.7	57.9	53.8	50.7	40.6	41.7	41.2	39.3
19	54.0	57.7	53.1	50.3	39.6	41.2	40.4	38.8
20	53.3	57.4	52.7	49.8	38.7	40.4	39.5	38.3
21	52.6	57.2	52.4	48.7	37.7	40.0	38.8	37.7
22	51.9	56.9	51.9	48.4	36.7	39.5	38.1	37.2
23	51.2	56.7	51.5	48.0	35.8	38.8	37.3	36.7
24	50.6	56.4	51.1	47.5	34.9	38.2	36.6	36.2
25	49.9	56.2	50.8	46.4	34.0	37.8	35.9	35.7
26	49.2	55.9	50.2	46.0	33.0	37.2	35.1	35.2
27	48.5	55.6	49.7	45.2	32.2	36.6	34.4	34.7
28	47.8	55.4	49.2	44.8	31.2	36.0	33.6	34.2
29	47.2	55.1	48.9	44.3	30.8	35.6	34.2	33.7
30	46.5	54.9	48.5	43.9	30.0	35.1	33.6	33.2

4.3.5. Dissolution rate

The dissolution profile of the pure CIL products was accomplished by 120-min-range in vitro studies in SGF without enzymes (pH=2±0.1). It can be observed on the dissolution curves of Figure 21 that after 5 min the dissolved CIL varied in a wide range showing the strong influence of particle sizes on the responses. On the dissolution curves at 5 min, a rapid increase of dissolution can be observed in the case of IJ results, which is a typical phenomenon when small particles possess a large surface area. Faster dissolution could be a consequence of the uniform, individual and rounded crystal habit as well, while in the case of the conventional products, the aggregated crystals delayed dissolution. At 120 min, the IJ CIL-7 sample with the smallest particle size led to the highest dissolution quantity. Based on our results, a clear correlation is revealed between the dissolution rate and the particle size; the smaller the particle size, the higher the dissolution rate. If the unique, small particles could remain in the final dosage form as well, the higher dissolved concentration of the API in the initial period of dissolution would improve bioavailability.

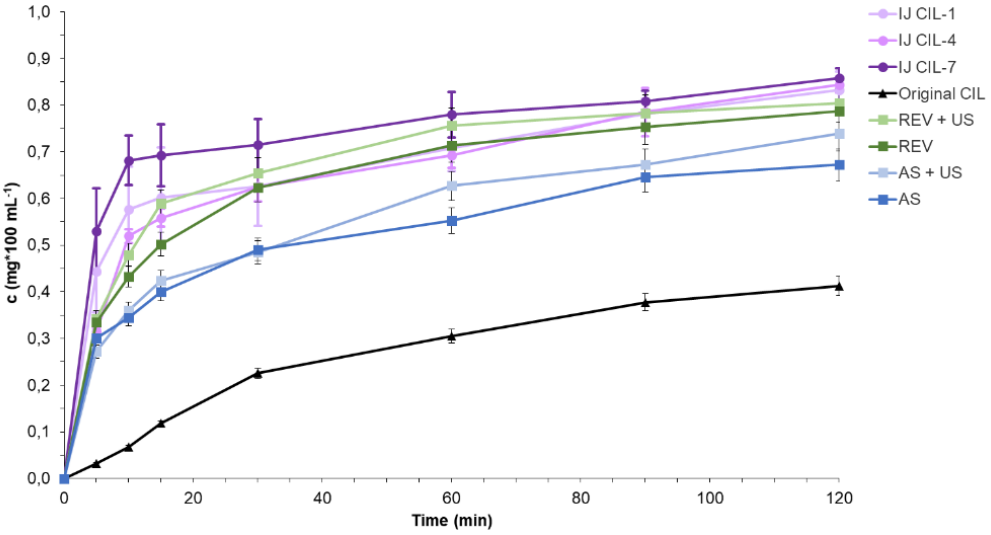

Figure 21 *Dissolution rate of the crystallized CIL products.*

4.3.6. Residual solvent quantity

Residual DMF content of the samples was analysed by hGC. DMF belongs to ICH Q3C(R7) Guideline Class 2, with an upper limit of residual concentration of 880 ppm [100]. These solvents are associated with less severe toxicity compared to Class 1 solvents, but they should be limited in order to protect patients from potential adverse effects. The DMF contents of the products of

IJ were between 4747 ppm and 5455 ppm, which exceeded the limit of the maximum requirement described. In order to reduce the solvent quantity, further development related to washing or other purifier procedure is still necessary. During the filtration step there is a possibility to use higher volumes or various compositions of washing solutions, or keep them on the filter surface for a longer period. The drying process could be accomplished at a higher temperature, and longer time which could also mean another mode for decreasing the residual solvent quantity. These experiments are intended to be performed in the future.

4.3.7. Statistical analysis

On the one hand, the statistical analysis was aimed to explore the effects of the IJ operating circumstances on key process parameters such as, particle size, roundness, percentage yield and dissolution rate. It was found that both the temperature difference and the post-mixing time had significant effect on particle size (d (0.5)), while they had no significant effects on roundness because of outliers in the data. As for the dissolution rate, the temperature difference verified a quadratic significant effect, thus when the temperature difference is higher, it enhances dissolution. Post-mixing time was found to have a significant relationship with the changes of percentage yield values. Therefore, increasing post-mixing time proved to improve yield. For all significant effects $p<0.038$. On the other hand, all of the conventional methods were compared with the IJ results in terms of particle size (d (0.5)) and roundness. Based on the unpaired t-test, the IJ method resulted in a significantly smaller particle size ($p<0.04$) in every case (Figure 22).

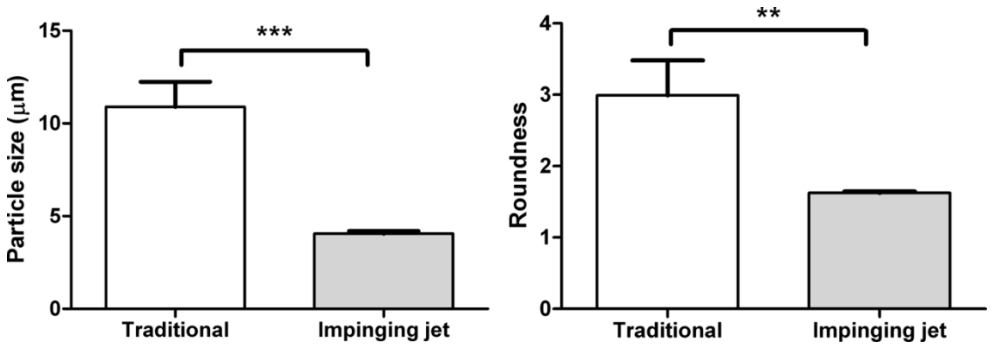

Figure 22 *Statistical comparison of the particle size (d (0.5)) and roundness of the crystallized CIL products.*

4.3.8. Conclusion

It was observed that the self-equipped IJ apparatus is a very effective and reproducible method for reducing the particle size of CIL and to attain a final product with suitable crystal

morphology and a narrow PSD. Post-mixing time and temperature difference are the significant factors in the case of CIL particle size modification. IJ resulted in significantly smaller and more uniform crystals compared to the original ground material, as well as compared to the traditional crystallization methods even with the application of ultrasound. This method resulted in stable orthorhombic polymorphic form (Form A) and enhanced the dissolution rate remarkably. Therefore, the combined cooling and IJ method is a promising approach to optimize the crystal habit, furthermore the practical application of the method in the manufacture is feasible in the case of poorly water-soluble drugs, if the crystallization parameters are chosen prudently.

4.4. Development of a continuous crystallization method with glycine

Based on our previous results in the batch processes the optimal parameters were converted to the novel continuous IJ antisolvent crystallization method with the use of glycine, as a model material at first. The solvent:antisolvent ratio was 1:1, 200 ppm KCl additive was added to the nearly saturated API solution, and feeding of the solutions was performed with linear velocity (4.06 m s^{-1}) at room temperature. Moreover, scale-up was also accomplished as the volume of the solutions was 20 times higher than in batch size. One complete experiment took 20 minutes and it was repeated 3 times. The parallel measurements were set with the same operational parameters to investigate the reproducibility of the method. In-process-monitoring was achieved with sampling in every minute in order to determine the consistency of the quality, as well as monitoring the key process parameters, for instance average particle size and roundness during the whole process [103].

4.4.1. Crystal habit and PSD

According to SEM images, which can be seen in Figure 23, it can be stated that the average particle size and the roundness of the particles are quite consistent independently of the sampling time, so the crystal morphology was not changed remarkably when the first and the last samples were compared with each other. The continuous mode resulted in small, bipyramidal shaped crystals with smooth surface. Due to the fast crystallization method and the lack of post-mixing time the edges and corners of the crystals are not rounded. These properties ensure the occurrence of individual crystals and ease the filtration of the product.

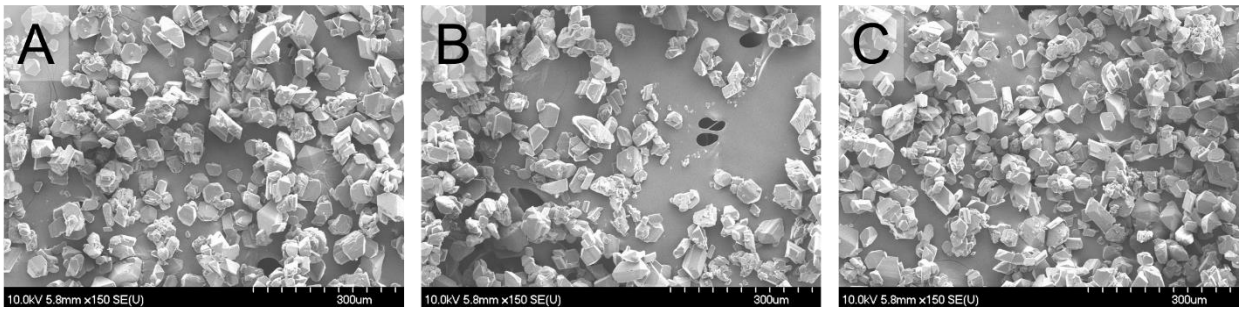

Figure 23 *SEM images of the products of continuous IJ crystallization method in the course of in process monitoring.*
A: sample in minute 1; B: sample in minute 10; C: sample in minute 20.

Based on micrometric data the average particle size (d (0.5) = 25.899 µm-34.313 µm) altered with low SD (2.54) and CV (0.08). This indicates the small variation between the process start and end points, and confirms the visual observations by SEM images. Based on PSD diagrams it can be stated that all of the twenty samples gave monodisperse distribution, and due to the constant circumstances of crystallization the difference between the samples was not remarkable (see Figure 24). The previous IJ batch process resulted in 52-62% percentage yield, which value was increased in the continuous mode to 64-70%. As the whole amount of the suspended crystals was filtered directly on the filtration surface, the material loss between the operating steps, i.e. crystallization and filtration, was eliminated. During the process neither obstruction nor operational difficulty was observed.

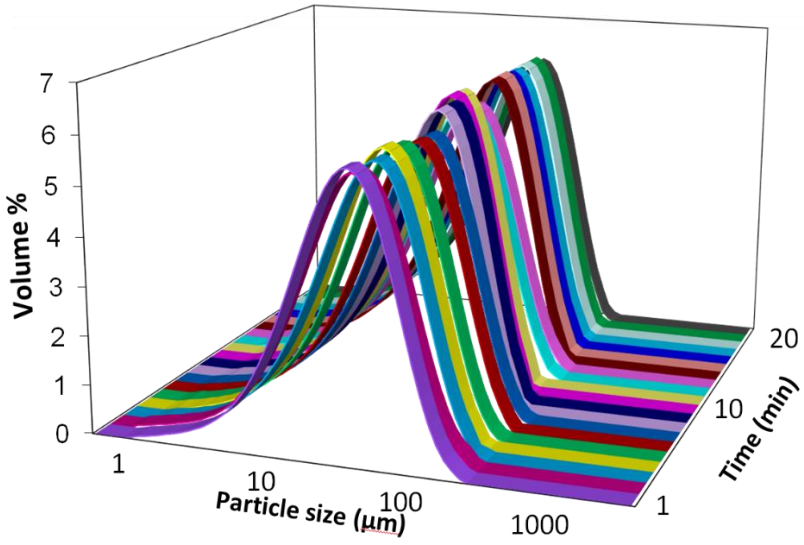

Figure 24 *Particle size distribution of the crystallized products by continuous IJ method [103].*

The average particle size results, such as d (0.5) and D [4,3] of the batch and continuous mode were compared with each other with a statistical software (GraphPad Prism5, GraphPad Software Inc., La Jolla, CA, USA). With the application of the two-sample t-test it was established that there was no significant difference between the batch (29,707-31,967 μm) and continuous mode (25,899-34,313 μm) regarding particle size.

4.4.2. Flowability

Flowability was measured with the use of PFT. The standard classification of powder flowability is based on the standard flow indices, and flow behaviour can be rated as free flowing (10<ff), easy flowing (4<ff<10), cohesive (2<ff<4), very cohesive (1<ff<2), and non-flowing (ff<1) [104]. The flowability of the IJ samples and the initial Gly is shown in Figure 25, at different levels of consolidating stress. The IJ crystallized products from batch process with the use of additive, without additive, as well as the continuous mode with additive are represented here. These results demonstrate that the initial material is a free flowing powder as it was expected from the large isodimensional shape of the particles. The IJ crystallized products without the use of additive contain needle-like crystals as described above, thus its flowability properties concur with this property, and it is generally a cohesive powder which could cause possible problems in the tableting process when the hopper empties. In contrast, both the batch and the continuous IJ products with the use of additives are mostly easy flowing, and their flowability properties are comparable. The use of these products could be suitable for further tableting procedures.

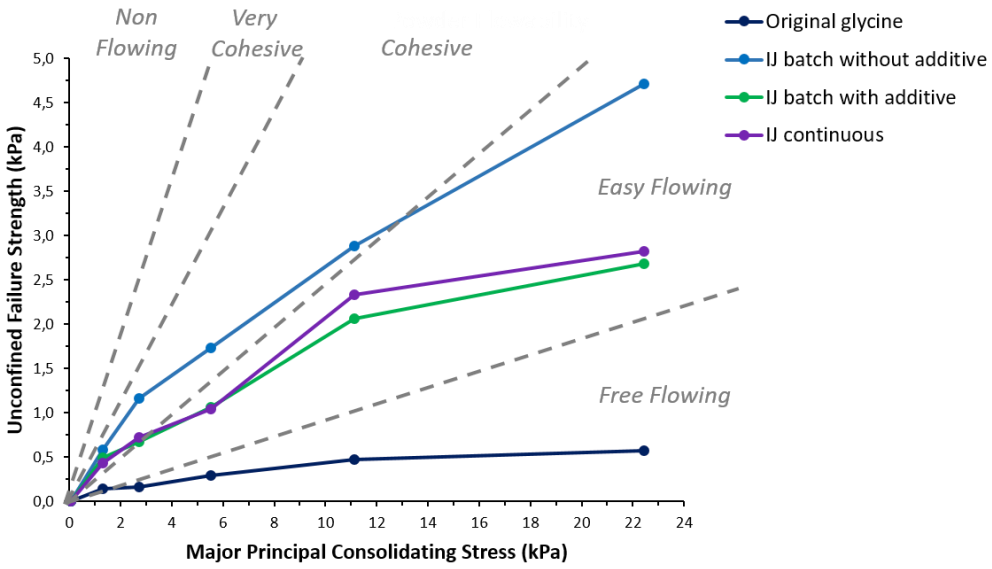

Figure 25 *Comparison of flowability properties of glycine IJ products.*

4.4.3. Polymorphism

XRPD was applied for the analysis of possible crystal structure transformations during the continuous process. The diffractograms were compared to the glycine polymorphic forms available in CSD and were demonstrated in a 3D figure (see Figure 26), because it makes it attainable to follow graphically the potential polymorphic form alterations. According to the XRPD results, all of the samples remained in the same crystal structure, the most common α-glycine, which is identical with the polymorphic form of the initial material.

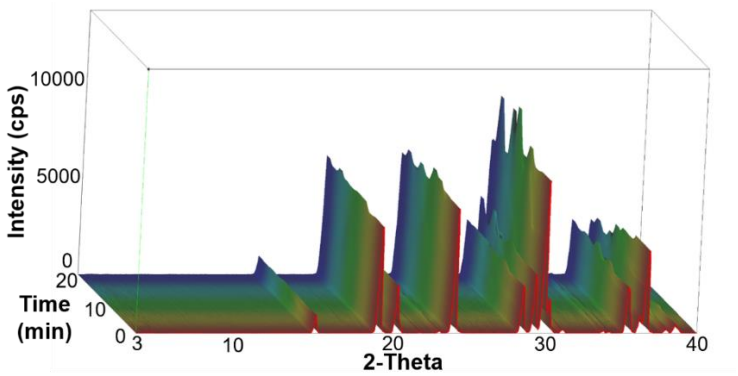

Figure 26 *Three-dimensional XRPD diffractograms of the crystallized glycine samples by IJ continuous method.*

Previous investigations revealed that DSC is already more sensitive to the presence of a small amount (less than 5%) of β-glycine in the Gly samples. On the thermograms the peak at about 254 ºC corresponds to the α-form, and the β-form occurs as an overlapped peak at about 251 ºC. Based on these, we assumed that the initial material contained the unstable β-form and this form can be detected in addition to the stable α-form in the IJ samples. The amount of the unstable form increased slightly from the beginning to the end of the process. This phenomenon might have been caused because of the presence of β-form in the initial material, since it can induce the production of the unstable form (see Figure 27).

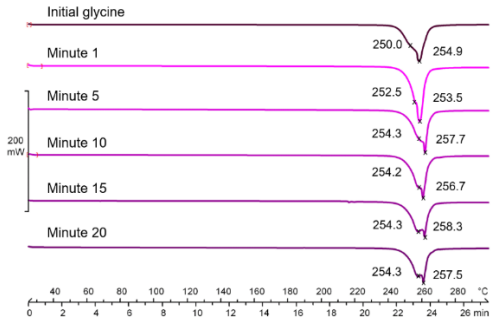

Figure 27 *DSC thermograms of the crystallized products by IJ continuous mode.*

4.4.4. Residual solvent quantity

According to the ICH Q3C (R7) guideline the residual solvent quantity has a maximum limit of 5000 ppm in the case of Group 3 solvents, where EtOH belongs to [100]. Based on our hGC measurements, all of the samples contained less than 100 ppm residual EtOH, which corresponds to the limit described in the guideline. The result of the IJ continuous mode is comparable with the values of the batch process, which means that the optimal batch operating parameters are suitable for the continuous mode regarding this data, and can produce a high quality product.

4.4.5. Residual potassium content

The KCl was used as an additive in our continuous crystallization process, and its concentration as well as the washing procedure of the samples were optimized previously in our batch process in order to minimize the residual quantity as much as possible in the final products. Regarding FAAS results the potassium quantity in all of the samples was less than 62 ppm, which shows a slight increase compared with the results in batch series B, but the difference is not significant.

4.4.6. Conclusion

One of the main purposes of the current work was to develop a robust continuous crystallization method with the use of the self-developed IJ device, and implement those operating parameters from the batch process. This latter can ensure the quality and the consistency of the key process parameters, such as particle size, PSD, roundness and polymorphism, in the case of glycine reproducibly. The percentage yield was increased remarkably compared to the batch process. Based on the results of the sample monitoring, physico-chemical properties of the crystals were consistent during the whole process and were comparable with the batch method results. The average particle size was reduced significantly (31.55 μm) compared to the initial material (680.69 μm) with an appropriate roundness, low residual solvent and potassium quantity. However, a slight alteration in the quantity of β-form was observed between the start and end points due to the presence of the unstable form in the initial material. The flowability values demonstrated that the samples have easy-flowing properties, which predicts good processability during tableting processes [103].

The results show that this scaled-up continuous method is simple and effective to improve the process efficiency, decrease the process time, but maintain the quality of the final product.

4.5. Development of IJ continuous crystallization method with cilostazol

After a successful implementation of IJ batch parameters for the novel IJ continuous method in the case of a model material, Gly, the poorly water-soluble drug, CIL was also tested with the application of the method. The previously optimized crystallization parameters for CIL (IJ CIL-7 factors) were selected for our scaled-up, continuous experiments. The robustness of the device was monitored with the same sampling procedure, every minute. The samples were analysed for the key process parameters, such as particle size, PSD, polymorphism, and dissolution rate.

4.5.1. Crystal morphology

Based on PSD analysis, all of the samples revealed monodisperse distribution from the beginning until the last samples in the end of one process. In Figure 28 the d (0.5) results were summarized. The values represent a very narrow range (d (0.5) = 4.021-5.797 μm) where the average particle size varied, the red lines indicate the smallest and the biggest sizes. The continuous results were comparable with the batch process average particle size results (d (0.5) = 3.6-4.8 μm), and although the values differed slightly, the difference was not significant based on statistical analysis. Compared to the batch process the percentage yield did not increase, it was between 80.19-86.52 %.

During the initial runs, smaller obstructions were observed in the course of our experiments, mainly in the second half of the process, as the bulk solution with the suspended crystals could not pass through the narrow part of the IJ unit. Finally, we came to the conclusion that the upper part of the unit should be closed during the process, thus the pressure can increase inside the unit, and the bulk solution could flow through the unit more easily.

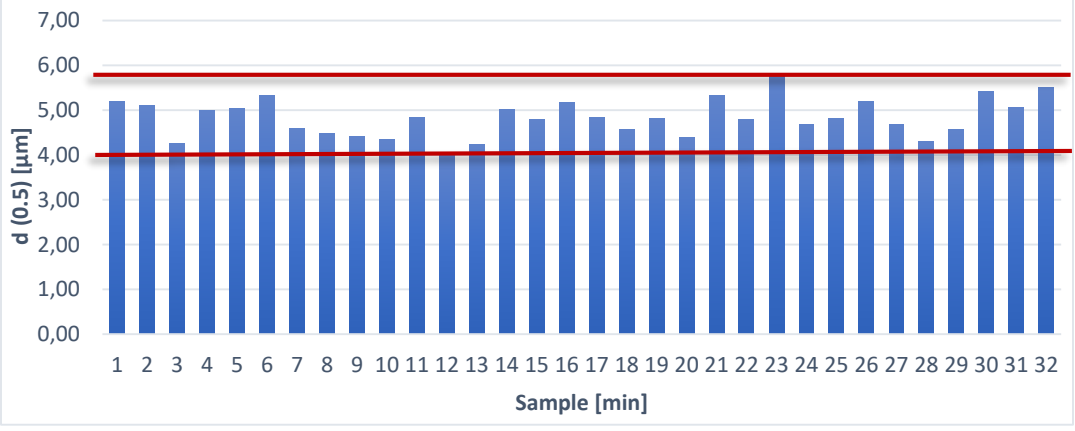

Figure 28 *Average particle size (d (0.5) of the CIL samples made by the IJ continuous method during the whole process.*

4.5.2. Polymorphism

XRPD results can be seen in Figure 29. The two dimensional figure demonstrates expressively the consistency of the CIL crystal structure through the process, as the lines in the figure are fixed and no alteration can be observed. The diffractograms were compared to the CIL polymorphic forms available in CSD and it can be stated that all of the samples contained the most stable polymorphic form, the orthorhombic Form A.

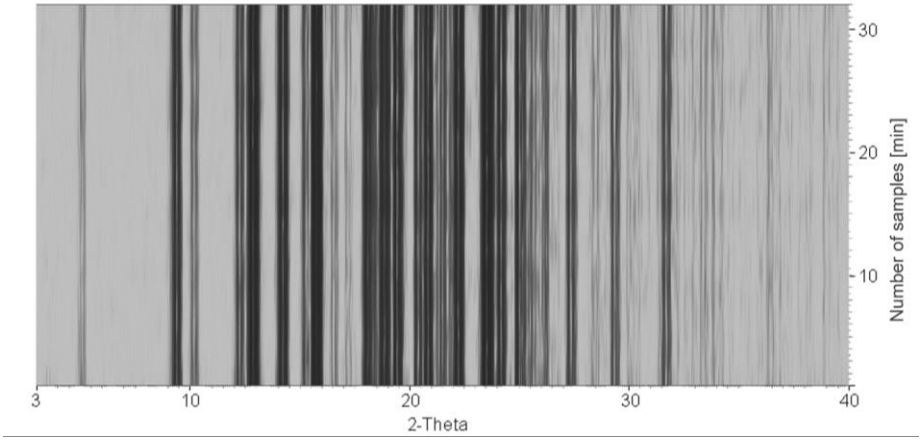

Figure 29 *Two-dimensional XRPD diffractograms of the crystallized CIL samples by IJ continuous method.*

The polymorphic forms of the samples was also determined by DSC (see Figure 30). The thermograms of the CIL samples displayed one endothermic peak at about 160 °C, which corresponded to Form A, confirming the XRPD results. The initial material as well as the batch process products contained the same polymorphic form, the most stable Form A.

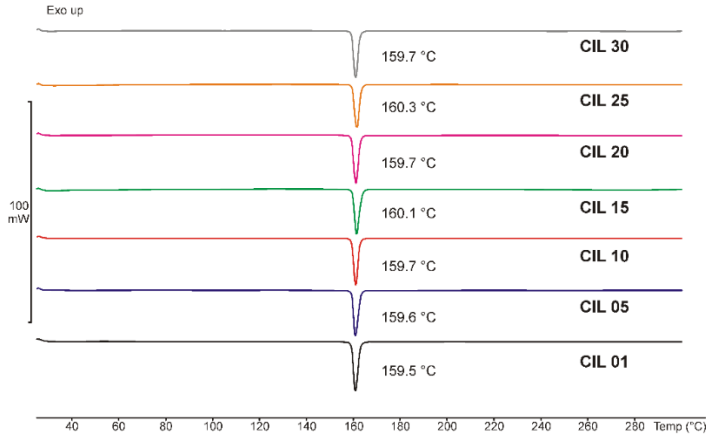

Figure 30 *DSC thermograms of the continuous IJ CIL method products.*

4.5.3. Dissolution rate

The in vitro dissolution rate was determined under the same circumstances as in the batch process, and this way the results could be compared. In Figure 31 the dissolution rate of six pure CIL crystallized materials are shown, sampling from different time points of the continuous process. It can be stated that the dissolution profile was similar to the batch process results in all of the continuous IJ products and the difference between them was also negligible, since the average particle size of the samples varied in a narrow range. At 5 min the dissolution was increased sharply and after 120 min just a slight difference could be detected between the samples. These observations proved that the continuous method was capable of producing the same quality compared with the batch process.

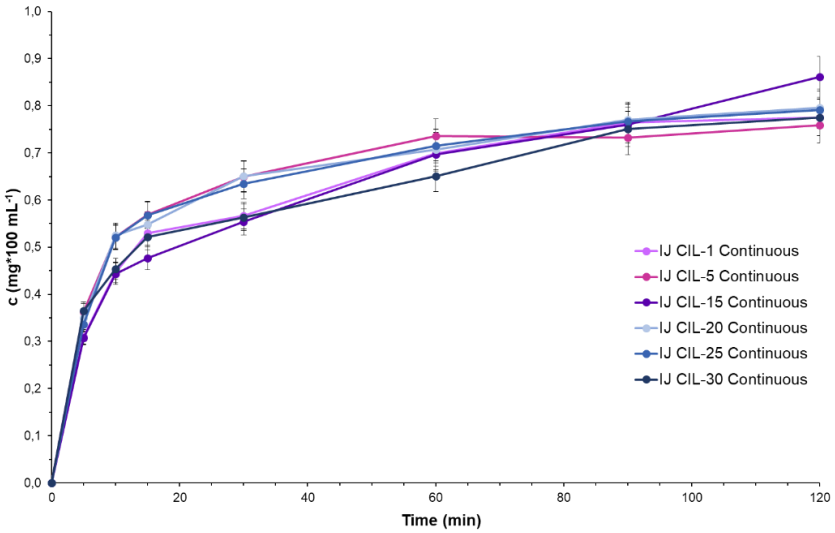

Figure 31 *Dissolution rate of the continuous IJ method products with the sampling of different period of time.*

4.5.4. Conclusion

The self-developed continuous IJ method was capable of producing a high quality product with small average particle size in the case of a poor water-soluble drug, CIL as well. The applied operating parameters of the batch process were converted to the continuous mode successfully. If the continuous IJ method using Gly is compared to the method using CIL, a small change was necessary in the method, as obstruction occurred during the crystallization of CIL. The main advantage of our continuous process is that the increased volume can be handled easily and fast, furthermore the method can produce crystals with improved morphology, reproducibly.

5. SUMMARY AND CONCLUSIONS

In this study the efficiency of the self-developed impinging jet crystallization method was investigated regarding its crystal habit modification effect in the case of a model material and in the case of a poorly water-soluble drug. The critical process parameters were optimized for both a batch and a continuous mode in order to achieve a stable and uniform crystalline product.

New approaches and practical relevance of the current research work:

A The self-developed impinging jet device proved to be an effective, fast and reproducible tool for particle size reduction of a model material, glycine. The process influencing factors were ascertained by means of a full factorial design.

- A novel X-ray powder diffractometry calibration approach was developed for the monitoring of the polymorph transformation in the case of β-glycine, which has not been reported previously.
- Our impinging jet method resulted in one order of magnitude smaller average particle size compared to the generally applied conventional crystallization methods which methods can reduce the particle size only within certain limits.
- The developed impinging jet crystallization technique enables the production of a stable polymorphic form with a low residual solvent quantity.

B This is the first description of combining the impinging jet crystallization method with the application of different concentrations of potassium chloride as an additive to modify the crystal habit of glycine particles.

- Crystal roundness was successfully improved with even low (100-200 ppm) KCl additive concentration.
- The distinct arrangement of the additive was determined in the final product and its residual quantity was adjusted to an optimal level.
- The critical operational parameters of crystallization were optimized for the desired crystal morphology with suitable flowability and low residual solvent quantity.

C The developed impinging jet method enabled us to reduce the particle size of a poorly water-soluble drug, cilostazol and ensure the quality of the final product, reproducibly.

- Significant improvement of the crystal habit of cilostazol was achieved by a combined impinging jet and cooling crystallization method.
- The critical process parameters were determined by a full factorial design, which were the post-mixing time and the temperature.
- Crystal morphology and dissolution rate were improved remarkably compared to the conventional crystallization methods.

D The batch process was successfully converted to a novel continuous impinging jet crystallization method not only with the use of a model material, glycine, but also in the case of a poorly water-soluble drug, cilostazol.

- The developed continuous method is simple and effective to improve the process efficiency, decrease the process time, but maintain the quality of the final product.
- Scale-up was achieved with an improved percentage yield compared to the batch method.
- During the process the operating parameters were optimized for the actual drug substance, furthermore the key process parameters, for instance particle size, particle size distribution and roundness were monitored, and the results revealed the consistency and robustness of the method.

Overall, it can be concluded that the developed batch and the streamlined continuous methods enable the production of a crystalline material with improved rheological properties, and this material could be applied directly in the tableting processes without further modifications, and the crystallization approach could be built into the manufacturing line of pharmaceutical formulations without large investments. The comparison of the different conventional crystallization methods revealed their particle size reduction capacity, and the results can ease the decision on which method is suitable for attaining the desired particle size range. The observations about the crucial process parameters can serve as a basis for the crystal habit optimization of other poorly water-soluble substances as well.

REFERENCES

1. L. Di, P.V. Fish, T. Mano: Bridging solubility between drug discovery and development. Drug Discov. Today 17 (2012) 486–495.
2. K. Zheng, Z. Lin, M. Capece, K. Kunnath, L. Chen, R.N. Davé: Effect of particle size and polymer loading on dissolution behavior of amorphous griseofulvin powder. J. Pharm. Sci. 108 (2019) 234–242.
3. T. Miletic, K. Kyriakos, A. Graovac, S. Ibric: Spray-dried voriconazole–cyclodextrin complexes: Solubility, dissolution rate and chemical stability. Carbohydr. Polym. 98 (2013) 122–131.
4. Y. Lu, N. Tang, R. Lian, J. Qi, W. Wu: Understanding the relationship between wettability and dissolution of solid dispersion. Int. J. Pharm. 465 (2014) 25–31.
5. N. Rasenack, B.W. Müller: Micron-size drug particles: common and novel micronization techniques. Pharm. Dev. Technol. 9 (2004) 1–13.
6. T. Patole and A. Deshpande: Co-crystallization - A technique for solubility enhancement. Int. J. Pharm. Sci. Res. 5 (2014) 3566–3576.
7. A.A. Thorat, S.V. Dalvi: Liquid antisolvent precipitation and stabilization of nanoparticles of poorly water soluble drugs in aqueous suspensions: Recent developments and future perspective. Chem. Eng. J. 181–182 (2012) 1–34.
8. Z. Gao, S. Rohani, J. Gong, J. Wang: Recent developments in the crystallization process: toward the pharmaceutical industry. Engineering 3 (2017) 343–353.
9. K. Pitt, R. Peña, J.D. Tew, K. Pal, R. Smith, Z.K. Nagy, J.D. Litster: Particle design via spherical agglomeration: A critical review of controlling parameters, rate processes and modelling. Powder Technol. 326 (2018) 327–343.
10. X. Han, C. Ghoroi, D. To, Y. Chen, R. Davé: Simultaneous micronization and surface modification for improvement of flow and dissolution of drug particles. Int. J. Pharm. 415 (2011) 185–195.
11. K.Vandana, Y.P. Raju, V.H. Chowdary, M. Sushma, N.V. Kumar: An overview on in situ micronization technique—an emerging novel concept in advanced drug delivery. Saudi Pharm. J. 22 (2014) 283–289.
12. A. Afrose, E.T. White, T. Howes, G. George, A. Rashid , L. Rintoul, N. Islam: Preparation of ibuprofen microparticles by antisolvent precipitation crystallization technique: characterization, formulation, and in vitro performance. J. Pharm. Sci. 107 (2018) 3060–3069.
13. J. Tao, S.F. Chow, Y. Zheng: Application of flash nanoprecipitation to fabricate poorly water-soluble drug nanoparticles. Acta Pharm. Sin. B 9 (2019) 4–18.
14. Y. Liu, C. Cheng, Y. Liu, R.K. Prud'homme, R.O. Fox: Mixing in a multi-inlet vortex mixer (MIVM) for flash nano-precipitation. Chem. Eng. Sci. 63 (2008) 2829–2842.
15. S.M. D'Addio, R.K. Prud'homme: Controlling drug nanoparticle formation by rapid precipitation. Adv. Drug. Deliv. Rev. 63 (2011) 417–426.
16. D. Zhang, S. Xu, S. Du, J. Wang, J. Gong: Progress of pharmaceutical continuous crystallization. Engineering 3 (2017) 354–364.

17. S. Ottoboni, C.J. Price, C. Steven, E. Meehan, A. Barton, P. Firth, A. Mitchell, F. Tahir: Development of a novel continuous filtration unit for pharmaceutical process development and manufacturing. J. Pharm. Sci. 108 (2019) 372–381.

18. F. Artusio, R. Pisano: Surface-induced crystallization of pharmaceuticals and biopharmaceuticals: A review. Int. J. Pharm. 547 (2018) 190–208.

19. J. Hilden, M. Schrad, J. Kuehne-Willmore, J. Sloan: A first-principles model for prediction of product dose uniformity based on drug substance particle size distribution. J. Pharm. Sci. 101 (2012) 2364–2371.

20. Y. Yang, D. Nie, Y. Liu, M. Yu, Y. Gan: Advances in particle shape engineering for improved drug delivery. Drug Discov. Today. 24 (2019) 575–583.

21. G. Perini, F. Salvatori, D.R. Ochsenbein, M. Mazzotti, T. Vetter: Filterability prediction of needle-like crystals based on particle size and shape distribution data. Sep. Purif. Technol. 211 (2019) 768–781.

22. J.M. Hacherl, E.L. Paul, H.M. Buettner: Investigation of impinging-jet crystallization with a calcium oxalate model system. AIChE J. 49 (2003) 2352–2362.

23. W.Y. Woo, , R.B.H. Tan, R.D. Braatz: Precise tailoring of the crystal size distribution by controlled growth and continuous seeding from impinging jet crystallizers. Cryst. Eng. Comm. 13 (2011) 2006–2014.

24. L.X. Liu, I. Marziano, A.C. Bentham, J.D. Litster, E.T. White, T. Howes: Influence of particle size on the direct compression of ibuprofen and its binary mixtures. Powder Technol. 240 (2013) 66–73.

25. T. Tari, R. Ambrus, G. Szakonyi, D. Madarász, P. Frohberg, I. Csóka, P. Szabó-Révész, Joachim Ulrich, Z. Aigner.: Optimizing the crystal habit of glycine by using an additive for impinging jet crystallization. Chem. Eng. Technol. 40 (2017) 1323–1331.

26. M. Jiang, Y.-E.D. Li, H.-H. Tung, R.D. Braatz: Effect of jet velocity on crystal size distribution from antisolvent and cooling crystallizations in a dual impinging jet mixer. Chem. Eng. Process. 97 (2015) 242–247.

27. L.Y. Lyn, H.W. Sze, A. Rajendran, G. Adinarayana, K. Dua, S. Garg: Crystal modifications and dissolution rate of piroxicam. Acta Pharm. 61 (2011) 391–402.

28. A. Dubbini, R. Censi, V. Martena, E. Hoti, M. Ricciutelli, L. Malaj, P.D. Martino: Influence of pH and method of crystallization on the solid physical form of indomethacin. Int. J. Pharm. 473 (2014) 536–544.

29. N. Blagden, M. de Matas, P.T. Gavan, P. York: Crystal engineering of active pharmaceutical ingredients to improve solubility and dissolution rates. Adv. Drug Deliv. Rev. 59 (2007) 617–630.

30. M. Kakran, N.G. Sahoo, L. Li, Z. Judeh: Particle size reduction of poorly water soluble artemisinin via antisolvent precipitation with a syringe pump. Powder Technol. 237, (2013) 468-476.

31. B. Farkas, P. Révész: Kristályosítástól a tablettázásig. Universitas Szeged Kiadó, Szeged (2007) 13–17.

32. S.J. Cooper: The effect of additive aggregation state on controlling crystallization. Crystallization of L-asparagine monohydrate in the presence of carboxylic acid functionality additives. Cryst. Eng. Comm. 3 (2001) 270–273.

33. G.R. Dillip, G. Bhagavannarayana, R. Pallepogu, D.P.R. Borelli: Effect of magnesium chloride on growth, crystalline perfection, structural, optical, thermal and NLO behavior of γ-glycine crystals. Chem. Phys. 134 (2012) 371–376.

34. D.J. Tobler, J.D. Rodriguez Blanco, K. Dideriksen, K.K. Sand, N. Bovet, L.G. Benning, S.L.S. Stipp: The effect of aspartic acid and glycine on amorphous calcium carbonate (acc) structure, stability and crystallization. Procedia Earth Planet. Sci. 10 (2014) 143–148.

35. K. Srinivasan: Crystal growth of α and γ glycine polymorphs and their polymorphic phase transformations. J. Cryst. Growth 311 (2008) 156–162.

36. B. Al-Taani, M. Sheikh-Salem, S. A. Taani: Influence of polyvinyl pyrrolidone addition during crystallization on the physicochemical properties of mefenamic acid crystals. Jordan J. Pharm. Sci. 2 (2009) 86–97.

37. G. Liu, T.B. Hansen, H. Qu, M. Yang, J.P. Pajander, J. Rantanen, L.P. Christensen: Crystallization of piroxicam solid forms and the effects of additives. Chem. Eng. Technol. 37 (2014) 1297–1304.

38. A. Zeng, X. Yao, Y. Gui, Y. Li, K.J. Jones, L. Yu: Inhibiting surface crystallization and improving dissolution of amorphous loratadine by dextran sulfate nanocoating. J. Pharm. Sci. in press (2019) 1–6.

39. W. Kaialy, H. Larhrib, B. Chikwanha, S. Shojaee, A. Nokhodchi: An approach to engineer paracetamol crystals by antisolvent crystallization technique in presence of various additives for direct compression. Int. J. Pharm. 464 (2014) 53–64.

40. M. Hrkovac, J. P. Kardum, N. Ukrainczyk: Influence of NaCl on granulometric characteristics and polymorphism in batch-cooling crystallization of glycine. Chem. Eng. Technol. 38 (2015) 139–146.

41. T. Tari, P. Szabó-Révész, Z. Aigner: Effect of additive on glycine crystal habit by impinging jet crystallization. BIWIC 2016 - 23rd International Workshop on Industrial Crystallization, Conference Proceedings, pp. 40–45, Magdeburg, Germany, 06-08. 09. 2016

42. W. Kaialy, M. Maniruzzaman, S. Shojaee, A. Nokhodchi: Antisolvent precipitation of novel xylitol-additive crystals to engineer tablets with improved pharmaceutical performance. Int. J. Pharm. 477 (2014) 282–293.

43. X. Yang, J. Lu, X. Wang, C. Ching: Effect of sodium chloride on the nucleation and polymorphic transformation of glycine. J. Cryst. Growth 310 (2008) 604–611.

44. C. Sekar, R. Parimaladevi: Effect of KCl addition on crystal growth and spectral properties of glycine single crystals. Spectrochim. Acta, Part A. 74 (2009) 1160–1164.

45. G. Han, P. S. Chow, R. B. H. Tan: Promoting and inhibiting effects of additives on the growth of polar γ-glycine and dl-alanine crystals. ISIC 18 Int. Symp. (2011)

46. D.J. am Ende, S.J. Brenek: Strategies to control particle size during crystallization processes. Am. Pharm. Rev. 7 (2004) 98–104.

47. Z. Aigner, Á. Szegedi, V. Szabadi, R. Ambrus, T. Sovány, P. Szabó-Révész: Comparative study of crystallization processes in case of glycine crystallization. Acta Pharm. Hung. 82 (2012) 61–68.

48. M. Matsumoto, Y. Wada, K. Onoe: Change in glycine polymorphs induced by minute-bubble injection during antisolvent crystallisation. Adv. Powder Technol. 26 (2015) 415–421.

49. C.-S. Su, C.-Y. Liao, W.-D. Jheng: Particle size control and crystal habit modification of phenacetin using ultrasonic crystallization. Chem. Eng. Technol. 38 (2015) 181–186.

50. R.S. Dhumal, S.V. Biradar, A.R. Paradkar, P. York: Particle engineering using sonocrystallization: Salbutamol sulphate for pulmonary delivery. Int. J. Pharm. 368 (2009) 129–137.

51. B. Gielen, T. Claes, J. Janssens, J. Jordens, L.C.J. Thomassen, T.V. Gerven, L. Braeken: Particle size control during ultrasonic cooling crystallization of paracetamol. Chem. Eng. Technol. 40 (2017) 1300–1308.

52. R.I. Sneha, P.R. Gogate: Ultrasound assisted crystallization of mefenamic acid: Effect of operating parameters and comparison with conventional approach. Ultrason. Sonochem. 34 (2017) 896–903.

53. M. Lenka, D. Sarkar: Combined cooling and antisolvent crystallization of l-asparagine monohydrate. Powder Technol. 334 (2018) 106–116.

54. M. Midler, E.L. Paul, E.F. Whittington, M. Futran, P.D. Liu, J. Hsu, S.H. Pan: Crystallization method to improve crystal structure and size. Patent US 5,314,506. (1994)

55. M.M. Gleeson, S. Kim, D.C. Kientzler, S. Kiang: Process for making sterile aripiprazole of desired mean particle size. Patent US 9,066,848 B2 (2015)

56. J. Cheng, C. Yang, M. Jiang, Q. Li, Z.-S. Mao: Simulation of antisolvent crystallization in impinging jets with coupled multiphase flow-micromixing-PBE. Chem. Eng. Sci. 171 (2017) 500–512.

57. T. Tari, Z. Fekete, P. Szabó-Révész, Z. Aigner: Reduction of glycine particle size by impinging jet crystallization. Int. J. Pharm. 478 (2015) 96–102.

58. H. Tamura, K. Kadota, Y. Shirakawa, Y. Tozuka, A. Shimosaka, J. Hidaka: Morphology control of amino acid particles in interfacial crystallization using inkjet nozzle. Adv. Powder Technol. 25 (2014) 847–852.

59. A. Bauer-Brandl: Polymorphic transitions of cimetidine during manufacture of solid dosage forms. Int. J. Pharm. 140 (1996) 195–206.

60. A. Bauer-Brandl: Erratum to polymorphic transitions of cimetidine during manufacture of solid dosage forms. Int. J. Pharm. 145 (1996) 253.

61. B. Calvignac, O. Boutin: The impinging jets technology: a contacting device using a SAS process type. Powder Technol. 191 (2009) 200–205.

62. Y. Dong, W.K. Ng, S. Shen, S. Kim, R.B.H. Tan: Controlled antisolvent precipitation of spironolactone nanoparticles by impingement mixing. Int. J. Pharm. 410 (2011) 175–179.

63. H.-H. Tung, E.L. Paul, M. Midler, J.A. McCauley: Crystallization of organic compounds – an industrial perspective. John Wiley & Sons Inc., New Jersey (2009) 196–204.

64. X.Y. Woo, R.B.H. Tan, R.D. Braatz: Modeling and computational fluid dynamics – population balance equation – micromixing simulation of impinging jet crystallizers. Cryst. Growth Des. 9 (2009) 156–164.

65. J. Kahn: FDA supports critical research to spur innovation for continuous manufacturing technology to support and advance drug and biologics development. (2018) https://www.fda.gov/NewsEvents/Newsroom/FDAInBrief/ucm615431.htm (Last accessed 14.04.2019)

66. M. Krishnan, M. Bisschops: Continuous processing is still processing. Pall Biotech® Sponsored Supplement. 18–21. https://tinyurl.hu/dUPo/ (Last accessed 14.04.2019)

67. K. Matsunamia, T. Nagatob, K. Hasegawab, H. Sugiyama: A large-scale experimental comparison of batch and continuous technologies in pharmaceutical tablet manufacturing using ethenzamide. Int. J. Pharm. 559 (2019) 210–219.

68. E.S. Lawton, G. Steele, P. Shering: Continuous crystallization of pharmaceuticals using a continuous oscillatory baffled crystallizer. Org. Process Res. Dev. 13 (2009) 1357–1363.

69. W.J. Liu, C.Y. Ma, X.Z. Wang: Novel impinging jet and continuous crystallizer design for rapid reactive crystallization of pharmaceuticals. Procedia Eng. 102 (2015) 499–507.

70. W.J. Liu, C.Y. Ma, J.J. Liu, Y. Zhang, X.Z. Wang: Continuous reactive crystallization of pharmaceuticals using impinging jet mixers. Aiche J. 63 (2017) 967–974.

71. Q. Su, Z.K. Nagy, C.D. Rielly: Pharmaceutical crystallisation processes from batch to continuous operation using MSMPR stages: Modelling, design, and control. Chem. Eng. Process. 89 (2015) 41–53.

72. M. Furuta, K. Mukai, D. Cork, K. Mae: Continuous crystallization using a sonicated tubular system for controlling particle size in an API manufacturing process. Chem. Eng. Process. 102 (2016) 210–218.

73. S. Ottoboni, C.J. Price, C. Steven, E. Meehan, A. Barton, P. Firth, A. Mitchell, F. Tahir: Development of a novel continuous filtration unit for pharmaceutical process development and manufacturing. J. Pharm. Sci. 108 (2019) 372–381.

74. R.P.D. Silva, M.F.S. Ambrosio, L.A. Piovesan, M.C.R. Freitas, D.L.M. Aguiar, B.A.C. Horta, E.K. Epprecht, R.A.D.S. San Gil, L.D.C. Visentin: New polymorph form of dexamethasone acetate. J. Pharm. Sci. 107 (2018) 672–681.

75. K. Mikó: Patentability of polymorphic crystalline forms of pharmaceutically active compounds. Hungarian Intellectual Property Office (2014) 2–11. http://www.sztnh.gov.hu/hirek/kapcsolodo/epo/Polymorphic_forms-1.pdf (Last accessed 14.04.2019)

76. K. Raza, P. Kumar, S. Ratan, R. Malik, S. Arora: Polymorphism: The phenomenon affecting the performance of drugs. SOJ Pharm. Pharm. 1 (2014) 2–10.

77. Á. Detrich, K.J. Dömötör, M.T. Katona, I. Markovits, J. Vargáné Láng: Polymorphic forms of bisoprolol fumarate. Preparation and characterization. J. Therm. Anal. Calorim. 135 (2019) 3043–3055.

78. K. Srinivasan, K.R. Devi, S.A. Azhagan: Characterization of α and γ polymorphs of glycine crystallized from water-ammonia solution. Cryst. Res. Technol. 46 (2011) 159–165.

79. M. Rabesiaka, M. Sghaier, B. Fraisse, C. Porte, J.-L. Havet, E. Dichi: Preparation of glycine polymorphs crystallized in water and physicochemical characterizations. J. Cryst. Growth 312 (2010) 1860–1865.

80. B.L.M. Lung-Somarriba, M. Moscosa-Santillan, C. Porte, A. Delacroix: Effect of seeded surface area on crystal size distribution in glycine batch cooling crystallization: a seeding methodology. J. Cryst. Growth 270 (2004) 624–632.

81. M.R.A. Bakar, Z.K. Nagy, A.N. Saleemi, C.D. Rielly: The impact of direct nucleation control on crystal size distribution in pharmaceutical crystallization processes. Cryst. Growth Des. 9 (2009) 1378–1384.

82. G. He, V. Bhamidi, S.R. Wilson, R.B.H. Tan, P.J.A. Kenis, C.F. Zukoski: Direct growth of γ-glycine from neutral aqueous solutions by slow, evaporation-driven crystallization. Cryst. Growth Des. 6 (2006)1746–1749.

83. S.V. Goryainov, E.V. Boldyreva, E.N. Kolesnik: Raman observation of a new (ζ) polymorph of glycine? Chem. Phys. Lett. (2006) 419, 496–500.

84. C.H. Lin, N. Gabas, J.P. Canselier, G. Pèpe: Prediction of the growth morphology of aminoacid crystals in solution: I. α-glycine. J. Cryst. Growth 191 (1998) 791–802.

85. I. Weissbuch, V.Y. Torbeev, L. Leiserowitz, M. Lahav: Solvent effect on crystal polymorphism: why addition of methanol or ethanol to aqueous solutions induces the precipitation of the least stable β form of glycine. Angew. Chem. Int. Ed. 117 (2005) 3290–3293.

86. E.S. Ferrari, R.J. Davey, W.I. Cross, A.M. Gillon, C.S. Towler: Crystallization in polymorphic systems: the solution-mediated transformation of β to α glycine. Cryst. Growth Des. 3 (2003) 53–60.

87. E.V. Boldyreva, V.A. Drebushchak, T.N. Drebushchak, I.E. Paukov, Y.A. Kovalevskaya, E.S. Shutova: Polymorphism of glycine, Part I. J. Therm. Anal. Calorim. 73 (2003) 409–418.

88. E.V. Boldyreva, V.A. Drebushchak, T.N. Drebushchak, I.E. Paukov, Y.A. Kovalevskaya, E.S. Shutova: Polymorphism of glycine, Part II. J. Therm. Anal. Calorim. 73 (2003) 419–428.

89. M. Louhi-Kultanen, M. Karjalainen, J. Rantanen, M. Huhtanen, J. Kallas: Crystallization of glycine with ultrasound. Int. J. Pharm. 320 (2006) 23–29.

90. U. Hayato, T. Toshio, K. Yukio, H. Hiroyoshi: Purification of cyclic adenosine monophosphate phosphodiesterase from human platelets using new-inhibitor sepharose chromatography. Biochem. Pharmacol. 33 (1984) 3339–3344.

91. D.B. Mahmoud, H. Shukr, E.R. Bendas: In vitro and in vivo evaluation of self-nanoemulsifying drug delivery systems of cilostazol for oral and parenteral administration. Int. J. Pharm. 476 (2014) 60–69.

92. E.-S. Ha, D.-H. Ha, D.-H. Kuk, W.-Y. Sim, I.-H. Baek, J.-S. Kim, H.J. Park, M.-S. Kim: Solubility of cilostazol in the presence of polyethylene glycol 4000, polyethylene glycol 6000, polyvinylpyrrolidone K30, and poly(1-vinylpyrrolidone-co-vinyl acetate) at different temperatures. J. Chem. Thermodyn. 113 (2017) 6–10.

93. G.W. Stowell, R.J. Behme, S.M. Denton, I. Pfeiffer, F.D. Sancilio, L.B. Whittall, R.R. Whittle: Thermally-prepared polymorphic forms of cilostazol. J. Pharm. Sci. 91 (2002) 2481–2488.

94. O. Mustapha, K.S. Kim, S. Shafique, D.S. Kim, S.G. Jin, Y.G. Seo, Y.S. Youn, K.T. Oh, B.J. Lee, Y.J. Park, C.S. Yong, J.O. Kim, H.G. Choi: Development of novel cilostazol–loaded solid SNEDDS using a SPG membrane emulsification technique: Physicochemical characterization and in vivo evaluation. Colloids Surf. B 150 (2017) 216–222.

95. O. Mustapha, K.S. Kim, S. Shafique, D.S. Kim, S.G. Jin, Y.G. Seo, Y.S. Youn, K.T. Oh, C.S. Yong, J.O. Kim, H.G. Choi: Comparison of three different types of cilostazol-loaded solid dispersion: Physicochemical characterization and pharmacokinetics in rats. Colloids Surf. B 154 (2017) 89–95.

96. X. Miao, C. Sun, T. Jiang, L. Zheng, T. Wang, S. Wang: Investigation of nanosized crystalline form to improve the oral bioavailability of poorly water soluble cilostazol. J. Pharm. Pharm. Sci. 14 (2011) 196–214.

97. K.S. Gouthami, D. Kumar, R. Thipparaboina, R.B. Chavan, N.R. Shastri: Can crystal engineering be as beneficial as micronisation and overcome its pitfalls?: A case study with cilostazol. Int. J. Pharm. 491 (2015) 26–34.

98. M.-S. Kim, S. Lee, J.-S. Park, J.-S. Woo, S.-J. Hwang: Micronization of cilostazol using supercritical antisolvent (SAS) process: Effect of process parameters. Powder Technol. 177 (2007) 64–70.

99. J.-I. Jinno, N. Kamada, M. Miyake, K. Yamada, T. Mukai, M. Odomi, H. Toguchi, G.G. Liversidge, K. Higaki, T. Kimura: Effect of particle size reduction on dissolution and oral absorption of a poorly water-soluble drug, cilostazol, in beagle dogs. J. Controlled Release 111 (2006) 56–64.

100. ICH International Conference on Harmonisation: ICH guideline Q3C(R7) on impurities: Guideline for residual solvents, Committee for Human Medicinal Products, October 2018.

101. C. Dahlberg, A. Millqvist-Fureby, M. Schuleit: Surface composition and contact angle relationships for differently prepared solid dispersions. Eur. J. Pharm. Biopharm. 70 (2008) 478–485.

102. F. Tian, N. Sandler, J. Aaltonen, C. Lang, D.J. Saville, K.C. Gordon, C.J. Strachan, J. Rantanen, T. Rades: Influence of polymorphic form, morphology, and excipient interactions on the dissolution of carbamazepine compacts. J. Pharm. Sci. 96 (2007) 584–594.

103. T. Tari, Z. Aigner: Folyamatos kristályosítási eljárás fejlesztése impinging jet módszerrel. Acta Pharm. Hung. 87 (2017) 69–75.

104. Brookfield Engineering Laboratories, Inc.: Brookfield Powder Flow Tester, Operating Instructions, Manual No. M09-1200. p 39.
http://www.huntercaprez.com/view/data/3906/Brookfield/Manual/PFT%20M09-1200.pdf
(Last accessed 14.04.2019)

ACKNOWLEDGEMENTS

I would like to express my greatest gratitude to my supervisor **Dr. Zoltán Aigner** for his support and patient guidance, as well as for his valuable and constructive suggestions during the planning and development of my research work.

I wish to sincere thank **Prof. Dr. Piroska Szabó-Révész**, former Head of the Pharmaceutical Technology Educational Program of the Doctoral School of Pharmaceutical Sciences and **Dr. Ildikó Csóka**, Head of the Institute of Pharmaceutical Technology and Regulatory Affairs for their useful advices and for providing me with the opportunity to work in the department.

I am very grateful to **Klára Kovács** for her enthusiastic encouragement and excellent technical assistance. My great thanks are also extended to all of **my colleagues** in the 3rd research group for their help and providing a friendly atmosphere.

I wish to thank **Prof. Dr.-Ing. habil. Dr. h.c. Joachim Ulrich**, Head of the Department of Thermal Process Technology, Martin Luther University Halle-Wittenberg for his professional support throughout my DAAD-MÖB 3-month research project (No. 39349) in the department.

I would like to thank all of **my co-authors, collaborators** and **colleagues from Gedeon Richter Plc., Budapest, Hungary** for their contribution to my Ph.D. work.

Finally, I would like to offer my special thanks to **my family** and **my friends** for their great support and love.

ANNEX

Related articles

I.

International Journal of Pharmaceutics 478 (2015) 96–102

Contents lists available at ScienceDirect

International Journal of Pharmaceutics

journal homepage: www.elsevier.com/locate/ijpharm

Reduction of glycine particle size by impinging jet crystallization

Tímea Tari, Zoltán Fekete, Piroska Szabó-Révész, Zoltán Aigner *

Department of Pharmaceutical Technology, University of Szeged, Eötvös u. 6, H-6720 Szeged, Hungary

ARTICLE INFO

Article history:
Received 25 June 2014
Received in revised form 7 November 2014
Accepted 8 November 2014
Available online 13 November 2014

Keywords:
Impinging jet crystallization
Particle size
Glycine
Crystal habit
Polymorphism
Residual solvent content

ABSTRACT

The parameters of crystallization processes determine the habit and particle size distribution of the products. A narrow particle size distribution and a small average particle size are crucial for the bioavailability of poorly water-soluble pharmacons. Thus, particle size reduction is often required during crystallization processes. Impinging jet crystallization is a method that results in a product with a reduced particle size due to the homogeneous and high degree of supersaturation at the impingement point.

In this work, the applicability of the impinging jet technique as a new approach in crystallization was investigated for the antisolvent crystallization of glycine. A factorial design was applied to choose the relevant crystallization factors. The results were analysed by means of a statistical program. The particle size distribution of the crystallized products was investigated with a laser diffraction particle size analyser. The roundness and morphology were determined with the use of a light microscopic image analysis system and a scanning electron microscope. Polymorphism was characterized by differential scanning calorimetry and powder X-ray diffraction. Headspace gas chromatography was utilized to determine the residual solvent content.

Impinging jet crystallization proved to reduce the particle size of glycine. The particle size distribution was appropriate, and the average particle size was an order of magnitude smaller (d(0.5) = 8–35 μm) than that achieved with conventional crystallization (d(0.5) = 82–680 μm). The polymorphic forms of the products were influenced by the solvent ratio. The quantity of residual solvent in the crystallized products was in compliance with the requirements of the International Conference on Harmonization.

1. Introduction

Crystallization is an important pharmaceutical industrial process. The majority of active pharmaceutical ingredients (APIs) and excipients can be produced by crystallization. The crystallization process determines the chemical purity and physical properties of the product, including its habit, particle size and crystal structure. The average particle size, the particle size distribution, and the habit of particles play decisive roles in pharmaceutical formulation. These parameters may influence the bioavailability and the processability. Direct tablet compression requires sufficiently large and isodimensional particles, but a small average particle size with a narrow particle size distribution is preferred for poorly water-soluble APIs. The marketable materials will be those that can be directly applied in the formulation of pharmaceutical products (Hacherl et al., 2003; Woo et al., 2011; Liu et al., 2013).

Crystallization methods that are commonly used in the pharmaceutical industry include cooling, antisolvent and precipitation processes. However, with these techniques the particle size can be reduced only within certain limits. New methods are therefore sought to decrease the particle size of APIs. One such may be sonocrystallization, which has been studied with various crystallization systems, but its advantages in various crystallization applications are disputed (McCausland et al., 2001; McCausland and Cains, 2003; Louhi-Kultanen et al., 2006). Other options involve the use of impinging jet crystallization and the application of multiple inlet vortex mixers (Liu et al., 2008; D'Addio and Prud'homme, 2011).

Midler et al. (1994) introduced and adapted the impinging jet technique in crystallization (Midler et al., 1994; Tung et al., 2009). The impinging jet mixer consists of two jet nozzles arranged diametrically opposite and facing each other. The impinging jet element can be used in a crystallization reactor or operated in non-submerged mode. A rich solution of the API and the antisolvent flow through the nozzles at a constant linear velocity, causing high supersaturation at the impingement point before the onset of nucleation. This process potentially results in rapid crystallization

* Corresponding author. Tel.: +36 62 545 577; fax: +36 62 545 571.
E-mail address: aigner@pharm.u-szeged.hu (Z. Aigner).

http://dx.doi.org/10.1016/j.ijpharm.2014.11.021
0378-5173/

in the absence of concentration gradients and produces a monodisperse population of small crystals with a high surface area. Impinging jet crystallization is often used in combination with ultrasound to achieve a further reduction in particle size. The direct production of small uniform crystals with high surface area that meet the bioavailability and dissolution requirements can eliminate the need for milling, which can give rise to dust issues, yield losses, long production times, polymorphic transformation or amorphization (Woo et al., 2009; Bauer-Brandl, 1996a,b; am Ende and Brenek, 2004; Calvignac and Boutin, 2009; Hacherl et al., 2003; Dong et al., 2011).

Glycine exists in three polymorphic forms under ambient conditions. Forms α and β are monoclinic (α, $P2_1/n$; β, $P2_1$), while γ is trigonal ($P3_1$). Other polymorphs have been observed at high pressure. In aqueous solution, form α is obtained by spontaneous nucleation (Rabesiaka et al., 2010; Goryainov et al., 2006; Lin et al., 1998). The less stable β glycine has been found to transform rapidly into form α in air or water, but the crystals remain unchanged if kept in a dry environment. The γ form of glycine is the stable form at room temperature and transforms to the α form when heated above 165 °C (Boldyreva et al., 2003a,b,b; Ferrari et al., 2003; Srinivasan, 2008). The addition of ethanol to an aqueous glycine solution induces precipitation of the β form (Weissbuch et al., 2005; Ferrari et al., 2003). The crystallization methods and conditions, the pH of the solution, and the presence of additives also influence the crystal morphology and the polymorphism (Dubbini et al., 2014).

Glycine is a widely used material for crystallization experiments (Srinivasan et al., 2011; Rabesiaka et al., 2010; Lung-Somarriba et al., 2004). It is fast-growing and its crystals are typically quite large, so it is a suitable model material for particle size reduction studies. In order to reduce the glycine particle size, Louhi-Kultanen et al. (2006) studied the effects of ultrasound during cooling crystallization on the polymorphism, crystal size distribution and heat transfer in batch cooling crystallization. Sonocrystallization proved to be a good tool for optimizing and controlling the nucleation and crystallization of glycine, and can be used as a size reduction method to produce a final product with uniform crystal morphology. The smallest average particle size achieved was about 100 μm. Aigner et al. (2012) examined the effects of several crystallization methods and their parameters (cooling, reverse antisolvent and antisolvent crystallization with ultrasound) on the average particle size, particle size distribution and roundness of glycine, and found that these methods are capable of reducing the average particle size only within a certain range. The particle size ranges (d(0.5)) obtained were as follows: 268–680 μm in cooling crystallization; 160–466 μm in reverse antisolvent crystallization; and 82–232 μm in antisolvent crystallization with ultrasound.

In the present work, the impinging jet antisolvent crystallization of glycine as model material were investigated by means of a factorial design for a further particle size decrease. The effects of a number of operating parameters, such as the linear velocity of feeding, the post-mixing time, the temperature difference and the solvent ratio, on the resulting particle size distribution and roundness were studied. A statistical program was used to evaluate the results. The particle size distribution was measured with a laser diffraction particle size analyser. Glycine crystals were analysed with a light microscopic image analysis system, scanning electron microscopy (SEM), differential scanning calorimetry (DSC) and powder X-ray diffraction (XRPD) in order to obtain images of the crystal shape, roundness and structure. The residual solvent content of the crystallized products was investigated by a headspace gas chromatographic method.

2. Materials and methods

2.1. Materials

The following components were used in the experimental work: glycine and ethanol 96% supplied by VWR Hungary; neutral oil (Miglyol 812) purchased from Sasol Germany GmbH; and purified water (Ph. Eur. quality).

2.2. Impinging jet crystallization

Crystallization experiments were carried out in a 250 mL round-bottomed, double-walled Schmizo crystallization reactor (Schmizo AG, Oftringen, Switzerland) equipped with an IKA Eurostar digital mixer (IKA-Werke GmbH & Co., Staufen, Germany).

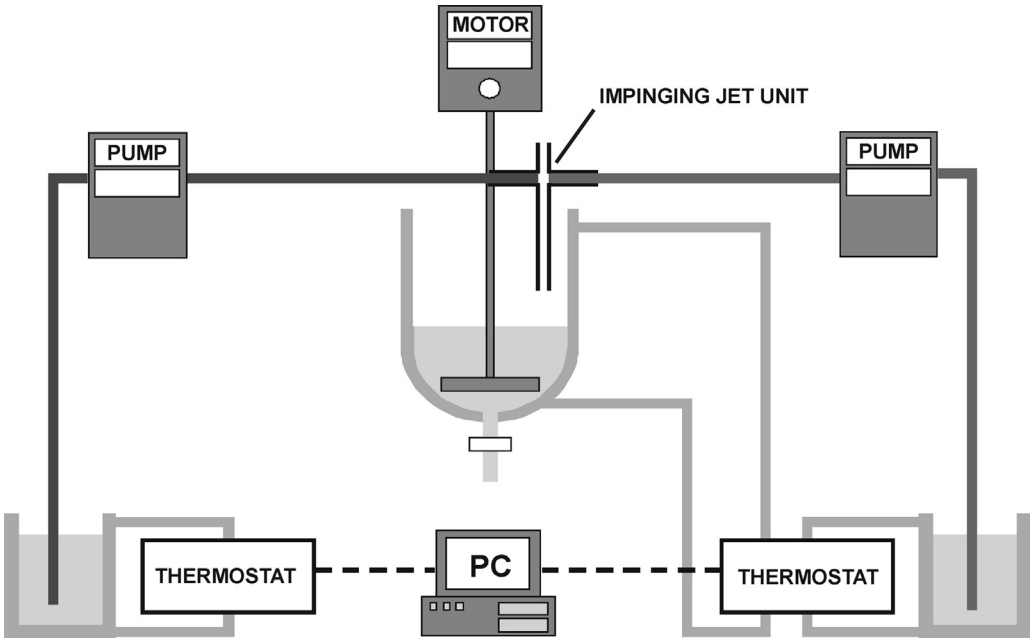

Fig. 1. Experimental apparatus with an impinging jet unit applied in non-submerged mode.

Temperatures were adjusted with a Thermo Haake P5/C10 (Thermo Haake, Karlsruhe, Germany) thermostat and a Julabo F32 (Julabo GmbH, Seelbach, Germany) cryothermostat controlled by Julabo EasyTemp 2.3e software. Two calibrated Rollpump Type 5198 peristaltic pumps (MTA Kutesz, Budapest, Hungary) were used for liquid feeding. The impinging jet unit was a locally developed device equipped with variable-diameter nozzles, used in non-submerged mode.

During the experiments, the two pumps dosed a nearly saturated aqueous solution of glycine at 25 °C (10.02 g of glycine dissolved in 50 mL of purified water) and the required amount of ethanol at defined temperatures. The stirring speed was 250 rpm. The crystallized products were filtered in porcelain filter and washed with 96% ethanol. After vacuum drying (40 °C, 24 h), the products were stored under normal conditions in closed containers. The experimental apparatus is outlined in Fig. 1.

2.3. Factorial design

A 3^2 full factorial design was applied to choose the relevant factors. In series A the influence of the linear velocity and the post mixing time, and in series B the influence of the temperature difference and the post mixing time were investigated on three operational parameters: roundness, d(0.5) and D[4,3].

The levels of the factors can be found in Table 1, while the samples are designated in Table 2. The experiments were performed in randomized sequence. The following approach, containing the interactions of the factors, was used to determine the response surface and the relative effects of the factors (b):

$$y = b_0 + b_1x_1 + b_2x_2 + b_3x_1^2 + b_4x_2^2 + b_5x_1x_2$$

Statistica for Windows 11 AGA software (StatSoft, Inc. Tulsa, USA) was used for the calculations. During the mathematical evaluations, the confidence interval was 95%, i.e. the differences were significant if $p < 0.05$.

2.4. Differential scanning calorimetry

The DSC analysis was carried out with a Mettler Toledo STAR^e thermal analysis system, version 9.30 DSC 821e (Mettler-Toledo AG, Greifensee, Switzerland), at a linear heating rate of 10 °C min^{-1}, with argon as carrier gas (100 mL min^{-1}). The sample weight was in the range 2–5 mg and examinations were performed in the temperature interval 25–300 °C, in a sealed 40 μL aluminium crucible having three leaks in the lid.

Table 1
Values of factors.

Factor	Low level (−)	Mid level (0)	High level (+)
Linear velocity (m s^{-1})	1.41	2.77	4.06
Post mixing time (min)	0	5	10
Temperature difference (°C)	0	12.5	25

2.5. X-ray powder diffractometry

Crystal structures were verified by measuring the X-ray powder diffraction patterns of crystallized samples and the initial material with a Bruker D8 Advance diffractometer (Bruker AXS GmbH, Karlsruhe, Germany) and compared with the structures in the Cambridge Structural Database (Cambridge Crystallographic Data Centre, CCDC, Cambridge, UK). The experiments were performed in symmetrical reflection mode with Cu Kα radiation (λ = 1.5406 Å), using Göbel Mirror bent gradient multilayer optics. The scattered intensities were measured with a Våntec-1 line detector. The angular range was from 3° to 40° in steps of 0.007°. Other measurement conditions were as follows: target, Cu; filter, Ni; voltage, 40 kV; current, 40 mA; measuring time, 0.1 s per step.

2.6. Investigation of crystal shape and roundness

The crystal shape and roundness of the crystallized products were measured with the LEICA Image Processing and Analysis System (LEICA Q500MC, LEICA Cambridge Ltd., Cambridge, UK). The particles were described in terms of their length, breadth, surface area, perimeter and roundness, which is a shape factor giving a minimum value of unity for a circle. This is calculated from the ratio of the perimeter squared to the area. The adjustment factor of 1.064 corrects the perimeter for the effect of the corners produced by the digitization of the image:

$$\text{Roundness} = \frac{\text{Perimeter}^2}{4\cdot\pi\cdot\text{Area}\cdot 1.064}$$

Table 2
Designation of samples.

Sample code	Linear velocity (m s^{-1})	Post mixing time (min)	Temperature difference (°C)
Series A	x_1	x_2	–
A1	1.41	0	0
A2	1.41	5	0
A3	1.41	10	0
A4	2.77	0	0
A5	2.77	5	0
A6	2.77	10	0
A7	4.06	0	0
A8	4.06	5	0
A9	4.06	10	0
Series B	–	x_2	x_1
B1	2.77	0	0
B2	2.77	5	0
B3	2.77	10	0
B4	2.77	0	12.5
B5	2.77	5	12.5
B6	2.77	10	12.5
B7	2.77	0	25
B8	2.77	5	25
B9	2.77	10	25

Table 3
Crystallization results in series A.

Sample	Linear velocity ($m\,s^{-1}$)	Post mixing time (min)	Roundness	d(0.5) (μm)	D[4,3] (μm)	Percentage yield
A1	1.41	0	2.977	15.792	21.497	62.84
A2	1.41	5	2.292	15.808	20.295	65.90
A3	1.41	10	2.089	31.222	37.498	67.22
A4	2.77	0	2.715	16.770	22.530	65.17
A5	2.77	5	2.251	26.057	31.610	64.14
A6	2.77	10	2.033	34.285	40.650	66.10
A7	4.06	0	2.116	14.029	17.175	64.97
A8	4.06	5	2.363	13.778	17.784	68.06
A9	4.06	10	1.961	31.948	38.076	68.72

Table 4
Crystallization results in series B.

Sample	Temperature difference (°C)	Post mixing time (min)	Roundness	d(0.5) (μm)	D[4,3] (μm)	Percentage yield
B1	0	0	1.825	10.142	13.329	82.25
B2	0	5	2.429	9.249	11.241	81.11
B3	0	10	2.935	9.368	11.563	80.54
B4	12.5	0	2.851	8.335	10.889	81.54
B5	12.5	5	2.186	8.524	10.803	85.59
B6	12.5	10	2.292	9.664	12.662	82.34
B7	25	0	2.071	8.575	11.599	80.60
B8	25	5	2.166	10.204	13.849	85.73
B9	25	10	2.513	8.835	11.636	84.33

The products were suspended in Miglyol 812 with ultrasound in order to ensure the presence of individual particles. Approximately 1000 particles per sample were examined.

2.7. Scanning electron microscopy

The morphology of the particles was examined by SEM (Hitachi S4700, Hitachi Scientific Ltd., Tokyo, Japan). A sputter coating apparatus (Bio-Rad SC 502, VG Microtech, Uckfield, UK) was applied to induce electric conductivity on the surface of the samples. The air pressure was 1.3–13.0 mPa.

2.8. Particle size distribution analysis

A Malvern Mastersizer laser diffraction analyser (Malvern Instruments Ltd., Malvern, UK) with a measuring range of 0.02–2000 μm was used to measure the crystal size distributions. The particle size distribution was determined in a dry method with a Scirocco dry powder feeder; air was used as the dispersion agent.

At least three repeated measurements were performed on each sample and the mean value was calculated. The tables with the results contain d(0.5) (defined as the diameter where half of the population lies below this value) and D[4,3] (the mean diameter over volume, also referred to as the DeBroukere mean).

2.9. Determination of residual solvent content

The residual solvent content was analysed by a headspace gas chromatographic method, with an Agilent 7890 A gas chromatograph (Agilent Technologies Inc., Santa Clara, CA, USA) with a DB-624 capillary column (60 m × 0.25 mm × 1.4 μm, nominal) equipped with an Agilent GC Sampler 80 and a flame ionization detector. The conditions of the gas chromatographic analysis were as follows: the oven temperature was initially maintained at 40 °C for 6 min, and then raised at a rate of 7 °C min^{-1} to 194 °C, where it was held for 0 min. The temperature of the injector was set at 220 °C and the detector temperature was set at 300 °C. Helium was used as carrier gas at a pressure of 34.8 psi. 1 mL samples were injected in split mode, with a split ratio of 8:1. The agitator temperature was 80 °C with a speed of 500 rpm, and the syringe temperature was 110 °C. The sample equilibration time was 20 min. The hydrogen gas and air flow rates were 30 and 350 mL min^{-1}, respectively.

The ethanol concentration of the standard solution was 100 μg mL^{-1}. The blank sample contained 500 mg of sodium sulfate dissolved in 1 mL of water for injection in a 20 mL headspace vial. The standard sample contained the same quantity of sodium sulfate dissolved in 1 mL of standard solution, while the sample solution contained 500 mg of sodium sulfate and 100 mg of crystallized glycine sample dissolved in 1 mL of water for injection.

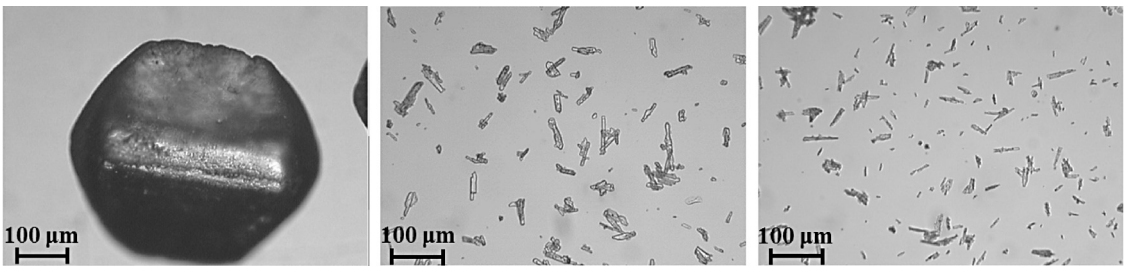

Fig. 2. Light microscopy images of glycine crystals.
(left: original crystal; middle: crystallized product A8; right: crystallized product B7).

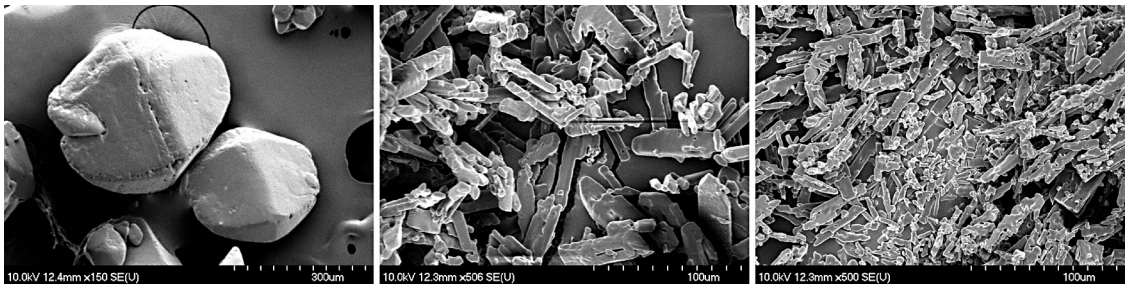

Fig. 3. SEM images of glycine crystals.
(left: original crystal; middle: crystallized product A8; right: crystallized product B7).

3. Results and discussion

The crystallization results for the two series are presented in Tables 3 and 4. Each assay was repeated three times; the Tables show the average results of roundness, d(0.5), D[4,3] and percentage yield.

The application of the impinging jet crystallization technique resulted in a smaller particle size as compared with the previously investigated conventional crystallization methods. The parallel crystallization processes with the same parameters produced the same particle size distribution, which confirmed the reproducibility of the method. In series A, increase of the post-mixing time improved the roundness, but increased the particle size of the product, which was in contrast with the announced goal. The average particle size increased to a greater extent particularly at a post-mixing time of 10 min. As the crystallization parameters had opposite effects on the particle size and roundness, it was favourable to apply a post-mixing time reduction. In series B, neither the temperature difference nor the post-mixing time influenced the particle size or roundness of the crystallized products significantly, but each individual parameter setting resulted in significantly smaller particles as compared with series A. The percentage yield in series B was higher due to the lower

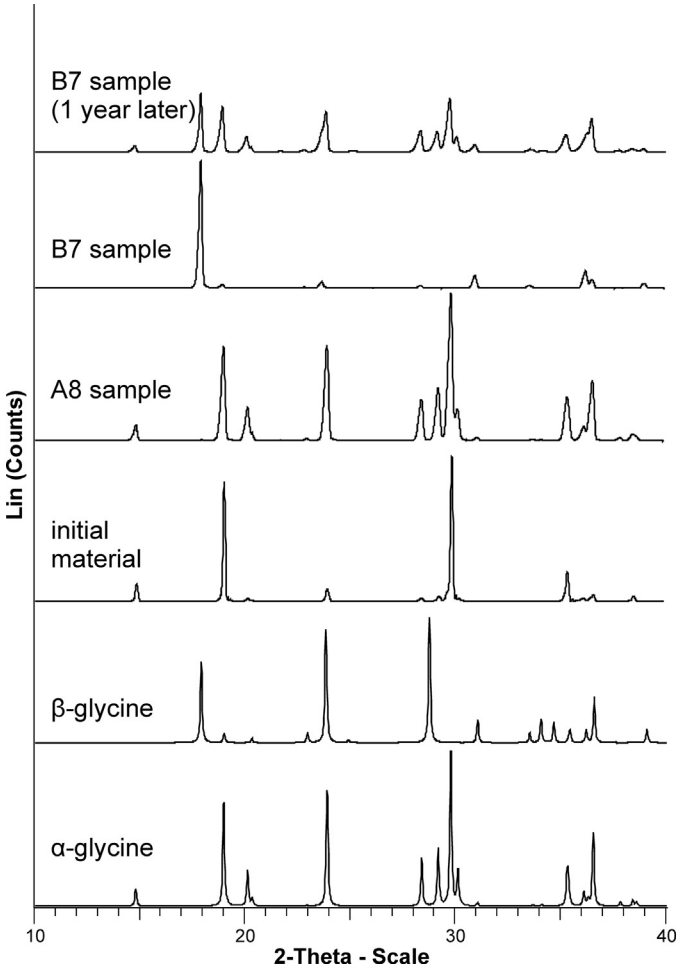

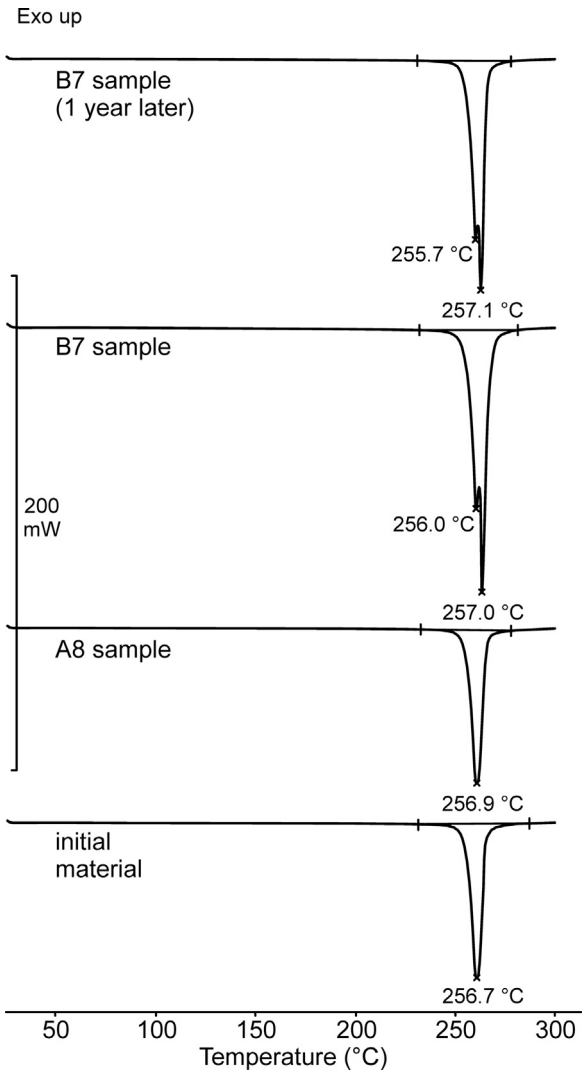

Fig. 5. DSC thermograms of the initial material and crystallized products.

Table 5
Factorial design results (series A).

Dependent variable	Polynomial function	r^2
Roundness	$y = 2.32 - 0.31x_1 - \underline{0.58x_2} + 0.04x_1^2 - 0.01x_2^2 + 0.37x_1x_2$	0.858
d(0.5)	$y = 22.19 - 1.02x_1 + \underline{16.94x_2} + 5.29x_1^2 - 5.46x_2^2 + 1.25x_1x_2$	0.937
D[4,3]	$y = 27.47 - 2.09x_1 + \underline{18.32x_2} + 6.24x_1^2 - 6.34x_2^2 + 2.45x_1x_2$	0.943

solubility of glycine in the 1:2 solvent–antisolvent mixture. The filterability of all the crystallized products was satisfactory.

The differences in crystal size and morphological parameters can be seen in the light microscopy and SEM images (Figs. 2 and 3). The original glycine contained large isodimensional crystals with a smooth surface. By contrast, the products with the smallest average particles in the two crystallization series consisted of small, irregular-shaped, needle-form crystals with a smooth surface and poorer roundness. The crystallized products exhibited a slight tendency to aggregate due to the small particle size, but this did not cause any problem for the laser diffraction particle size analysis measurements and allowed the application of the dry method.

The polymorphism of the initial material and the products was examined with a powder X-ray diffraction apparatus and compared with the structures in the Cambridge Structural Database (refcodes GLYCIN02 (α) and GLYCIN (β)) (Fig. 4). It was found that both the initial material and the series A products consisted of the pure stable α polymorph. In contrast, the series B products contained mostly the less stable β polymorph, and a small amount of the α polymorph. According to the literature data (Weissbuch et al., 2005; Ferrari et al., 2003), the appearance of the β polymorph is caused by the presence (and the concentration) of ethanol in the crystallization process. While the 1:1 solvent–antisolvent ratio favoured the formation of the stable α form, the higher ethanol ratio resulted in the appearance of the less stable β polymorph.

Transformation of the β form into the α polymorph began during storage. The pure β form had been generated as described in the literature (Boldyreva et al., 2003a). Powder mixtures of various compositions (0 + 100, 10 + 90, 20 + 80 α + β forms, and so on) were prepared from the two polymorphs and the calibration curve was recorded. The calibration curve based on the characteristic peak area of the α form (peaks at 29.225, 29.827 and 30.172 2θ) was as follows: y (α form %) = −1.7465 x (net area) + 158.25 (R^2 = 0.991). The initial β form content of the series B samples was between 72 and 96%. After 1 year of storage, the β form content had decreased to 13–17%. The series A products did not change during this storage period. It was found that the 1:1 solvent ratio used in the crystallization processes was crucial for the formation of the stable polymorphic form.

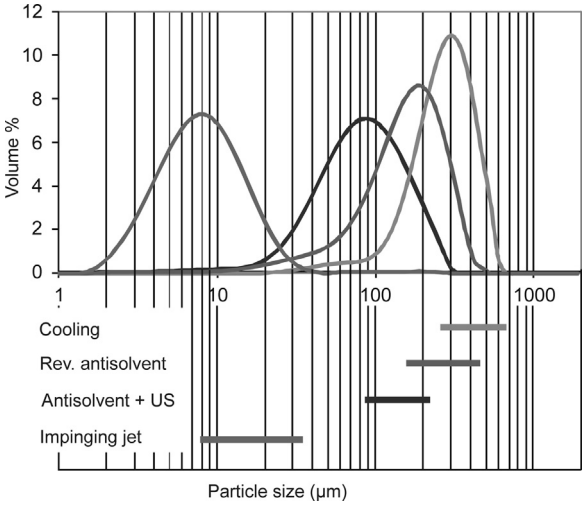

Fig. 6. Particle size distribution and average particle size range produced by different crystallization methods.
(top: particle size distribution of the product with the smallest average particle size achieved with the given method; bottom: average particle size ranges (d(0.5)) attained with the given method).

DSC studies confirmed the results of the powder X-ray analysis. The thermograms of the initial material and the series A products contained one endothermic peak at about 257 °C, which corresponds to the melting point of the α form (Srinivasan, 2008). In contrast, the thermograms of the series B samples displayed two endothermic peaks. The lower-temperature peak corresponded to the melting point of the β form, while the second peak was caused by the melting of the α form. It was not possible to specify the proportion of the polymorphs because the two endothermic peaks overlapped. After storage for one year, the thermograms of the series B samples were similar to the previously recorded ones. It has been reported that the phase transition of the γ form to the α polymorph causes a small endothermic peak at about 179 °C (Srinivasan, 2008). Our results indicated that our samples did not contain any γ form (Fig. 5).

The growth of the crystals during impinging jet crystallization is rapid, due to the homogeneous and high degree of supersaturation, so that the chance of the occurrence of solvent inclusion is high. Ethanol (used as antisolvent) belongs in the ICH Q3C(*R*2) Guideline Class 3 group (where the residual solvent concentration is at most 5000 ppm), and it was therefore necessary to determine its concentration in the crystallized products (ICH, 2011). The residual solvent contents of the crystallized samples were determined by headspace gas chromatography (Grodowska and Parczewski, 2010). Our results indicated that the ethanol content of the initial sample was less than the limit of quantification, and it was therefore assumed that ethanol was not used in the preparation of this material. The maximum residual solvent content of the series A samples was 9 ppm, while the samples in series B contained a maximum 145 ppm of ethanol. The measured residual solvent content of the samples was low relative to the maximum values prescribed in the ICH requirements, which demonstrated the applicability of the impinging jet method in the antisolvent crystallization of glycine despite the extremely rapid nucleation.

Statistical analysis results relating to the effects of the crystallization parameters on the roundness and particle size are presented in Table 5, where the statistically significant factors are underlined.

In the case of series A, only the post-mixing time exhibited a significant linear relationship with the changes in roundness, d (0.5) and D[4,3] results (the response surface r^2 results were 0.858, 0.937 and 0.943, respectively). Neither the linear nor the quadratic relationship of the linear velocity and the interaction effect of the two independent variables displayed a significant effect on the change in these dependent variables. An increase of the post-mixing time increased the average particle size, but reduced the roundness, and the post-mixing time therefore had to be reduced to achieve the desired small particles. We assume that an increase

of the linear velocity would cause a further particle size reduction, but the pump capacity was limited, so that the velocity could not be increased as compared with the original parameters described in the crystallization studies. The investigated parameters did not cause significant changes in the particle size and roundness in series B.

Fig. 6 depicts the particle size distributions of the products with the smallest particles and the average particle size ranges produced by impinging jet crystallization and the previously investigated crystallization methods (Aigner et al., 2012). Those studies had shown that the largest particles were achieved by conventional cooling crystallization. The reverse antisolvent and antisolvent methods with the application of ultrasound were also able to achieve slight reductions in the average particle size of glycine. The impinging jet technology resulted in a further one order of magnitude reduction in particle size.

4. Conclusions

Glycine crystals grow rapidly and the crystal size is typically quite large, and glycine is therefore an ideal model material for particle size reduction experiments. Application of the impinging jet method in antisolvent crystallization led to a reproducible decrease in the average particle size of glycine, with suitable low residual organic solvent quantity and roundness. A factorial design was applied to choose the relevant crystallization factors, and the results were analysed by means of a statistical program. The average particle size was an order of magnitude smaller ($d(0.5) = 8–35\ \mu m$) as compared with the results of several other crystallization methods (cooling, reverse antisolvent and antisolvent crystallization with the application of ultrasound, where $d(0.5)$ was between 82 and 680 μm). Production of the stable polymorphic form required the application of a 1:1 water–ethanol ratio.

The impinging jet crystallization method has proved to be a good tool for optimizing and controlling the nucleation and crystallization of organic materials such as glycine. Furthermore, it can be used as a very effective size reduction method to attain a final product with suitable crystal morphology and a narrow particle size distribution.

Acknowledgements

The authors wish to thank Rita Ambrus for her contribution to the SEM analysis. We are grateful for the support of DAAD-MÖB project No. 39349.

References

Aigner, Z., Szegedi, Á., Szabadi, V., Ambrus, R., Sovány, T., Szabó-Révész, P., 2012. Comparative study of crystallization processes in case of glycine crystallization. Acta Pharmaceutica Hungarica 82, 61–68.
Bauer-Brandl, A., 1996a. Polymorphic transitions of cimetidine during manufacture of solid dosage forms. Int. J. Pharm. 140, 195–206.
Bauer-Brandl, A., 1996b. Erratum to polymorphic transitions of cimetidine during manufacture of solid dosage forms. Int. J. Pharm. 145, 253.
Boldyreva, E.V., Drebushchak, V.A., Drebushchak, T.N., Paukov, I.E., Kovalevskaya, Y. A., Shutova, E.S., 2003a. Polymorphism of glycine. Thermodynamic aspects. Part I. Relative stability of the polymorphs. J. Therm. Anal. Calorim. 73, 409–418.
Boldyreva, E.V., Drebushchak, V.A., Drebushchak, T.N., Paukov, I.E., Kovalevskaya, Y. A., Shutova, E.S., 2003b. Polymorphism of glycine. Thermodynamic aspects. Part II. Polymorphic transitions. J. Therm. Anal. Calorim. 73, 419–428.
Calvignac, B., Boutin, O., 2009. The impinging jets technology: a contacting device using a SAS process type. Powder Technol. 191, 200–205.
D'Addio, S.M., Prud'homme, R.K., 2011. Controlling drug nanoparticle formation by rapid precipitation. Adv. Drug. Deliv. Rev. 63, 417–426.
Dong, Y., Ng, W.K., Shen, S., Kim, S., Tan, R.B.H., 2011. Controlled antisolvent precipitation of spironolactone nanoparticles by impingement mixing. Int. J. Pharm. 410, 175–179.
Dubbini, A., Censi, R., Martena, V., Hoti, E., Ricciutelli, M., Malaj, L., Martino, P.D., 2014. Influence of pH and method of crystallization on the solid physical form of indomethacin. Int. J. Pharm. 473, 536–544.
am Ende, D.J., Brenek, S.J., 2004. Strategies to control particle size during crystallization processes. Am. Pharm. Rev. 7, 98–104.
Ferrari, E.S., Davey, R.J., Cross, W.I., Gillon, A.M., Towler, C.S., 2003. Crystallization in polymorphic systems: the solution-mediated transformation of β to α glycine. Cryst. Growth Des. 3, 53–60.
Goryainov, S.V., Boldyreva, E.V., Kolesnik, E.N., 2006. Raman observation of a new (ζ) polymorph of glycine? Chem. Phys. Lett. 419, 496–500.
Grodowska, K., Parczewski, A., 2010. Organic solvents in the pharmaceutical industry. Acta Pol. Pharm. Drug Res. 67, 3–12.
Hacherl, J.M., Paul, E.L., Buettner, H.M., 2003. Investigation of impinging-jet crystallization with a calcium oxalate model system. AIChE J. 49, 2352–2362.
ICH International Conference on Harmonisation of Technical Requirements for Registration of Pharmaceuticals for Human Use, ICH harmonised tripartite guideline validation of Impurities: Guideline for residual solvents Q3C(R5), (February 2011).
Lin, C.H., Gabas, N., Canselier, J.P., Pèpe, G., 1998. Prediction of the growth morphology of aminoacid crystals in solution: I. è-glycine. J. Cryst. Growth 191, 791–802.
Liu, L.X., Marziano, I., Bentham, A.C., Litster, J.D., White, E.T., Howes, T., 2013. Influence of particle size on the direct compression of ibuprofen and its binary mixtures. Powder Technol. 240, 66–73.
Liu, Y., Cheng, C., Liu, Y., Prud'homme, R.K., Fox, R.O., 2008. Mixing in a multi-inlet vortex mixer (MIVM) for flash nano-precipitation. Chem. Eng. Sci. 63, 2829–2842.
Louhi-Kultanen, M., Karjalainen, M., Rantanen, J., Huhtanen, M., Kallas, J., 2006. Crystallization of glycine with ultrasound. Int. J. Pharm. 320, 23–29.
Lung-Somarriba, B.L.M., Moscosa-Santillan, M., Porte, C., Delacroix, A., 2004. Effect of seeded surface area on crystal size distribution in glycine batch cooling crystallization: a seeding methodology. J. Cryst. Growth 270, 624–632.
McCausland, L.J., Cains, P.W., 2003. Ultrasound to make crystals. Chem. Indust. 5, 15–16.
McCausland, L.J., Cains, P.W., Martin, P.D., 2001. Use the power of sonocrystallization for improved properties. Chem. Eng. Prog. 97, 56–61.
Midler, M., Paul, E.L., Whittington, E.F., Futran, M., Liu, P.D., Hsu, J., Pan, S.H., 1994. Crystallization method to improve crystal structure and size. Patent US 5,314,506.
Rabesiaka, M., Sghaier, M., Fraisse, B., Porte, C., Havet, J.-L., Dichi, E., 2010. Preparation of glycine polymorphs crystallized in water and physicochemical characterizations. J. Cryst. Growth 312, 1860–1865.
Srinivasan, K., 2008. Crystal growth of α and γ glycine polymorphs and their polymorphic phase transformations. J. Cryst. Growth 311, 156–162.
Srinivasan, K., Devi, K.R., Azhagan, S.A., 2011. Characterization of α and γ polymorphs of glycine crystallized from water-ammonia solution. Cryst. Res. Technol. 46, 159–165.
Tung, H.-H., Paul, E.L., Midler, M., McCauley, J.A., 2009. Crystallization of Organic Compounds – An Industrial Perspective. John Wiley & Sons Inc., New Jersey, pp. 196–204.
Weissbuch, I., Torbeev, V.Y., Leiserowitz, L., Lahav, M., 2005. Solvent effect on crystal polymorphism: why addition of methanol or ethanol to aqueous solutions induces the precipitation of the least stable β form of glycine. Angew. Chem. Int. Ed. 117, 3290–3293.
Woo, X.Y., Tan, R.B.H., Braatz, R.D., 2009. Modeling and computational fluid dynamics – population balance equation – micromixing simulation of impinging jet crystallizers. Cryst. Growth Des. 9, 156–164.
Woo, W.Y., Tan, R.B.H., Braatz, R.D., 2011. Precise tailoring of the crystal size distribution by controlled growth and continuous seeding from impinging jet crystallizers. Cryst. Eng. Comm. 13, 2006–2014.

II.

Tímea Tari[1,*]
Rita Ambrus[1]
Gerda Szakonyi[2]
Dániel Madarász[3]
Patrick Frohberg[4]
Ildikó Csóka[1]
Piroska Szabó-Révész[1]
Joachim Ulrich[4]
Zoltán Aigner[1]

Optimizing the Crystal Habit of Glycine by Using an Additive for Impinging Jet Crystallization

Additives selectively inhibit or enhance the growth of crystal faces and effectively change the crystal morphology. For the first time, potassium chloride was used as additive during impinging jet crystallization of glycine. The structure of the powder particles was evaluated by X-ray powder diffraction, differential scanning calorimetry, scanning electron microscopy with energy dispersive X-ray spectroscopy, headspace gas chromatography, and flame atomic absorption spectrometry. Even a minor amount of KCl had a significant effect on the crystal roundness and reduced the particle size significantly, despite of the extremely rapid nature of the crystallization process. This method resulted in the α-polymorph of glycine with an appropriate low residual additive content and a minimal residual organic solvent content. The arrangement and the optimal concentration of the additive were determined.

Keywords: Additives, Glycine, Impinging jet crystallization, Particle size, Polymorphism

Received: November 11, 2016; *revised:* April 06, 2017; *accepted:* May 03, 2017

DOI: 10.1002/ceat.201600634

1 Introduction

The main purpose of crystallization is to produce the most appropriate form of an active compound in terms of manufacturability, in the pharmaceutical, food, or cosmetic industries. The crystal habit, such as the particle size, shape and surface, influences the processability [1–3]. A small average particle size and a narrow particle size distribution (PSD) are frequent requirements in case of poorly water-soluble drugs (Biopharmaceutics Classification System (BCS) class II). These parameters can increase the dissolution rate from dosage forms, enhance the bioavailability of the drug products, and influence the stability and uniformity of the active agent incorporated in tablets [4, 5]. The roundness of the crystals affects their flowability and fluency and the agglomeration of the particles during the tableting process, both in case of direct tablet compression and in case of wet granulation. A spherical crystal shape and a smooth surface are known to improve the flowability and assure the presence of individual particles [6].

During the course of impinging jet crystallization, the rich solution of the active pharmaceutical ingredient (API) and the antisolvent flow through two jet nozzles arranged diametrically opposite to and facing each other. At the impinging point, where the mixing of small volumes of the two solutions occurs, high supersaturation evolves before the onset of nucleation, which produces a monodisperse population of small crystals with a high surface area [7, 8]. The PSD can be adjusted by modifying the crystallization parameters, including the linear velocity of the fluid flow, the temperature of the liquids, or the post-mixing time [9]. On the other hand, modifying the crystal shape is hardly feasible because of the momentary and extremely rapid nature of the crystallization process.

Glycine crystals are well known to grow rapidly; their particle size is typically large, and therefore glycine is an ideal model material for crystal habit modification experiments [10, 11]. Glycine has three polymorphic forms including α-, β-, and γ-polymorphs under normal conditions. Under high pressure, δ- and ζ-polymorphs have also been observed [12]. The formation of these polymorphs can be influenced by various experimental conditions and different crystallization parameters [13]. α-Glycine is metastable under ambient conditions, and in aqueous solution, it develops by spontaneous nucleation as the main polymorph. Its crystal structure is monoclinic (space

[1]Dr. Tímea Tari, Dr. Rita Ambrus, Dr. Ildikó Csóka, Prof. Piroska Szabó-Révész, Dr. Zoltán Aigner
tari.timea@pharm.u-szeged.hu
University of Szeged, Department of Pharmaceutical Technology and Regulatory Affairs, Eötvös Street 6, 6720 Szeged, Hungary.
[2]Dr. Gerda Szakonyi
University of Szeged, Institute of Pharmaceutical Analysis, Somogyi Street 4, 6720 Szeged, Hungary.
[3]Dr. Dániel Madarász
University of Szeged, Department of Applied and Environmental Chemistry, Rerrich Béla square 1, 6720 Szeged, Hungary.
[4]Dr. Patrick Frohberg, Prof. Joachim Ulrich
Martin Luther University Halle-Wittenberg, Center of Engineering Sciences, Thermal Process Technology, Hoher Weg 7, 06120 Halle, Germany.

group (s.gr.) $P2_1/n$). β-Glycine is the least stable form at all temperatures, and its formation is driven by the addition of methanol or ethanol to the aqueous solutions. It is also characterized by a monoclinic crystal structure (s.gr. $P2_1$). Thermodynamically, γ-glycine is the most stable form under ambient conditions, although most commonly the α-form crystallizes in aqueous solutions and it does not usually transform into the γ-form under these conditions. The γ-form is known to develop in acidic and basic water solutions containing additives like acetic acid, ammonia, or inorganic salts. Its crystal structure is trigonal (s.gr. $P3_1$). These three polymorphs exist in the zwitter-ionic form within the crystals, and they differ in terms of how the $^{+}NH_3–CH_2–COO^{-}$ groups are linked by the hydrogen bonds [14–16].

Additives selectively inhibit or enhance the growth of crystal faces via several mechanisms and effectively change the crystal morphology [17–19]. Parameters such as the concentration and type of the additives can influence the occurrence of the different polymorphs [20–22]. The additives used for the crystallization process can influence the dissolution rate, the hardness, and therefore even the efficiency of the tablets [23–25]. Yang et al. [26] investigated the effects of sodium chloride on the nucleation and transformation of two polymorphs of glycine. They found that the aqueous solution of NaCl favored the formation of the γ-form, and the final crystals were larger than the initial crystal size. Sekar and Parimaladevi [27] applied a slow evaporation method for glycine crystallization using a high concentration of potassium chloride (4–18 %, i.e., 4000–18 000 ppm) as additive. They observed that the additive preferentially adsorbed on the (011) crystal face of α-glycine and inhibited its growth along the *c*-axis, while enhancing the growth along the *a*-axis [27]. Han et al. [28] examined the effects of malonic and DL-aspartic acids as additives on the growth of γ-glycine and *DL*-alanine side faces. These amino acids usually grow with a needle-like morphology from their aqueous solutions and are elongated along the polar *c*-axis. It was found that both of the additives inhibited the side growth along the *c*-axis [28]. In summary, the additives are clearly shown to affect the crystal morphology in case of long-lasting crystallization methods, but for fast crystallization methods like impinging jet crystallization, the effects of additives on morphology control have not yet been investigated.

Previously, it was demonstrated that impinging jet crystallization is a very effective method for the particle size reduction of organic materials such as glycine, yielding reproducible products with a small average particle size and a narrow PSD [29]. In any case, the applied rapid antisolvent crystallization method gave needle-like crystals during our experiments, which is considered as an unfavorable shape.

In the present work, the purpose was to produce glycine crystals with suitable roundness besides a small average particle size, a narrow PSD, and a stable polymorphic form. To the authors' knowledge, the current research is the first example of combining the impinging jet crystallization method with the application of different concentrations of potassium chloride as an additive to modify the crystal habit of glycine particles. Further aims were to adjust the optimal concentration of the additive and to optimize the crystallization parameters.

2 Materials and Methods

2.1 Materials

Glycine and ethanol 96 % were supplied by VWR (Leuven, Belgium) and potassium chloride was obtained from Scharlau (Barcelona, Spain). Purified water of Ph. Eur. quality was used for the experimental work.

2.2 Impinging Jet Crystallization

The impinging jet unit was used in the non-submerged mode with given-diameter nozzles (d = 0.6 mm). During the experiments, two calibrated peristaltic pumps (Rollpump Type 5198; MTA Kutesz, Budapest, Hungary) fed the near-saturated aqueous solution of glycine containing different concentrations of potassium chloride and the antisolvent (ethanol 96 %). The glycine concentrations of the saturated solutions were varied between 20.05 and 23.48 % (m/v), corresponding to the solubility-increasing effect of the various concentrations of added potassium chloride. After preparation of the saturated glycine solution, 2 mL of additive solution were added subsequently to avoid crystallization in the nozzles. The feeding was accomplished with constant linear velocity (4.06 m s^{-1}) and with a solvent/antisolvent ratio of 1:1, at 25 °C. The crystallization experiments were carried out in a 250-mL round-bottom, double-walled Schmizo crystallization reactor (Schmizo, Oftringen, Switzerland) equipped with an IKA Eurostar digital overhead stirrer (IKA-Werke, Staufen, Germany) and an Anker-type mixer. The stirring speed was 250 rpm.

Constant temperature was provided by a Thermo Haake P5/C10 (Thermo Haake, Karlsruhe, Germany) thermostat and a Julabo F32 (Julabo GmbH, Seelbach, Germany) cryothermostat controlled by the Julabo EasyTemp 2.3e software. The crystallized products were filtered in a porcelain filter and washed with 40 mL of an ethanol-water mixture of ratio 1:1, to minimize the quantity of residual potassium. After vacuum drying (40 °C, 24 h), the products were stored in closed containers under normal conditions. The experimental apparatus is outlined in Fig. 1.

2.3 Characterization of the Glycine Particles Produced by Impinging Jet Crystallization

2.3.1 Investigation of the Crystal Morphology

The crystal shape of the crystallized products was investigated using the Leica Image Processing and Analysis System (Leica Q500MC; Leica Cambridge Ltd., Cambridge, UK). Crystal length, breadth, surface area, perimeter, and roundness were analyzed for approximately 1000 particles per sample. Roundness is a shape factor giving a minimum value of unity for the circle shape. The roundness value for the perfect sphere shape equals 1.00. Roundness is calculated as the ratio of the perimeter squared and the surface area. The adjustment factor of 1.064 corrects the perimeter for the effect of the corners produced by the digitization of the image:

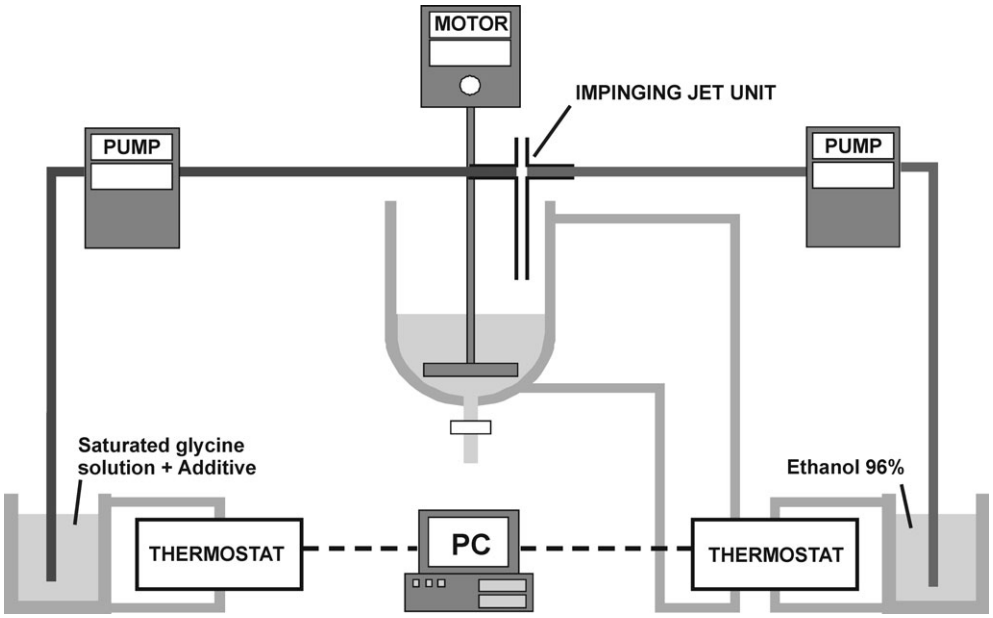

Figure 1. Experimental apparatus.

$$\text{roundness} = \frac{\text{perimeter}^2}{4\pi\,\text{area} \times 1.064} \quad (1)$$

The morphology of the particles was analyzed by scanning electron microscopy (SEM) (Hitachi S-4700; Hitachi Scientific Ltd., Tokyo, Japan) using a working distance of 15 mm, an accelerating voltage of 10 kV, and an emission current of 10 mA. A sputter coating apparatus (Bio-Rad SC 502; VG Microtech, Uckfield, UK) was used to induce electric conductivity on the surface of the samples applying a gold-palladium coating. The argon gas pressure was 1.3–13.0 mPa and the time was 90 s.

2.3.2 Particle Size Distribution Analysis

The PSD was analyzed by a Malvern Mastersizer laser diffraction analyzer (Malvern Instruments Ltd., Malvern, UK) in a dry method with a Scirocco dry powder feeder, using air as the dispersion agent, and defining a measuring range of 0.02–2000 µm. Two repeated measurements were performed on each sample and the mean value was calculated. The tables with the results contain $d(0.5)$, the diameter where half of the population lies below, and $D[4,3]$, the mean diameter over the volume.

2.3.3 Identification of Polymorphism

X-ray powder diffractometry (XRPD) and differential scanning calorimetry (DSC) were used to identify the crystal structure of the products. The XRPD experiments were performed with a Bruker D8 Advance diffractometer (Bruker AXS GmbH, Karlsruhe, Germany) using the symmetrical reflection mode with CuKα radiation (λ = 1.5406 Å) and Göbel mirror bent gradient multilayer optics. Scattered intensities were measured with a Våntec-1 line detector. The angular range included 3 to 40° in steps of 0.01°. Other relevant measurement conditions were as follows: target, Cu; filter, Ni; voltage, 40 kV; current, 40 mA; measuring time, 0.1 s step^{-1}. The diffraction patterns of the crystallized samples were compared with those of the structures available in the Cambridge Structural Database (Cambridge Crystallographic Data Centre (CCDC), Cambridge, UK).

The DSC analysis was carried out with a Mettler Toledo DSC 821^e thermal analysis system, equipped with the STAR^e software version 9.30 (Mettler-Toledo AG, Greifensee, Switzerland). The measuring parameters were as follows: 10 °C min^{-1} linear heating rate, argon as carrier gas (100 mL min^{-1}), 2–5 mg sample weight, 25–300 °C temperature interval. A sealed 40-µL aluminum crucible with three leaks in the lid was used for the measurements.

2.4 Factorial Design

A 3^2 full factorial design was applied to identify the relevant factors affecting the impinging jet-crystallized product. In series I and II, the influence of the additive concentration and the post-mixing time on three independent variables, i.e., on roundness, $d(0.5)$, and $D[4,3]$, was investigated. Tab. 1 shows the influential levels of these two factors. The experiments were performed in a randomized sequence. The following equation describing the interactions of the factors was used to determine the response surface and the relative effects of each factor investigated (b):

$$y = b_0 + b_1x_1 + b_2x_2 + b_3x_1^2 + b_4x_2^2 + b_5x_1x_2 \quad (2)$$

Statistica for Windows 12 AGA software (StatSoft Inc., Tulsa, OK, USA) was used for the calculations. The confidence interval was chosen to be 95 %, i.e., the differences were regarded as significant at $p < 0.05$.

Table 1. Values of factors investigated by the 3^2 full factorial design.

Factor	Low level (–)	Mid level (0)	High level (+)
Series I			
KCl concentration [ppm]	0	1000	2000
Post-mixing time [min]	0	5	10
Series II			
KCl concentration [ppm]	0	100	200
Post-mixing time [min]	0	5	10

2.5 Determination of the Residual Solvent Content

The residual solvent content was analyzed by a headspace gas chromatographic method using a Varian CP-3800 gas chromatograph (Varian, Walnut Creek, CA, USA) with a DB-624 capillary column (60 m × 0.25 mm × 1.4 µm, nominal) equipped with a Tekmar Dohrmann 7000 headspace autosampler and a flame ionization detector. The conditions for the gas chromatographic analysis were as follows: the oven temperature was initially maintained at 40 °C for 6 min and then raised to 194 °C at a rate of 7 °C min^{-1}, at which the sample was held for 0 min. The temperature of the injector was set to 220 °C and the detector temperature was set to 270 °C. Helium was used as the carrier gas at a volume of 1.5 mL min^{-1}.

Aliquots of 1 mL were injected in split mode, with a split ratio of 8:1. The platen temperature was 80 °C, the loop temperature was 90 °C, and the transfer line temperature was 110 °C. The sample equilibration time was 20 min. The gas flow rates of hydrogen, air, and nitrogen were 30, 300, and 25 mL min^{-1}, respectively. The ethanol concentration of the standard solution was 100 $\mu g\,mL^{-1}$. The blank sample contained 500 mg of sodium sulfate dissolved in 1 mL water for injection in a 20-mL headspace vial. The standard sample contained the same quantity of sodium sulfate dissolved in 1 mL of standard solution, while the sample solution contained 500 mg sodium sulfate and 100 mg crystallized glycine with the KCl sample dissolved in 1 mL water for injection.

2.6 Determination of the KCl Content

2.6.1 Qualitative Determination of the KCl Content

SEM (Hitachi S-4700 cold field emission microscope type II) with energy dispersive X-ray spectroscopy (EDS) (Röntec XFlash energy dispersive X-ray spectrometer, Berlin, Germany) was used to examine the topology, the composition, and the elemental map of the samples. The resolution limit of this unit was 1.5 nm; the rate of magnification was 2500×. The samples were made conductive by sputter-coating, producing an approximately 3-nm gold-palladium surface layer to avoid charging effects.

2.6.2 Quantitative Determination of the KCl Content

Determination of the KCl concentration of the samples was performed by flame atomic absorption spectrometry (FAAS). A Perkin Elmer 4100 ZL (Überlingen, Germany) flame atomic absorption spectrometer equipped with a deuterium background correction system and an air-acetylene burner was used for the determination of the potassium content. The conventional working parameters for the instrument were as follows: a wavelength of 766.5 nm, a spectral bandwidth of 0.7 nm, an acetylene flow rate of 2.5 L min–1, and a nebulizer flow rate of 8.0 mL min–1. The concentration of the standard potassium stock solution was 1000 ppm (Acidum-2 Ltd., Debrecen, Hungary); the calibration series were made using a 0.2 M HNO3 solution and the stock solution in various quantities. The sample solutions were also prepared using the 0.2 M HNO3 solution.

3 Results and Discussion

3.1 Crystal Morphology

The crystallization results for the two series of experiments are presented in Tabs. 2 and 3, showing the percentage yield, the average values of roundness, the particle size ($d(0.5)$ and $D[4,3]$), and the residual potassium content of the products.

In our initial pilot research, a high concentration (5000–8000 ppm) of KCl was applied as additive, but these concentrations did not prove to be suitable to achieve the appropriate morphology in case of the impinging jet method. Thus, in series I, the concentration of additive was decreased, and the concentration range of 1000–2000 ppm of KCl was found to produce the desired effect: it improved the crystal roundness and reduced the particle size. An increasing post-mixing time was found to adversely affect these properties. The additive concentration of 1000 ppm KCl and 0 min of post-mixing time were demonstrated to yield crystals with the most favorable properties, indicating that a lower concentration of additive contributes to the optimal glycine particle shape and to a lower level of residual impurity in case of impinging jet crystallization. Therefore, in series II, the additive concentration was decreased sharply.

In series II, the morphology of the glycine crystals was also found to be modified, even by a small amount of KCl added, in comparison to the samples without additive. This series of experiments clearly demonstrated that using low concentrations of KCl resulted in even better properties of the crystal habit compared to using higher concentrations of the additive. Even 100 ppm of additive appreciably improved the roundness of the crystals. A KCl concentration of 200 ppm and 0 min of post-mixing time were found to yield the smallest particle size and the most favorable roundness. The laser diffraction analysis of all samples demonstrated a monodisperse PSD. In Fig. 2, the PSD diagrams of the most favorable samples of series I and II, and of the sample without additive, are illustrated and compared to each other. Differences in particle size between the samples produced by the different parameters can be recognized.

Table 2. Crystallization results in series I.

KCl concentration [ppm]	Post-mixing time [min]	Percentage yield [wt %]	Roundness [–]		Particle size [µm]		Residual potassium [ppm]
			Mean	SD	$d(0.5)$	$D[4,3]$	
0	0	52.27	2.36	1.05	37.728	44.959	1
0	5	56.53	2.62	1.36	39.662	46.803	1
0	10	56.81	2.34	0.95	39.082	44.206	1
1000	*0*	*54.55*	*1.86*	*0.63*	*31.929*	*41.233*	*123*
1000	5	60.97	2.03	0.84	34.162	38.606	167
1000	10	61.62	2.25	0.84	36.125	40.441	182
2000	0	51.56	2.16	0.93	36.682	42.789	184
2000	5	61.90	2.09	0.82	37.031	48.429	233
2000	10	61.81	2.20	0.90	40.854	46.361	364

Table 3. Crystallization results in series II.

KCl concentration [ppm]	Post-mixing time [min]	Percentage yield [wt %]	Roundness [–]		Particle size [µm]		Residual potassium [ppm]
			Mean	SD	$d(0.5)$	$D[4,3]$	
0	0	52.27	2.36	1.05	37.728	44.959	1
0	5	56.53	2.62	1.36	39.662	46.803	1
0	10	56.81	2.34	0.95	39.082	44.206	1
100	0	58.48	1.68	0.42	37.814	44.684	33
100	5	58.78	1.65	0.39	33.970	40.311	30
100	10	60.88	1.67	0.48	38.446	43.444	31
200	*0*	*59.58*	*1.63*	*0.41*	*30.877*	*38.443*	*35*
200	5	56.29	1.65	0.36	33.562	39.237	22
200	10	60.78	1.62	0.38	36.083	41.909	48

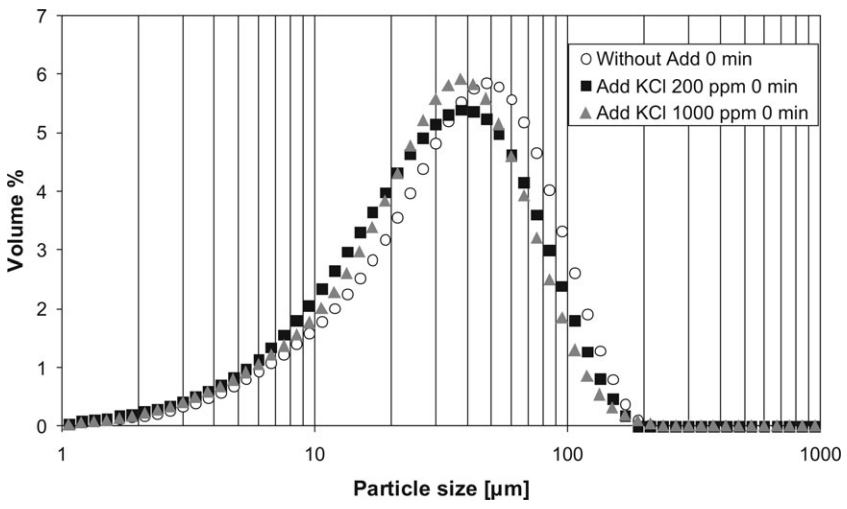

Figure 2. Particle size distributions of selected samples. Add: additive.

The quantitative measurement of the residual potassium content of the products was carried out by FAAS, as this is the most frequently used detector technique for the quantitative determination of this element. The crystal samples produced by using a higher concentration (1000–2000 ppm) of KCl as additive were found to have a residual potassium content of 123–364 ppm. These values were found to be proportional to the length of the post-mixing time. A longer post-mixing time increased the residual potassium content because a higher amount of KCl was allowed to get adsorbed on the surface of the glycine crystals. The products generated in series II contained by one order of magnitude less potassium (22–48 ppm) compared to those produced in series I.

The percentage yield in the two series ranged between 52 and 62 %. An increasing effect of the KCl addition was noticeable for this parameter. The presence of KCl increased the solubility of glycine; therefore, the increased saturation concentration of glycine resulted in a higher supersaturation value in the same water-ethanol mixture. Hence, if a bigger amount of glycine was dissolved, higher supersaturation occurred. This condition is preferred over the higher percentage yield. The supersaturation also influenced the crystal habit; it increased the nucleation rate and was favorable for the smaller particle size, and it also improved the crystal roundness. The optimal supersaturation and KCl concentration were achieved in series II. Besides, the percentage yield also depended on the post-mixing time: With increasing post-mixing time, the yield was also increased. During post-mixing, crystal growth could be considered to increase the percentage yield. Without post-mixing time, the nuclei had no time to grow further, since they were filtered off immediately. The filterability of all the crystallized products was satisfactory in our small-volume system, since the obtained filter cake did not inhibit the removal of the solution and did not decrease the flow rate of the dispersion medium.

The SEM images show the differences in crystal size and morphological parameters of the experimental products. Those crystals with the smallest average particle size and the most favorable roundness are presented in Fig. 3. The original glycine contained large isodimensional crystals with a smooth surface. The products yielded by the impinging jet crystallization process were shown to have a significantly smaller average particle size. The sample without additive consisted of irregularly shaped, needle-like crystals with a smooth surface and poor roundness, and also exhibited a slight tendency to aggregate. On the other hand, the products crystallized with the KCl additive contained bipyramidal-shaped, small-size, individual crystals with a smooth surface. The crystals produced by using 200 ppm of the additive show the most favorable morphology, as confirmed by the analytical data.

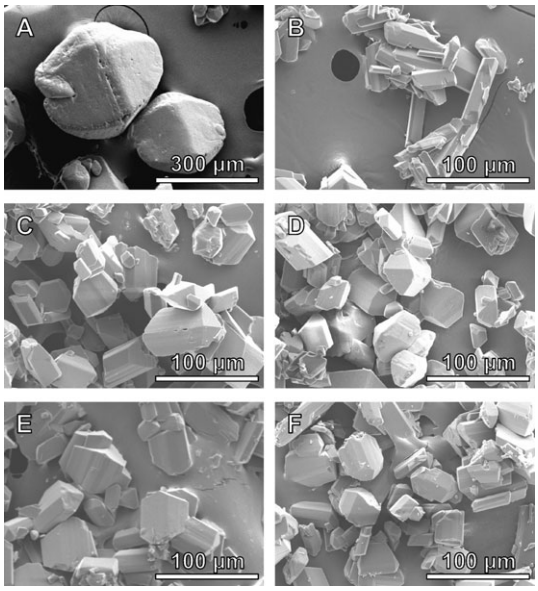

Figure 3. SEM images of glycine crystals. (a) Initial glycine, (b) without additive, (c) with KCl 1000 ppm, (d) with KCl 2000 ppm, (e) with KCl 100 ppm, (f) with KCl 200 ppm.

3.2 Polymorphism

The polymorphism of the initial material and the products was examined immediately after vacuum drying, by both XRPD and DSC, in parallel. The XRPD diffractograms were compared with the structures available in the Cambridge Structural Database (Fig. 4). Based on the XRPD analysis, both the initial material and all the products were found to contain only the stable α-polymorph. The more sensitive DSC measurements, however, revealed two polymorphs (Fig. 5). The thermograms of the original glycine and of the products also contained two endothermic peaks at about 251 and 254 °C. The first peak corresponds to a small amount of the less stable β-form. The second one is the melting point of the α-form. It was not possible to specify the proportion of the polymorphs because the two endothermic peaks overlapped. Based on the literature, a higher additive concentration favors the formation of γ-glycine, as it was mentioned above [27]. The phase transition of the γ-form to the α-polymorph causes a small endothermic peak at about 179 °C. Our results indicate that our samples did not contain any amount of the γ-form, supporting the notion that the low concentrations of KCl applied did not change the crystal structure and the initial α-form was preserved in all the crystallized products.

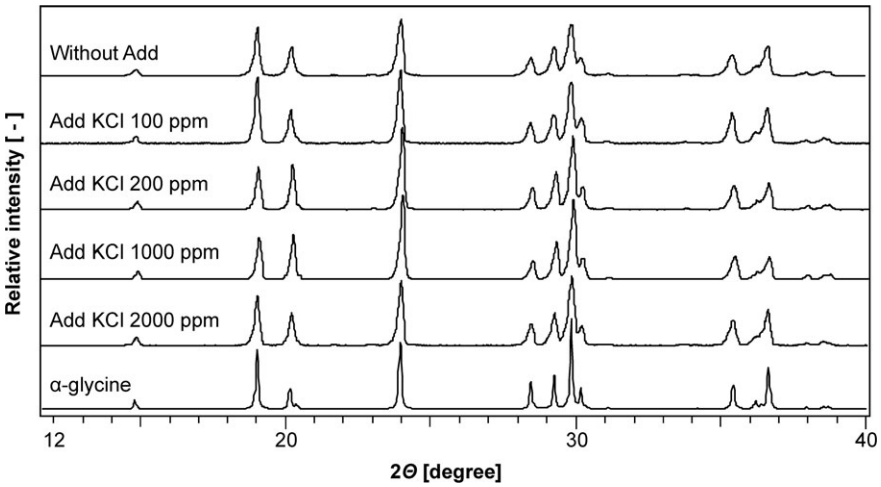

Figure 4. XRPD diffractograms of the initial material and of the crystallized products. Add: additive.

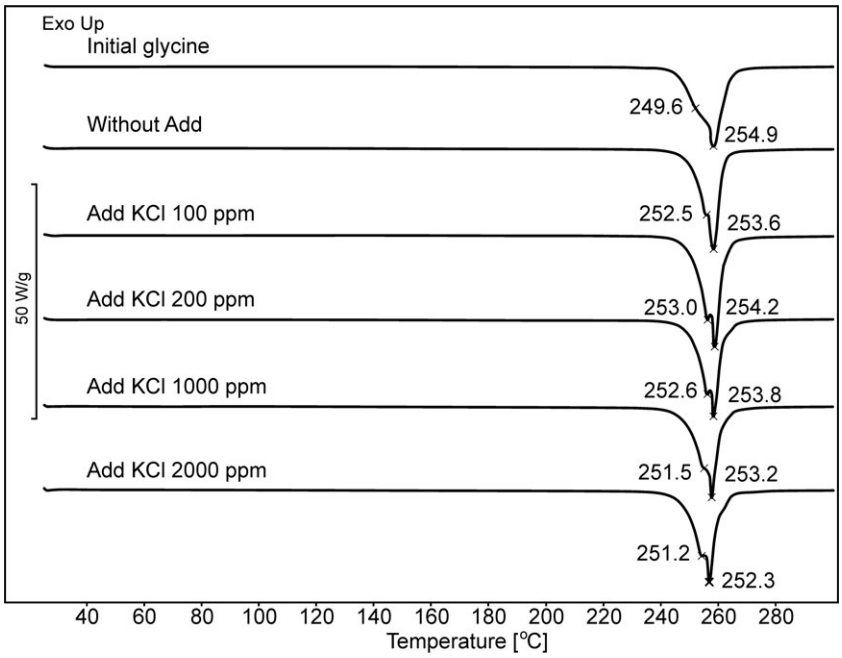

Figure 5. DSC thermograms of the initial material and of the crystallized products. Add: additive.

3.3 Statistical Analysis

The statistical analysis aimed to explore the effects of the crystallization parameters on the roundness and particle size of the crystals, and the results can be seen in Tab. 4. In series I, the KCl concentration was revealed to exhibit a significant quadratic effect on the particle size, while it had no significant effect on the roundness because of outlier data. However, in series II, a tendency between the obtained data and an effect of the x_1 factor was noticeable. The KCl concentration was found to have a significant linear relationship with the changes in roundness, as well as with the $d(0.5)$ and $D[4,3]$ values. Thus, increasing the concentration of the additive within a certain range (0–200 ppm) was shown to improve the roundness and to reduce the average particle size. For all significant effects, $p < 0.036$.

Table 4. Factorial design results (x_1: KCl concentration; x_2: post-mixing time).

Dependent variable	Polynomial function	r^2
Series I		
Roundness	$y = 2.21 - 0.29x_1 + 0.14x_2 - 0.25x_1^2 + 0.05x_2^2 + 0.03x_1x_2$	0.74
$d(0.5)$	$y = 37.03 - 0.64x_1 + 3.24x_2 - 4.43x_1^2 - 0.12x_2^2 + 1.41x_1x_2$	0.99
$D[4,3]$	$y = 43.76 + 0.54x_1 + 0.68x_2 - 5.50x_1^2 + 1.28x_2^2 + 2.16x_1x_2$	0.77
Series II		
Roundness	$y = 1.92 - 0.79x_1 - 0.03x_2 - 0.38x_1^2 + 0.08x_2^2 - 0.03x_1x_2$	0.97
$d(0.5)$	$y = 36.36 - 5.32x_1 + 2.40x_2 + 0.58x_1^2 - 0.94x_2^2 + 1.93x_1x_2$	0.76
$D[4,3]$	$y = 42.67 - 5.46x_1 + 0.49x_2 + 0.22x_1^2 - 0.82x_2^2 + 2.11x_1x_2$	0.71

3.4 Residual Solvent and Potassium Content

The residual ethanol content of the samples was analyzed by headspace gas chromatography due to the high risk of the occurrence of solvent (antisolvent) inclusions that may be associated with such an extremely rapid crystallization technique as used here. Ethanol belongs to the International Council for Harmonisation (ICH) Q3C(R5) Guideline Class 3, with an upper limit of residual concentration of 5000 ppm [30]. The ethanol contents of the products of series I and II were between 38 and 80 ppm, which is minimal compared to the maximum value defined in the ICH requirements.

The arrangement of the residual KCl content within the samples was examined by SEM-EDS. Within the products containing high concentrations (5000 ppm) of the additive, the KCl crystals were found to be arranged separately and individually, as seen in Fig. 6 visualizing K and Cl as bright spots. In case of low additive concentrations (100–200 ppm), in the SEM-EDS elemental maps, well-defined separate KCl crystals were not recognized; KCl was only found to be adsorbed widespread on the crystal faces all over the sample surfaces. In case of higher concentrations, those K and Cl ions not able to adsorb to the faces because of their high quantity arranged themselves separately and individually next to the glycine crystals. Based on the literature, KCl prefers to adsorb to the (011) crystal face of glycine and inhibits further incorporation of glycine molecules into the crystal lattice along the c direction [27]. Thus, the adsorption of KCl inhibits the lengthwise growth of the crystals: in case of this rapid crystallization method, the enhancing effect of KCl in the a direction is smaller than the inhibiting effect displayed in the c direction, while crystal growth in direction b is not affected by KCl. This way, it is possible that the additive also has a decreasing effect on the particle size. During the post-mixing period, the growth in directions a and b becomes prominent, as the faces have more time to grow without limit. Presumably, the lack of the post-mixing period causes the more favorable roundness.

4 Conclusions

The current research is the first example of combining the impinging jet crystallization method with the application of potassium chloride as an additive. The combination method was demonstrated to improve the crystal habit of glycine, despite the extremely rapid nature of the crystallization process. Even low concentrations of the

Figure 6. SEM image and EDS elemental maps of potassium and chlorine for the arrangement of KCl crystals within the glycine products containing 5000 ppm of additive. SE: SEM-EDS.

additive proved sufficient for an appropriate effect: As little as 100 and 200 ppm of KCl could significantly improve the roundness and reduce the particle size of the glycine crystal products. Based on the 3^2 full factorial design applied to identify the relevant factors affecting the impinging jet-crystallized product, the post-mixing time was demonstrated to be another important process parameter. A KCl concentration of 200 ppm and 0 min of post-mixing time were found to yield the smallest particle size and the most favorable roundness.

Residual KCl crystals were found to be arranged separately and individually within the products containing high concentrations of the additive, while those containing low concentrations of the additive were found to have residual KCl adsorbed on the crystal faces all over the sample surfaces. The crystallized product was characterized by low residual solvent and potassium contents. The newly applied jet crystallization method yielded a stable polymorph. Therefore, this study supports the notion that combining impinging jet crystallization with the application of an additive produces microparticles with the desired crystal morphology when the parameters of crystallization are chosen correctly.

Acknowledgment

The authors are grateful for the support of the DAAD-MÖB, project no. 39349.

The authors have declared no conflict of interest.

Abbreviations

API	active pharmaceutical ingredient
DSC	differential scanning calorimetry
EDS	energy dispersive X-ray spectroscopy
FAAS	flame atomic absorption spectrometry
PSD	particle size distribution
SEM	scanning electron microscopy
s.gr.	space group
XRPD	X-ray powder diffractometry

References

[1] M. Tanaka, S. Yamanaka, Y. Shirakawa, A. Shimosaka, J. Hidaka, *Adv. Powder Technol.* **2011**, *22*, 125–130. DOI: 10.1016/j.apt.2010.09.012

[2] H. Tamura, K. Kadota, Y. Shirakawa, Y. Tozuka, A. Shimosaka, J. Hidaka, *Adv. Powder Technol.* **2014**, *25*, 847–852. DOI: 10.1016/j.apt.2013.12.010

[3] C.-S. Su, C.-Y. Liao, W.-D. Jheng, *Chem. Eng. Technol.* **2015**, *38*, 181–186. DOI: 10.1002/ceat.201300573

[4] J. Xu, K. Q. Luo, *Chem. Eng. Res. Des.* **2014**, *92*, 2542–2549. DOI: 10.1016/j.cherd.2014.03.018

[5] N. Variankaval, A. S. Cote, M. F. Doherty, *AIChE J.* **2008**, *54*, 1682–1688. DOI: 10.1002/aic.11555

[6] M. S. Hassan, R. Lau, *Int. J. Pharm.* **2011**, *413*, 93–102. DOI: 10.1016/j.ijpharm.2011.04.033

[7] M. Midler, E. L. Paul, E. F. Whittington, M. Futran, P. D. Liu, J. Hsu, S. H. Pan, *US Patent 5 314 506*, **1994**.

[8] X. Y. Woo, R. B. H. Tan, R. D. Braatz, *Cryst. Growth Des.* **2009**, *9*, 156–164. DOI: 10.1021/cg800095z

[9] M. Jiang, Y.-E. D. Li, H.-H. Tung, R. D. Braatz, *Chem. Eng. Process.* **2015**, *97*, 242–247. DOI: 10.1016/j.cep.2015.09.005

[10] A. M. R. Bakar, K. Z. Nagy, N. A. Saleemi, D. C. Rielly, *Cryst. Growth Des.* **2009**, *9*, 1378–1384. DOI: 10.1021/cg800595v

[11] G. He, V. Bhamidi, S. R. Wilson, R. B. H. Tan, P. J. A. Kenis, C. F. Zukoski, *Cryst. Growth Des.* **2006**, *6*, 1746–1749. DOI: 10.1021/cg0602515

[12] S. V. Goryainov, E. V. Boldyreva, E. N. Kolesnik, *Chem. Phys. Lett.* **2006**, *419*, 496–500. DOI: 10.1016/j.cplett.2005.11.123

[13] M. Matsumoto, Y. Wada, K. Onoe, *Adv. Powder Technol.* **2015**, *26*, 415–421. DOI: 10.1016/j.apt.2014.11.014

[14] E. V. Boldyreva, V. A. Drebushchak, T. N. Drebushchak, I. E. Paukov, Y. A. Kovalevskaya, E. S. Shutova, *J. Therm. Anal. Calorim.* **2003**, *73*, 409–418. DOI: 10.1023/A:1025405508035

[15] E. V. Boldyreva, V. A. Drebushchak, T. N. Drebushchak, I. E. Paukov, Y. A. Kovalevskaya, E. S. Shutova, *J. Therm. Anal. Calorim.* **2003**, *73*, 419–428. DOI: 10.1023/A:1025457524874

[16] I. Weissbuch, V. Y. Torbeev, L. Leiserowitz, M. Lahav, *Angew. Chem., Int. Ed.* **2005**, *44*, 3226–3229. DOI: 10.1002/anie.200500164

[17] S. J. Cooper, *CrystEngComm* **2001**, *3*, 270–273. DOI: 10.1039/B108827K

[18] G. R. Dillip, G. Bhagavannarayana, P. Raghavaiah, B. Deva Prasad Raju, *Mater. Chem. Phys.* **2012**, *134*, 371–376. DOI: 10.1016/j.matchemphys.2012.03.004

[19] D. J. Tobler, J. D. Rodriguez Blanco, K. Dideriksen, K. K. Sand, N. Bovet, L. G. Benning, S. L. S. Stipp, *Procedia Earth Planet. Sci.* **2014**, *10*, 143–148. DOI: 10.1016/j.proeps.2014.08.047

[20] K. Srinivasan, *J. Cryst. Growth* **2008**, *311*, 156–162. DOI: 10.1016/j.jcrysgro.2008.10.084

[21] B. Al-Taani, M. Sheikh-Salem, S. A. Taani, *Jordan J. Pharm. Sci.* **2009**, *2*, 86–97.

[22] G. Liu, T. B. Hansen, H. Qu, M. Yang, J. P. Pajander, J. Rantanen, L. P. Christensen, *Chem. Eng. Technol.* **2014**, *37*, 1297–1304. DOI: 10.1002/ceat.201400206
[23] W. Kaialy, H. Larhrib, B. Chikwanha, S. Shojaee, A. Nokhodchi, *Int. J. Pharm.* **2014**, *464*, 53–64. DOI: 10.1016/j.ijpharm.2014.01.026
[24] W. Kaialy, M. Maniruzzaman, S. Shojaee, A. Nokhodchi, *Int. J. Pharm.* **2014**, *477*, 282–293. DOI: 10.1016/j.ijpharm.2014.10.015
[25] M. Hrkovac, J. P. Kardum, N. Ukrainczyk, *Chem. Eng. Technol.* **2015**, *38*, 139–146. DOI: 10.1002/ceat.201400462
[26] X. Yang, J. Lu, X. Wang, C. Ching, *J. Cryst. Growth* **2008**, *310*, 604–611. DOI: 10.1016/j.jcrysgro.2007.11.072
[27] C. Sekar, R. Parimaladevi, *Spectrochim. Acta, Part A* **2009**, *74*, 1160–1164. DOI: 10.1016/j.saa.2009.09.026
[28] G. Han, P. S. Chow, R. B. H. Tan, *ISIC 18 Int. Symp. on Industrial Crystallization*, Zurich, September **2011**.
[29] T. Tari, Z. Fekete, P. Szabó-Révész, Z. Aigner, *Int. J. Pharm.* **2015**, *478*, 96–102. DOI: 10.1016/j.ijpharm.2014.11.021
[30] EMA/CHMP/ICH/82260/2006, *ICH Guideline Q3C (R5) on Impurities: Guideline for Residual Solvents*, European Medicines Agency, London **2015**.

III.

Effect of additive on glycine crystal habit by impinging jet crystallization

T. Tari, P. Szabó-Révész, Z. Aigner

Department of Pharmaceutical Technology, University of Szeged, Szeged, Hungary
tari.timea@pharm.u-szeged.hu

Crystal morphology is a very important factor in the processability of active agents and excipients. Thus, it is beneficial if the product of crystallization already possesses the desired particle size, shape and surface. In our previous work it was found that impinging jet crystallization is a very effective particle size reduction method for organic materials, such as glycine, and it results reproducible samples with narrow particle size distribution. However, that rapid antisolvent crystallization method causes unfavorable shaped, needle-like crystals. Due to the momentary and extremely rapid method, the changing of morphology is hardly feasible. In the present work our purpose was to produce glycine crystals with suitable roundness besides small average particle size, narrow particle size distribution and stable polymorphic form. The impinging jet crystallization process supplemented with different concentration of additives was applied for modifying the crystal habit of glycine particles. The effects of operating parameters, such as the post mixing time and the KCl concentration, were investigated by full factorial design.

1 Introduction

The crystal habit, such as particle size, shape and surface, influences the processability of active agents even in pharmaceutical, food or cosmetic industry. The method and the parameters of crystallization processes determine these properties. The small average particle size, narrow particle size distribution and suitable crystal shape of the poorly water-soluble drugs (BCS II) are very important factors in the field of formulation [1].
Impinging jet crystallization is an antisolvent method. The rich solution of the active agent and the antisolvent flow through two jet nozzles arranged diametrically opposite and facing each other. At the impinging point will be high supersaturation producing a monodisperse population of small crystals. As well as in our previous work, it was proved that impinging jet crystallization is a very effective particle size reduction method for organic materials such as glycine, and in case of the rapid crystallization, the change of crystal morphology is hardly feasible [2].
Glycine crystals grow rapidly, their particle size is typically large. Glycine exists in three polymorphic forms under ambient conditions. Forms α (space group: $P2_1/n$) and β (s. g.: $P2_1$) are monoclinic, while γ (s. g.: $P3_1$) is trigonal. α-glycine is obtained by spontaneous nucleation in aqueous solution as the main polymorph from pure aqueous solutions and it is stable at ambient conditions. The γ-form is the most stable at low temperature, but it transforms to the α-form at high temperature. The β-form is the less stable polymorph at all conditions [3].
Additives selectively inhibit or enhance growth of crystal faces with several mechanisms and effectively change the morphology. For example, the additive molecule is able to adsorb to the competent crystal face and then it is incorporated into the crystal lattice or after the adsoption it can desorb. The probable mode of the bonding depends on the molecular arrangement and the crystal structure. The concentration and type of additives can influence the occurance of the different polymorphic forms, also the additives can improve the dissolution rate or control the impurity in the products [4]. *C. Sekar et al*. used high concentration of potassium chloride additive for the slow evaporation crystal-

lization method of glycine. The preferential adsorption of KCl to the (011) crystal face was confirmed in case of the α-form, and the high concentration of KCl resulted the γ-form [5].
In the present work, our purpose was to produce glycine crystals by impinging jet crystallization with suitable roundness besides small average particle size, narrow particle size distribution and stable polymorphic form. The impinging jet process supplemented with different concentration of additives was applied for modifying the crystal habit of glycine particles. The effect of different potassium chloride concentrations and post mixing times were studied by means of a 3^2 full factorial design.

2 Experimental methods

2.1 Materials

Glycine and ethanol 96% were supplied by VWR (Leuven, Belgium); potassium chloride was obtained from Scharlau (Barcelona, Spain); purified water (Ph. Eur. quality).

2.2 Impinging jet crystallization

Crystallization experiments were carried out in a double-walled Schmizo crystallization reactor equipped with an IKA Eurostar digital mixer and the stirring speed was 250 rpm. The constant 25 °C temperature was adjusted with a Thermo Haake P5/C10 thermostat. Two calibrated peristaltic pumps were used for the saturated glycine solution with different concentration of additive and the ethanol 96% feeding to the impinging jet unit with permanent velocity. The schematic representation of the experimental apparatus is outlined in Fig. 1.
Two series were prepared and the parameters were chosen based on our previous results. In Serie I. the KCl concentrations were 0; 1000; 2000 ppm, in Serie II. they were 0; 100; 200 ppm. In case of both series the other examined parameter was the post mixing time, the values were 0; 5 and 10 min.

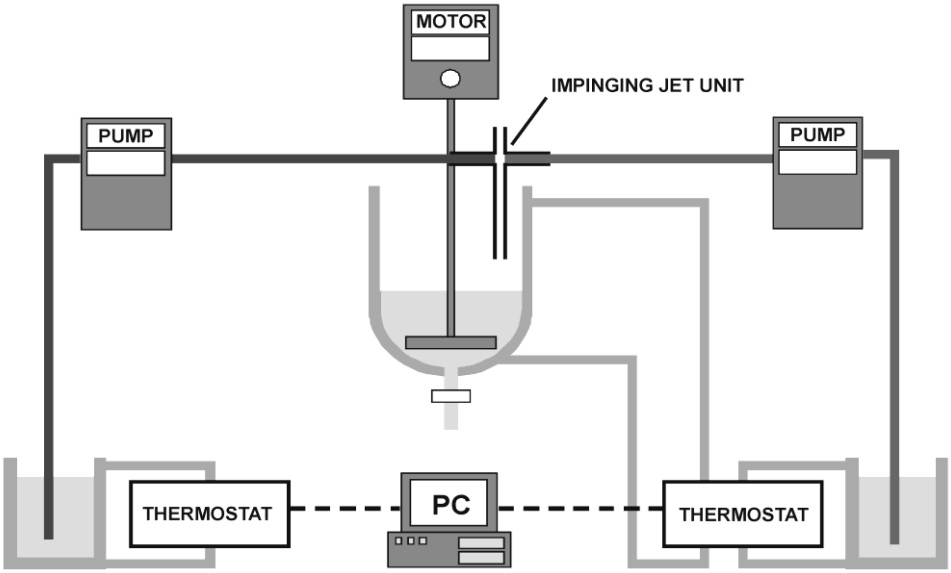

Fig. 1: Experimental apparatus

2.3 Methods

Roundness and morphology of the crystals were determined with the use of light microscopic image analysis system and scanning electron microscope (SEM). The particle size distribution was investigated with a laser diffraction particle size analyser. Polymorphism was characterized by differential scanning calorimetry (DSC) and powder X-ray

diffraction (XRPD). Headspace gas chromatography (GC) was utilized to determine the residual solvent content. The amount of the residual potassium of the products was detected by flame atomic absorption spectrometry (FAAS). The topology, the composition and the elemental map of the samples were examined by scanning electron microscope equipped with element dispersive X-ray spectroscopy (SEM-EDS). The results were analysed by means of a statistical program.

3 Results and Discussion

3.1 Crystal morphology

The crystallization results for the two series are presented in Tables 1 and 2. The percentage yield, the average results of roundness, d(0.5), D[4,3] and the residual potassium contant of the products are shown in the tables.

Tab. 1: Crystallization results in Serie I.

KCl conc.	Post mixing time	Percentage yield	Roundness		Particle size		Residual potassium
					d(0.5)	D[4,3]	
(ppm)	(min)	(m%)	Mean	SD	(µm)	(µm)	(ppm)
0	0	52.27	2.36	1.05	37.728	44.959	1
0	5	56.53	2.62	1.36	39.662	46.803	1
0	10	56.81	2.34	0.95	39.082	44.206	1
1000	**0**	**54.55**	**1.86**	**0.63**	**31.929**	**41.233**	**123**
1000	5	60.97	2.03	0.84	34.162	38.606	167
1000	10	61.62	2.25	0.84	36.125	40.441	182
2000	0	51.56	2.16	0.93	36.682	42.789	184
2000	5	61.90	2.09	0.82	37.031	48.429	233
2000	10	61.81	2.20	0.90	40.854	46.361	364

In Serie I. the added high concentration of KCl improved the crystal roundness and reduced the particle size. The increase of the post mixing time affected these properties adversely. The 1000 ppm KCl additive with 0 minute post mixing resulted in the crystals with the most favorable properties of habit.

Tab. 2: Crystallization results in Serie II.

KCl conc.	Post mixing time	Percentage yield	Roundness		Particle size		Residual KCl
					d(0.5)	D[4,3]	
(ppm)	(min)	(m%)	Mean	SD	(µm)	(µm)	(ppm)
0	0	52.27	2.36	1.05	37.728	44.959	1
0	5	56.53	2.62	1.36	39.662	46.803	1
0	10	56.81	2.34	0.95	39.082	44.206	1
100	0	58.48	1.68	0.42	37.814	44.684	33
100	5	58.78	1.65	0.39	33.970	40.311	30
100	10	60.88	1.67	0.48	38.446	43.444	31
200	**0**	**59.58**	**1.63**	**0.41**	**30.877**	**38.443**	**35**
200	5	56.29	1.65	0.36	33.562	39.237	22
200	10	60.78	1.62	0.38	36.083	41.909	48

In Serie II. the morphology of the crystals was also modified by the added small amount of KCl compared to the samples without additive. 100 ppm of additive has already im-

proved the roundness appreciably. This serie resulted in even better properties of the crystal habit compared to the higher concentrations. The 200 ppm KCl with 0 minute effected the smallest particle size and the most favorable roundness.
The amount of the residual potassium of the products was detected quantitatively by FAAS. In case of the higher concentration additive the values were between 123 and 364 ppm. The longer post mixing time increased the quantity. The products of Serie II. contained an order of magnitude less potassium (22–48 ppm) compared to the results of Serie I.
The differences in crystal size and morphological parameters can be seen in the SEM images, those products are presented which had the smallest average particle size and the most favorable roundness (Fig. 2). The original glycine contained large isodimensional crystals with a smooth surface. The products of impinging jet crystallization possess significantly smaller average particle size. The sample without additive consisted of irregular-shaped, needle-form crystals with smooth surface and poor roundness, also exhibited a slight tendency to aggregate. On the other hand the products crystallized with additive contained bypiramidal-shaped, small size, individually crystals with smooth surface. The crystals of 200 ppm additive show the most favorable morphology confirmed the measured data.

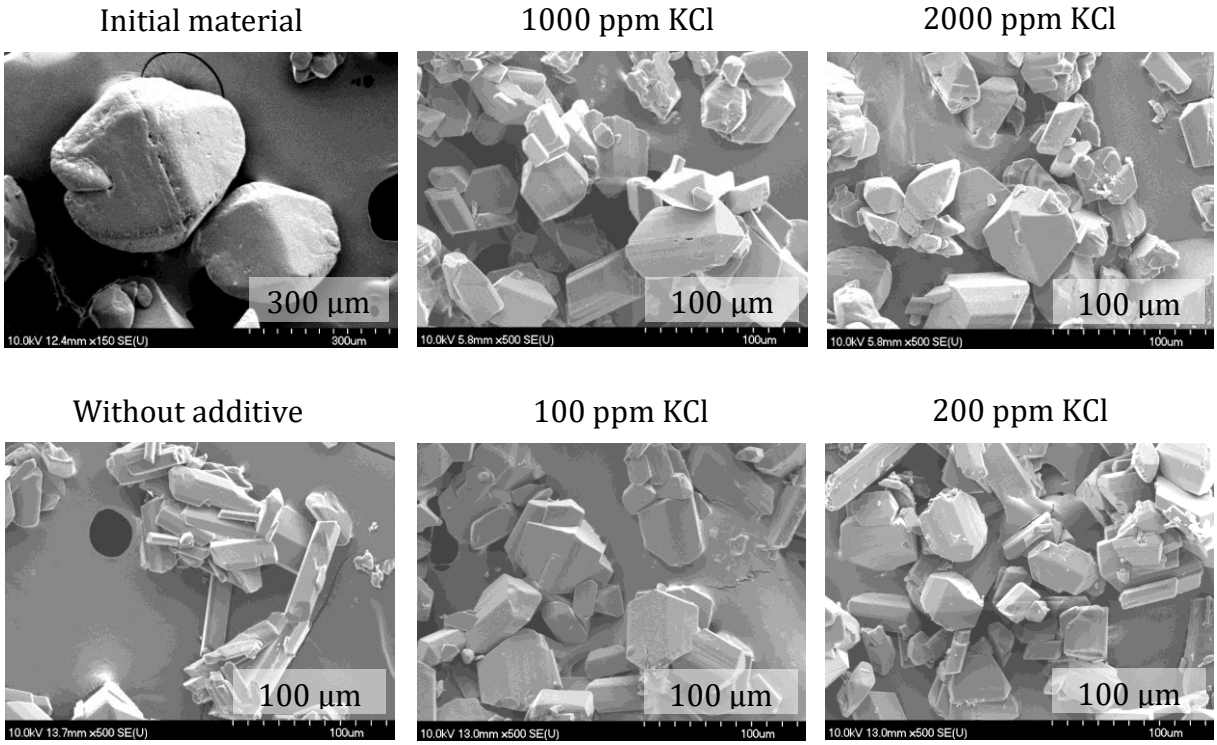

Fig. 2: SEM images of glycine crystals

3.2 Polymorphism

The polymorphism of the initial material and the products were examined with XRPD and DSC apparatus. The XRPD diffractograms were compared with the structures in the Cambridge Structural Database (Fig. 3). It was found that both the initial material and all the products consisted of the pure stable α-polymorph. The more sensitive DSC measurements represented two polymorphs (Fig. 4). The thermograms of the original glycine and the products also contained two endothermic peaks at about 251 °C and 254 °C. The first peak refers to a little amount of the less stable β-form. The second one is the melting point of the α-form. It was not possible to specify the proportion of the polymorphs because the two endothermic peaks were overlapped.

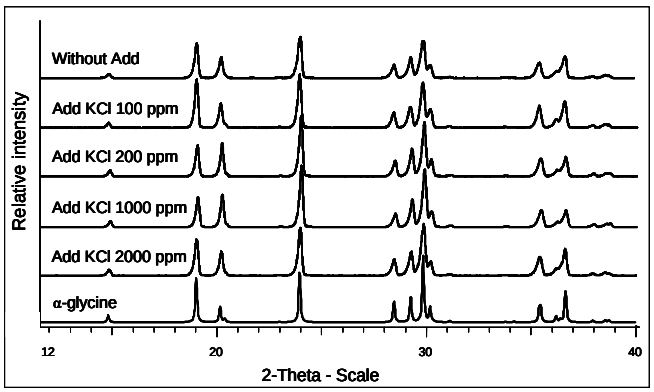

Fig. 3: XRPD diffractograms of the crystallized products

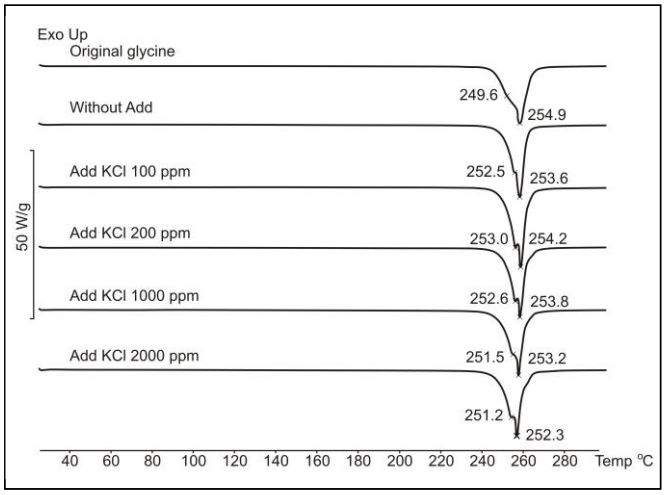

Fig. 4: DSC thermograms of the initial material and the crystallized products

3.3 Statistical analysis

Statistical analysis results related to the effects of the crystallization parameters on the roundness and the particle size. In case of Serie I. the KCl concentration exhibited a significant quadratic relationship with the changes in particle size, but this parameter did not display significant effect on the change of roundness. But in Serie II. the KCl concentration denoted a significant linear relationship with the change of roundness as well as the d(0.5) and D[4,3] results. An increase of the concentration improved the roundness and reduced the average particle size. The confidence interval was 95% and the alpha value indicating significant factors was 0.05. In case of all significant effects the $p<0.036$.

3.3 Residual solvent and potassium content

The residual ethanol content of the samples was detected due to the high risk of the occurrence of solvent inclusion which can happen during an extremely rapid crystallization. The ethanol quantity of the products was between 38 ppm and 80 ppm, which values were low relative to the maximum value – 5000 ppm – prescribed in the ICH requirements.

The arrangement of the KCl in the samples was examined by SEM-EDS. The KCl crystals were arranged separately and individually in the products containing high concentration additive, in Fig. 5 the bright spots denoted the K and the Cl. In case of low concentration additive the KCl arrenged diffuse on the samples, adsorbed to the crystal faces. Based on the literature KCl prefers adsorbing to the (011) crystal face of glycine and inhibits further glycine molecules incorporation into the crystal lattice along the „c" direction.

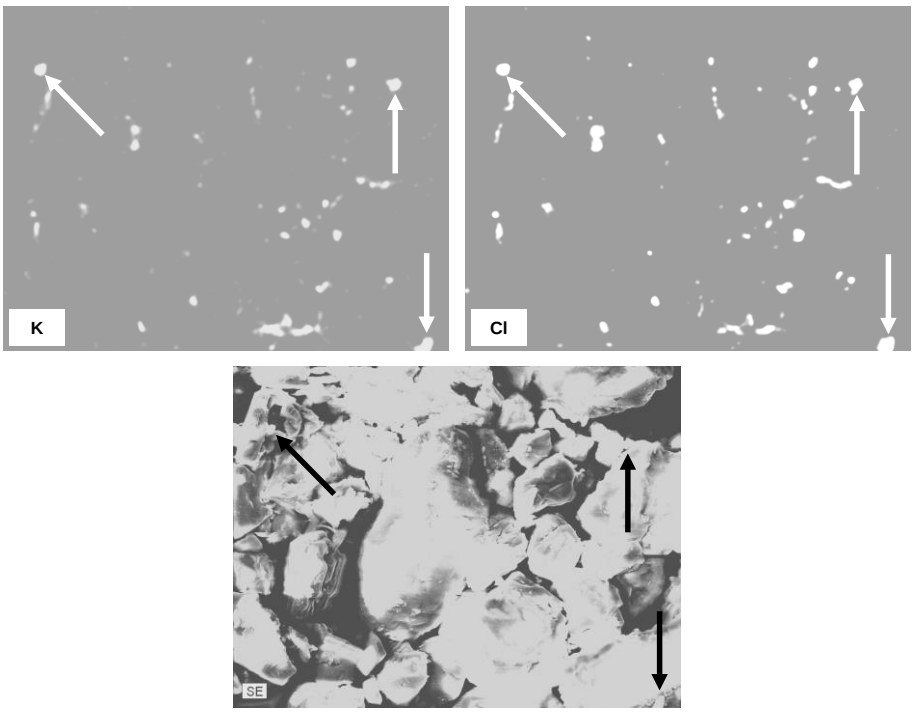

Fig. 5: The arrangement of KCl crystals in product
which contains high concentration additive by SEM-EDS

4 Conclusions

Impinging jet crystallization method supplemented with KCl additive was able to improve crystal habit of glycine despite of the extremely rapid process. For the suitable effect it was sufficient to apply low concentration of additives, already 100 and 200 ppm KCl could significantly advance the roundness and reduce the particle size. The KCl crystals were arranged separately and individually in the product containing high concentration additive and adsorbed to the (011) crystal face. That adsorption inhibited the lengthwise growing along the „c" direction of the glycine crystals. The product contained low residual solvent and potassium quantity. The method resulted in a stable polymorphic form. Thereby, the desired crystal morphology could be produced in only one step if the parameters of crystallization are chosen correctly.

References

(1) Xu, J.; Luo, K. Q. Enhancing the solubility and bioavailability of isoflavone by particle size reduction using a supercritical carbondioxide-based precipitation process. *Chem. Eng. Res. Des.* **2014,** *92,* 2542–2549.
(2) Tari, T.; Fekete, Z.; Szabó-Révész, P.; Aigner, Z. Reduction of glycine particle size by impinging jet crystallization. *Int. J. Pharm.* **2015,** *478,* 96–102.
(3) Boldyreva, E. V.; Drebushchak, V. A.; Drebushchak, T. N.; Paukov, I. E.; Kovalevskaya, Y. A.; Shutova, E. S. Polymorhism of glycine. Thermodynamic aspects. Part I. Relative stability of the polymorphs. *J. Therm. Anal. Calorim.* **2003,** *73,* 409–418.
(4) Kaialy, W.; Maniruzzaman, M.; Shojaee, S.; Nokhodchi, A. Antisolvent precipitation of novel xylitol-additive crystals to engineer tablets with improved pharmaceutical performance. *Int. J. Pharm.* **2014,** *477,* 282–293.
(5) Sekar, C.; Parimaladevi, R. Effect of KCl addition on crystal growth and spectral properties of glycine single crystals. *Spectrochim. Acta A* **2009,** *74,* 1160–1164.

IV.

Acta Pharmaceutica Hungarica 87. 69-76 2017.

Folyamatos kristályosítási eljárás fejlesztése impinging jet módszerrel

TARI TÍMEA*, AIGNER ZOLTÁN

Szegedi Tudományegyetem, Gyógyszerésztudományi Kar, Gyógyszertechnológiai és Gyógyszerfelügyeleti Intézet, H-6720 Szeged, Eötvös u. 6.
**Levelezési cím: tari.timea@pharm.u-szeged.hu*

Summary

Tari, T., Aigner, Z.: ***Development of continuous crystallization process using impinging jet method***

Introduction: *Nowadays, in pharmaceutical industry, it is a great challenge to convert technologies from batch to continuous mode. Our aim was to develop a continuous antisolvent crystallization method using impinging jet nozzles in case of glycine as model material and optimize the crystallization parameters for high quality product.*

Methods: *Impinging jet mixer was applied in non-submerged mode in a double-walled crystallization reactor, and samples were separated from the crystallized product at given intervals during continuous crystallization. Properties of the samples were examined by several analytical methods (laser diffraction particle size analyser, light microscopic image analysis system, scanning electron microscope, differential scanning calorimetry, powder X-ray diffraction, etc.)*

Results: *Morphology, average particle size, particle size distribution, residual solvent and additive potassium quantity of the continuous crystallized products were not changed significantly compared to the batch process. The main polymorph was the α form, during progression of crystallization, increasing of small amount of β-polymorphic form was observed. Percentage yield was improved compared to the batch crystallization method.*

Conclusion: *It was found, that the continuous impinging jet crystallization is suitable for producing of high quality, uniform product in large quantity. The method also proved to be reproducible.*

Keywords: *continuous crystallization, impinging jet, glycine, crystal habit, polymorphism*

Összefoglalás

Bevezetés: *A gyógyszeriparban manapság nagy kihívást jelent a hagyományos szakaszos technológiák átalakítása folyamatos eljárásokká. Jelen munkánkban célunk volt egy folyamatos antiszolvens kristályosítási módszer fejlesztése impinging jet technikával, glicin modell anyag esetében, és a kristályosítási paraméterek optimalizálása magas minőségű termék előállítása céljából.*

Módszerek: *Az impinging jet egységet a dupla-falú kristályosító reaktoron kívül elhelyezve („non-submerged" mód) alkalmaztuk, és a folyamatos kristályosítás során a kristályosított termékből adott időközönként mintákat különítettünk el. A termékminták tulajdonságait számos analitikai módszerrel vizsgáltuk (lézer diffrakciós szemcseméret analízis, fénymikroszkópos képanalizálás, pásztázó elektronmikroszkóp, differenciális pásztázó kaloriméter, porröntgen diffraktométer, stb.)*

Eredmények: *A folyamatos kristályosítással készült termék morfológiája, átlagos szemcsemérete, szemcseméret-eloszlása, maradék oldószer- és additív-tartalma nem változott a szakaszos előállítással készített termékhez képest. A kristályosított termék α-polimorf volt, mellette a folyamat előrehaladása során a β-polimorf forma kismértékű növekedését detektáltuk. A kitermelési százalék javult a szakaszos módszerhez képest.*

Összegzés: *Megállapítottuk, hogy a folyamatos impinging jet kristályosítás alkalmas reprodukálható, egyenletes minőségű, nagy mennyiségű termék előállítására.*

Kulcsszavak: *folyamatos kristályosítás, impinging jet, glicin, kristály habitus, polimorfia*

1. Bevezetés

A gyógyszeriparban manapság egyre inkább teret hódít a folyamatos technológiák kialakítása mind a kutatás-fejlesztés, mind a gyártás területén. A folyamatos eljárásnak számos előnye van a korábban alkalmazott szakaszos módszerekkel szemben, amelyek közül legmeghatározóbbak a költségek, az idő- és a helyigény jelentős csökkentése [1, 2]. A folyamatos módszer egységesebb terméket eredményez, hiszen a gyártási tételek közötti minőségi különbségek kiküszöbölhetőek, jobb kitermelés érhető el, a minőségi ellenőrzés könnyebben megvalósítható, az automatizálásuk egyszerűbben kivitelezhető [3, 4].

A hagyományos kristályosítási eljárások fejlesztése laborméretű reaktorokban kezdődnek, és a jelentős méretnövelés során nem minden esetben

vihetők át egyszerűen az optimális paraméterek ipari méretekbe. Nagyobb gyártási mennyiség eléréséhez nagy méretű reaktorok, drága készülékek szükségesek, melyeknek tisztítása időigényesebb, minden külön lépést validálni szükséges. A felsoroltak mindegyike a gyártásból kiesett időt jelentik. Folyamatos kristályosítás során elegendő egy kisméretű reaktor használata, hiszen a termék eltávolítása folyamatosan történik, használatuk gazdaságosabb [5-7]. Célszerű tehát a már létező és engedélyezett szakaszos eljárást átalakítani folyamatos módszerré, hiszen a megalkotott tervezési tér („design space") elemeit követve biztosítható az állandó minőségű termék, és lehetőség nyílik a mai szigorú szabályozások mellett is a gyorsabb engedélyeztetési eljárásra [8]. A megfelelő kristályosítási módszer megválasztásával pénz és energia spórolható, hiszen ha már a hatóanyaggyártás során optimális tulajdonságokkal rendelkezik a termék, nincs szükség további utóműveletek elvégzésére (pl. szemcseméret csökkentés, frakcionalizálás, egyéb technológiai műveletek) [9, 10].

A kristályhabitus, mint a szemcseméret, -felület és -alak, nagymértékben befolyásolják a hatóanyagok gyógyszerformába történő feldolgozhatóságát [11]. A kis átlagos szemcseméret és a szűk szemcseméret-eloszlás gyakori követelmény a rossz vízoldékonyságú (Biopharmaceutics Classification System, BCS II. csoportba tartozó) hatóanyagok esetében. Ezek a paraméterek befolyásolhatják az oldódási sebességet, biohasznosíthatóságot, stabilitást, a tablettákban a hatóanyagok eloszlatottságának egységességét [12, 13]. A megfelelő kerekdedségű és sima felszínű szemcsék agglomerációra kevésbé hajlamosak, így szűrhetőségük és porreológiai, folyási tulajdonságuk is kedvezőbbek. A szemcsék habitusa additívek hozzáadásával is módosítható, hiszen az additívek szelektíven gátolják vagy elősegítik az egyes kristályoldalak növekedését többféle mechanizmuson keresztül. Hatásuk függ többek között az anyagi minőségüktől és koncentrációjuktól, továbbá befolyásolhatják a hatóanyagok polimorfiáját, ezzel oldékonyságukat, a készített tabletták szilárdságát, hatékonyságát [14-16].

Impinging jet (IJ, „összeütköző sugarak") antiszolvens kristályosítás során a hatóanyagot tartalmazó telített oldat és az antiszolvens két külön, egymással szemben álló csövön keresztül áramlik nagy sebességgel. A kis térfogatú keverési térben az oldatok találkoznak, ahol nagy intenzitású mikrokeverés jön létre, homogén és nagy szuperszaturáció jelentkezik a nukleáció megindulása előtt, így elérhető a szűk szemcseméret-eloszlású, kis átlagos szemcseméretű termék előállítása. A szemcseméret-eloszlás és a kristály habitus befolyásolható a kristályosítási paraméterek változtatásával, mint például az áramlási sebesség, hőmérséklet vagy az utókeverési idő módosításával. A pillanatszerű, gyors kristályosítási folyamat következtében viszont a kristályok morfológiája nehezen befolyásolható [17-19].

A glicin a legegyszerűbb kémiai szerkezetű aminosav. Jellemzően gyors kristálynövekedéssel nagy méretű kristályokban kristályosodik, így különösen jól alkalmazható a habitus módosító és szemcseméret csökkentő eljárások hatékonyságának modellezésére. A glicinnek standard körülmények között három polimorf módosulata ismert: α-, β- és γ-forma. A módosulatok megjelenését befolyásolják a különböző kristályosítási paraméterek, mint pl. az oldószer és az antiszolvens minősége és aránya, a hőmérséklet, a különböző koncentrációjú additívek jelenléte. Vizes közegből spontán nukleációval képződő fő polimorfja az α-glicin. A kristályszerkezete monoklin (tércsoport: $P2_1/n$) és normál körülmények között ez a forma metastabil. A β-glicin a legkevésbé stabil módosulat, bizonyos idő elteltével átalakul α-polimorffá, kristályszerkezete szintén monoklin (tércsoport: $P2_1$). Megjelenését elősegíti az etanol és metanol jelenléte vizes közegben. Termodinamikailag a γ-glicin a legstabilabb polimorf forma standard körülmények között, melynek kristályszerkezete trigonális (tércsoport: $P3_1$). Azonban az α-glicin gyakrabban fordul elő vizes közegben, és nem alakul át ezen körülmények között γ-formává [20-22].

Korábbi vizsgálatainkban glicin kristályosításánál alkalmaztuk az impinging jet módszert és szemcseméret csökkentő hatását összehasonlítottuk a konvencionális kristályosítási eljárásokkal szemben. Megállapítottuk, hogy a hűtéses, az antiszolvens, illetve a reverz antiszolvens módszerekhez képest is több mint egy nagyságrendnyi szemcseméret csökkentést eredményezett az új módszer, megfelelő szemcseméret-eloszlás és maradék oldószer-tartalom mellett [23]. Továbbá megfelelő koncentrációjú kálium-klorid additív alkalmazásával elérhető a szemcsék kerekdedségének javítása, így közel szférikus szemcsék állíthatók elő alacsony maradék kálium-tartalom és stabil polimorf forma mellett [24].

Jelen munkánkban egy saját fejlesztésű impinging jet eszköz folyamatos kristályosítási eljárásban való alkalmazhatóságát vizsgáltuk nagy térfo-

gatú oldatok felhasználásával, additív jelenlétében. Célunk volt, hogy a módszer biztosítson megfelelő kitermelést, reprodukálható, gyors és pontos legyen. A korábbi vizsgálataink alapján optimalizált kristályosítási paramétereket alkalmaztuk glicin modell anyag esetében, és összehasonlítottuk a termék fizikai-kémiai tulajdonságait a szakaszos eljárás eredményeivel.

2. Anyagok és vizsgálati módszerek

2.1. Anyagok

Munkánk során a glicint, mint modell anyagot alkalmaztuk, melyet a VWR forgalmaz (Leuven, Belgium). Az antiszolvensként használt 96%-os etanol szintén a VWR terméke. Az additívként alkalmazott kálium-kloridot a Scharlau forgalmazza (Barcelona, Spanyolország). Oldószerként Ph. Hg. VIII. minőségű tisztított vizet használtunk.

2.2. Impinging jet kristályosítás

Az impinging jet egység külső elemként (non-submerged) volt alkalmazva a duplafalú, kerekített aljú Schmizo kristályosító reaktorral (Schmizo AG, Oftringen, Svájc), amelyben a folyamatos keverést egy IKA Eurostar digitális motorral meghajtott anker-típusú keverő biztosította 250 rpm fordulatszámmal (IKA-Werke GmbH & Co., Staufen, Németország). A folyadékok adagolását két azonos típusú kalibrált perisztaltikus pumpa végezte (Rollpump Type 5198, MTA Kutesz, Budapest, Magyarország). A 200 ppm KCl additívet tartalmazó telített glicin oldat és a 96%-os etanol állandó sebességgel (4,06 m/s) áramlott, 1:1 arányban az adott átmérőjű csöveken keresztül az impinging jet elem keverő terébe [24]. A kísérleteket állandó hőmérsékleten, 25 °C-on végeztük, amelyet Julabo F32 (Julabo GmbH, Seelbach, Németország) kriotermosztáttal biztosítottunk, Julabo EasyTemp 2.3e software vezérlésével. A folyamatos kristályosítás során keletkezett szuszpenzió szűrése szűrőnucson folyamatosan történt, ennek során percenként különítettünk el a nedves kristály frakciókat. A minták 40 °C-on, 24 óráig történő vákuum szárítása után zárt edényekben voltak tárolva. A teljes berendezés felépítése az ***1. ábrán*** látható.

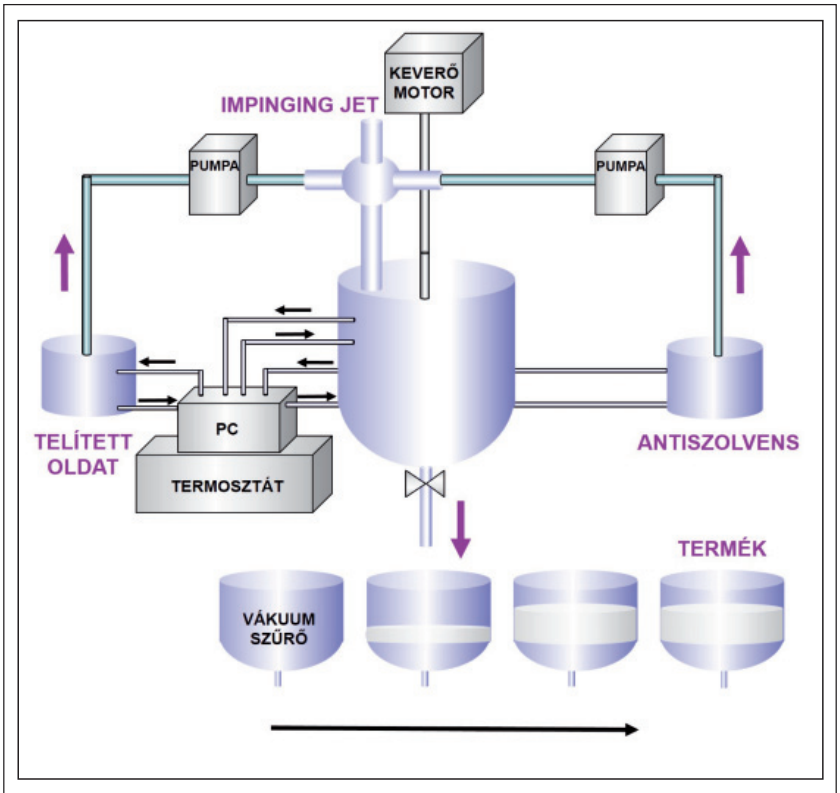

1. ábra: A saját fejlesztésű impinging jet kristályosítási rendszer sematikus felépítése

2.3. Termékek analitikai vizsgálatai

2.3.1. Kristály habitus és szemcseméret-eloszlás vizsgálata

A kristályosított termékek kerekdedségének és szemcseméretének vizsgálatát LEICA fénymikroszkópos képanalizátor (Leica LEICA Q500MC, LEICA Cambridge Ltd., Cambridge, UK), valamint pásztázó elektronmikroszkóp (SEM, Hitachi S-4700, Hitachi Scientific Ltd., Tokyo, Japán) segítségével végeztük. A SEM minták felületét aranypalládium bevonattal láttuk el a megfelelő elektromos vezetőképesség biztosítása céljából, Bio-Rad SC 502 készülék (VG Microtech, Uckfield, UK) alkamazásával.

A minták szemcseméret-eloszlását Malvern Mastersizer 2000 lézerdiffrakciós szemcseméret analizáló berendezéssel (Malvern Instruments Ltd., Malvern, UK) határoztuk meg, száraz módszerrel Scirocco száraz poradagoló segítségével. Két párhuzamos mérést alkalmaztunk minden minta esetében, a táblázatok az átlag értékeket tartalmazzák.

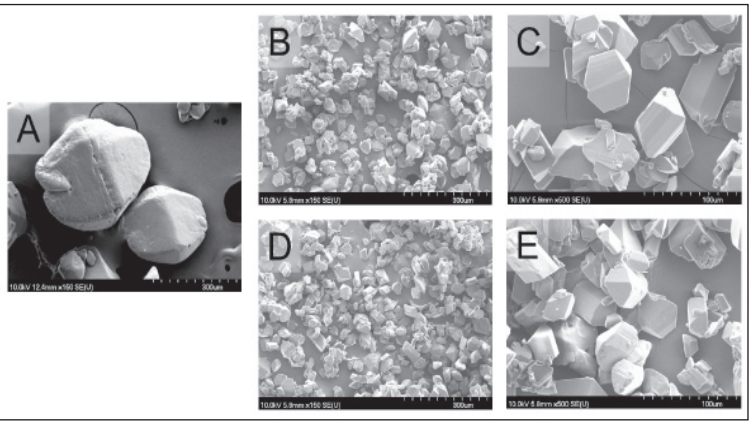

2. ábra: Minták SEM felvételei
A: kiindulási glicin (150x), B: termék 1. perc (150x), C: termék 1. perc (500x), D: termék 20. perc (150x), E: termék 20. perc (500x)

2.3.2. Polimorfia vizsgálata

A termékek polimorfiáját porröntgen (XRPD) készülék és differenciáló pásztázó kaloriméter (DSC) segítségével vizsgáltuk. Az XRPD mérésekhez Bruker D8 Advance diffraktométert (Bruker AXS GmbH, Karlsruhe, Németország) alkalmaztunk. A vizsgálatok fő paraméterei a következők voltak: szögtartomány: 3°-40° 2-Theta; lépésköz: 0,01°. A kristályosított termékek diffraktogramjait a Cambridge Szerkezeti Adatbázis adataival hasonlítottuk össze (Cambridge Crystallographic Data Centre, CCDC, Cambridge, UK).

A DSC analízis Mettler Toledo DSC 821^e (Mettler-Toledo AG, Greifensee, Svájc) berendezéssel történt. Az adatok értékelését STAR^e ver. 9.30 software-rel végeztük. A vizsgálatok paraméterei: hőmérsékleti tartomány: 25-300 °C; fűtési sebesség: 10 °C/perc.

2.3.3. Szennyezők vizsgálata

A minták maradék oldószer-tartalmának meghatározása headspace gázkromatográfiás módszerrel történt, vizsgálatainkat Varian CP-3800 gázkromatográffal (Varian, Inc., Walnut Creek, CA, USA) végeztük, DB-624 kapilláris oszlopon (60 m x 0.25 mm x 1.4 μm, nominal) kiegészítve Tekmar Dohrmann 7000 headspace automatikus mintavevővel és lángionizáló detektorral.

A kristályosítási additívként alkalmazott kálium maradék koncentrációjának pontos mérésére Perkin Elmer 4100 ZL (Überlingen, Németország) atomabszorpciós lángspektrométert alkalmaztunk (FAAS), deutérium háttér korrekciós rendszerrel és levegő-acetilén láng alkalmazásával.

3. Eredmények értékelése

3.1. Kristály habitus és szemcseméret-eloszlás

Az impinging jet antiszolvens kristályosítás során megnövelt térfogattal (1000-1000 ml) végeztük el kísérleteinket, a kristályosító reaktorban utókeverés nélkül folyamatosan történt a szuszpenzió továbbhaladása a szűrőbe, ahol percenként történt a mintavétel. Egy kristályosítási kísérlet időtartama 20 perc volt, a megadott paraméterekkel 3 párhuzamos mérést végeztünk. A továbbiakban az eredmények átlagértékeit mutatjuk be.

A SEM felvételeken látható, hogy a kiindulási anyag lekerekített oldalú, nagy, izodimenziós szemcsékből áll, ezzel szemben az impinging jet kristályosított termékek szemcsemérete jelentősen csökkent, alakja bipiramidális, felszíne sima. A gyors kristályosítási eljárásból adódóan az élek és csúcsok nincsenek lekerekedve. Ezek a tulajdonságok biztosítják, hogy a kristályok egyedi szemcsé-

I. táblázat
Kristályosított minták szemcseméret-eloszlása

Minta [perc]	d (0,1) [μm]	d (0,5) [μm]	d (0,9) [μm]
1.	8,524	27,934	70,382
2.	7,701	25,899	68,285
3.	8,520	29,278	74,356
4.	8,360	28,265	69,346
5.	8,758	29,969	75,320
6.	9,292	33,190	82,260
7.	9,577	34,313	84,812
8.	9,657	33,825	77,717
9.	9,674	34,066	78,151
10.	8,990	30,854	70,155
11.	8,864	30,308	69,338
12.	8,567	29,334	72,748
13.	8,626	29,748	74,385
14.	9,605	34,028	77,861
15.	9,627	33,880	77,352
16.	9,259	32,922	76,072
17.	9,197	32,470	75,244
18.	9,367	33,379	76,586
19.	9,417	33,622	77,036
20.	9,358	33,719	78,712
Átlag	**9,047**	**31,550**	**75,306**
Szórás	**0,54**	**2,54**	**4,35**
Relatív szórás	**0,06**	**0,08**	**0,06**

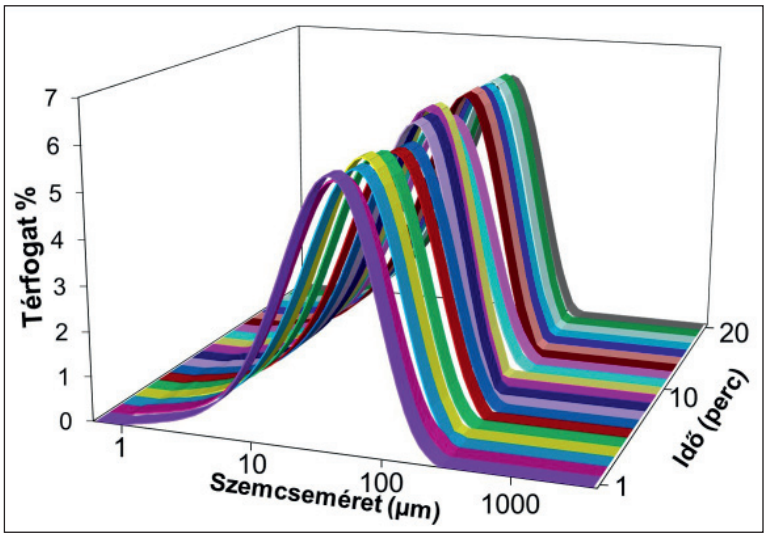

3. ábra: Impinging jet kristályosított termékek szemcseméret-eloszlása

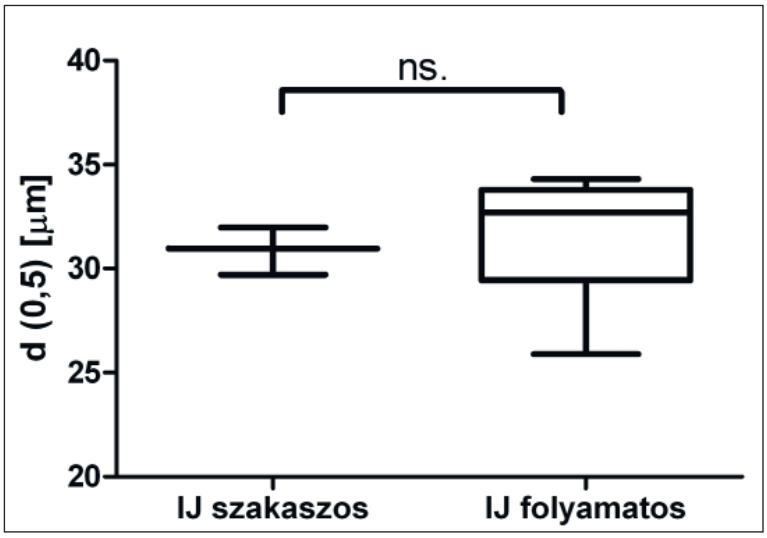

4. ábra: Átlagos szemcseméret összehasonlítása a szakaszos kristályosítási eljárás termékeivel

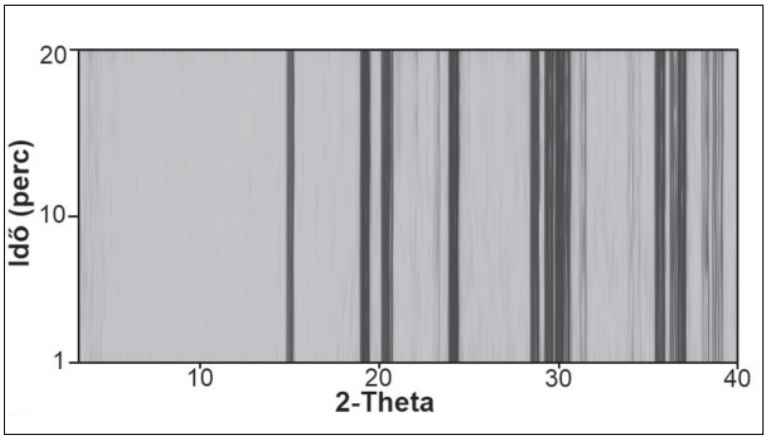

5. ábra: A termékek kétdimenziós XRPD diffraktogramjai

ket alkotnak, aggregációra kevéssé hajlamosak. A ***2. ábrán*** a kiindulási anyag és a folyamatos kristályosítás során az első és a huszadik percben vett minták SEM felvételei láthatóak, különböző nagyítással készítve. A képek alapján megfigyelhető, hogy nem történt jelentős változás a kristály morfológiában a kristályosítás teljes időtartama alatt.

A kristályosított minták mikrometriai adatait az ***I. táblázatban*** foglaltuk össze. Feltüntettük a 20-20 minta szemcseméret analízisére vonatkozó d (0,1), d (0,5) és d (0,9) értékeket, átlagot, szórást és relatív szórást számoltunk. Az alacsony szórásértékek azt igazolják, hogy a kristályosítási folyamat során nem változnak jelentősen az említett paraméterek.

A szemcseméret-eloszlási görbék alapján kijelenthető, hogy a 20 minta mindegyike monodiszperz eloszlást mutat, az állandó kristályosítási körülményeknek köszönhetően az eloszlás lefutása is azonos (***3. ábra***).

A korábbi szakaszos eljárás 52-62% kitermelési százalékot eredményezett, amelyhez képest növekedés volt tapasztalható, hiszen a folyamatos módszerrel 64-70%-ra emelkedett a kitermelés értéke. A keletkezett glicin szuszpenzió teljes mennyisége a szűrőfelületre jutott, így elkerülhető volt a műveletek közötti anyagveszteség. A folyamat során az impinging jet elem elzáródása, illetve egyéb működési nehézség nem volt megfigyelhető.

A szakaszos és folyamatos módszerrel előállított minták átlagos szemcseméret különbségét statisztikai szoftverrel, kétmintás t-próba segítségével hasonlítottuk össze (GraphPad Prism 5, GraphPad Software Inc., La Jolla, CA, USA), amely alapján megállapítottuk, hogy a szakaszos (29,707-31,967 µm) és a folyamatos (25,899-34,313 µm) módszer termékei között nincs szignifikáns különbség (***4. ábra***).

3.2. Polimorfia

A kiindulási anyag és a kristályosított termékek kristályszerkezetét XRPD

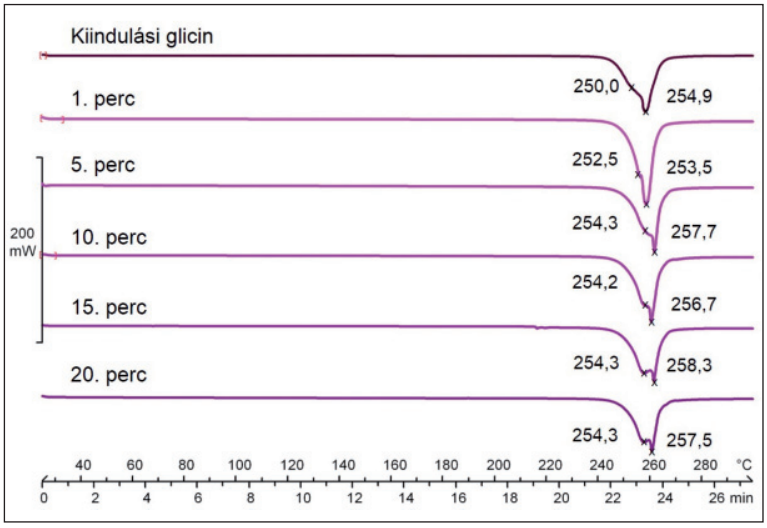

6. ábra: A kiindulási glicin és a termékek DSC termogramjai

berendezéssel vizsgáltuk, és az eredményeket a Cambridge Szerkezeti Adatbázis diffraktogramjaihoz hasonlítottuk. A mérések alapján mind a kiindulási glicin, mind a termékek kristályformája a leggyakrabban előforduló α-polimorf volt. A kristályosítási folyamat során nem tapasztaltunk a polimorfiában eltérést. Eredményeinket az ***5. ábrán*** szemléltetjük.

Korábbi vizsgálataink során megállapítottuk, hogy a DSC termoanalitikai módszer érzékenyebb az instabil β-glicin jelenlétére [24]. Ennél az analitikai eljárásnál a β-formára jellemző, 251 ºC-nál jelentkező csúcs már kis (5% alatti) mennyiségben is megjelenik, amely az α-glicin 254 ºC-os endoterm csúcsához kapcsolódva, kis vállként jelentkezik, ezért pontos mennyisége nem határozható meg. A porröntgen vizsgálatok során ez a mennyiség még nem detektálható. Ezek alapján már a kiindulási glicin is tartalmazott kis mennyiségben β-polimorfot. A kristályosított termékekben ugyancsak megfigyelhető volt az α- és β-forma keverékének megjelenése, a kristályosítás folyamatának előrehaladásával a β-glicin mennyisége kis mértékben növekedett. A növekedés oka feltehetőleg a kezdeti β-polimorf jelenléte, amely indukálta az instabil forma megjelenését (***6. ábra***).

3.3. Maradék oldószer- és maradék kálium-tartalom

A headspace gázkromatográfiás mérések alapján meghatároztuk a termékek maradék oldószer-tartalmát. A gyors kristályosítási folyamat következtében előfordulhat, hogy a kristálynövekedés során oldószer zárványok keletkeznek a szemcsékben, így fontos a pontos meghatározásuk. Az etanol az ICH Q3C (R5) irányelv szerint a 3. csoportba tartozik, a maximális értéke 5000 ppm lehet [25]. A termékekben 38 ppm és 80 ppm közötti maradék etanol koncentráció volt mérhető, így ez megfelelt az előírt követelményeknek.

A habitus javítása céljából alkalmazott kálium mennyiségét a termékekben FAAS mérések alapján határoztuk meg. A maradék kálium koncentrációja 22-48 ppm közé esett a mintákban, amely nem jelent nagy mértékű szennyezettséget.

4. Összefoglalás

A fejlesztett impinging jet antiszolvens kristályosítási módszer glicin modell anyag esetében alkalmasnak bizonyult a folyamatos kristályosítás kivitelezésére. A módszer reprodukálható és pontos, valamint rövid idő alatt magas kitermeléssel, jó minőségű termék állítható elő. A korábbi, szakaszos kristályosítás során optimalizált paraméterek jól alkalmazhatóak a folyamatos technológia esetén is, hiszen a termékek fizikai-kémiai tulajdonságai nem térnek el szignifikánsan a szakaszos módszer mintáihoz képest. A kapott kristályok átlagos szemcsemérete (31,55 μm) szignifikánsan csökkent a kiindulási anyaghoz (680,69 μm) képest, megfelelő kerekdedség, stabil polimorf módosulat, alacsony maradék oldószer- és kristályosítási additív (kálium) tartalom mellett. Összegezve, a szakaszos kristályosítási módszerek folyamatos technológiává történő konvertálásával elérhető a magasabb kitermelési százalék, valamint az előállításhoz szükséges idő jelentős csökkentése, a termék fizikai-kémiai tulajdonságainak változása nélkül.

Köszönetnyilvánítás

A szerzők köszönetet mondanak *Ambrus Ritának* a pásztázó elektronmikroszkópos felvételek elkészítéséért, és *Szakonyi Gerdának* az atomabszorpciós lángspektrométer használatában nyújtott segítségért.

IRODALOM

1. *Acevedo, D., Peña, R., Yang, Y., Barton, A., Firth, P., K. Nagy, Z. K.*: Chem. Eng. Process. *108*, 212–219 (*2016*).
2. *Plumb, K.*: Chem. Eng. Res. Des. *83*, 730–738 (*2005*).
3. *Gerogiorgis, D. I., Barton, P. I.*: Steady-state optimization of a continuous pharmaceutical process. 10th In-

ternational Symposium on Process Systems Engineering (2005) 927–932
4. *Quon, J. L., Zhang, H., Alvarez, A., Evans, J., Myerson, A. S., Trout, B. L.*: Cryst. Growth Des. *12*, 3036–3044 (*2012*).
5. *Lawton, E. S., Steele, G., Shering, P.*: Org. Process Res. Dev. *13*, 1357–1363 (*2009*).
6. *Liu, W., Ma, C. Y., Xue, Z., Wang*: Procedia Eng. *102*, 499–507 (*2015*).
7. *Liu, W., Ma, C. Y., Liu, J. J., Zhang, Y., Wang, X. Z.*: AIChE J. *63*, 967–974 (*2017*).
8. *Su, Q., Nagy, K. Z., Rielly, C. D.*: Chem. Eng. Process. *89*, 41–53 (*2015*).
9. *Farkas Béla, Révész Piroska*: Kristályosítástól a tablettázásig. Universitas Szeged Kiadó, Szeged, 2007. 13–17. old.
10. *Furuta, M., Mukai, K., Cork, D., Mae, K.*: Chem. Eng. Process. *102*, 210–218 (*2016*).
11. *Tamura, H., Kadota, K., Shirakawa, Y., Tozuka Y., Shimosaka, A., Hidaka, J.*: Adv. Powder Technol. *25*, 847–852 (*2014*).
12. *Hassan, M. S., Lau, R.*: Int. J. Pharm. *413*, 93–102 (*2011*).
13. *Variankaval, N., Cote S. A., Doherty, M. F.*: AIChE J. *54*(7), 1682–1688 (*2008*).
14. *Tobler. D. J., Rodriguez Blanco, J.D., Dideriksen, Sand, K. K., Bovet, N., Benning, L. G., Stipp, S. L. S.*: Procedia Earth and Planetary Science *10*, 143–148 (*2014*).
15. *Yang, X., Lu, J., Wang, X.-J., Ching, C.-B.*: J. Cryst. Growth *310*, 604–611 (*2008*).
16. *Sekar, C., Parimaladevi, R.*: Spectrochimica Acta Part A *74*, 1160–1164 (*2009*).
17. *Midler, M., Paul, E. L., Whittington, E. F., Futran, M., Liu, P. D., Hsu, J., Pan, S. H.*: Patent US 5 314 506 (1994).
18. *Woo, X.Y., Tan, R. B.H., Braatz, R. D.*: Cryst. Growth Des. *9*, 156–164 (*2009*).
19. *Jiang, M., Li, Y.-E. D., Tung, H.-H., Braatz, R. D.*: Chem. Eng. Process. *97*, 242–247 (*2015*).
20. *Bakar, A. M. R., Nagy, Z. K., Saleemi, A. N., Rielly, C. D.*: Cryst. Growth Des. *9*(3), 1378–1384 (*2009*).
21. *Boldyreva, E. V.; Drebushchak, V. A.; Drebushchak, T. N.; Paukov, I. E.; Kovalevskaya, Y. A.; Shutova, E. S.*: J. Therm. Anal. Calorim. *73*, 409–418 (*2003*).
22. *Weissbuch, I., Torbeev, Yu. V., Leiserowitz, L., Lahav, M.*: Angew. Chem. *117*, 3290–3293 (*2005*).
23. *Tari, T., Fekete, Z., Szabó-Révész, P., Aigner, Z.*: Int. J. Pharm. *478*, 96–102 (2015).
24. *Tari, T., Ambrus, R., Szakonyi, G., Madarász, D., Frohberg, P., Csóka, I., Szabó-Révész, P., Ulrich, Joachim, Aigner, Z.*: Chem. Eng. Technol. *40*(7), 1–10 (*2017*).
25. International Conference on Harmonisation: ICH guideline Q3C(R5) on impurities: Guideline for residual solvents, EMA/CHMP/ICH/82260/2006 Committee for Human Medicinal Products (2015).

Érkezett: 2017. június 19.

NYILATKOZAT SAJÁT MUNKÁRÓL

Név: **dr. Tari Tímea**

A doktori értekezés címe:

Crystal habit optimization by means of impinging jet crystallization method

Én, *dr. Tari Tímea* teljes felelősségem tudatában kijelentem, hogy a Szegedi Tudományegyetem Gyógyszertudományok Doktori Iskolában elkészített doktori (Ph.D.) disszertációm saját kutatási eredményeimre alapulnak. Kutatómunkám, eredményeim publikálása, valamint disszertációm megírása során a Magyar Tudományos Akadémia Tudományetikai Kódexében lefektetett alapelvek és ajánlások szerint jártam el.

Szeged, 2019. április 15.

dr. Tari Tímea